WELCOME

The Organizing Committee kindly welcomes you to the International Baltic Sea Region conference "Functional materials and nanotechnologies" **FM&NT-2010**. The conference is organized in co-operation with projects **ERANET "MATERA"** and **National Research programme in Materials Science of Latvia.**

The purpose of the conference is to bring together scientists, research staff, engineers, and students from universities, research institutes and related industrial companies aware in the field of advanced material science and materials technologies trends and future activities.

Scientific Themes are following:

- **Advanced inorganic materials for photonics, energetics and microelectronics**
- **Organic materials for photonics and nanoelectronics**
- **Advanced methods for investigation of nanostructures**
- **Perspective biomaterials and medicine technologies**
- **Development of technologies for design of nanostructured materials, nanoparticles, and thin films**
- **Design of functional materials and nanocomposites and development of their technologies**

International Organizing Committee

- **Andris Sternbergs (chairperson)**, Institute of Solid State Physics, University of Latvia, Latvia, MATERA
- **Juras Banys**, Vilnius University, Lithuania
- **Gunnar Borstel**, University of Osnabrück, Germany
- **Niels E. Christensen**, University of Aarhus, Denmark
- **Robert A. Evarestov**, St. Petersburg State University, Russia
- **Claes-Goran Granqvist**, Uppsala University, Sweden
- **Dag Høvik**, The Research Council of Norway, Norway, MATERA
- **Marco Kirm**, Institute of Physics, University of Tartu, Estonia
- **Vladislav Lemanov**, Ioffe Physical Technical Institute, Russia
- **Witold Łojkowski**, Institute of High Pressure Physics, Poland
- **Sisko Sipilä**, Finnish Funding Agency for Technology and Innovation, Finland, MATERA
- **Ingólfur Torbjörnsson**, Icelandic Centre for Research, Iceland, MATERA
- **Marcel H. Van de Voorde**, University of Technology Delft, The Netherlands

International Program Committee

- **Inta Muzikante (chairperson),** Institute of Solid State Physics, University of Latvia, Latvia, MATERA
- **Liga Berzina-Cimdina,** Institute of Biomaterials and Biomechanics, Riga Technical University, Latvia
- **Janis Grabis,** Institute of Inorganic Chemistry, Riga Technical University, Latvia
- **Leonid V. Maksimov,** Vavilov State Optical Institute, Russia
- **Linards Skuja,** Institute of Solid State Physics, University of Latvia, Latvia
- **Maris Springis,** Institute of Solid State Physics, University of Latvia, Latvia
- **Ilmars Zalite,** Institute of Inorganic Chemistry, Riga Technical University, Latvia
- **Janis Zicans,** Institute of Polymers, Riga Technical University

Local Committee:

Liga Grinberga, Anatolijs Sarakovskis, Jurgis Grube, Maris Kundzins, Raitis Siatkovskis, Anastasija Jozepa, Anna Muratova, Krisjanis Smits, Aivars Vembris, Guna Doke, Ilze Smeltere, Jelena Butikova.

The Organizing Committee sincerely hopes that the Conference will give all the participants new insights into the wide spread development of functional materials and nanotechnologies and will enhance the circulation of information released at the meeting.

On behalf of FM&NT-2010 organizers thank you all for coming and we wish you most successful and enjoyable Conference.

Edited by: Andris Sternbergs, Inta Muzikante, Liga Grinberga (ISSP UL)
Typesetting: Anatolijs Sarakovskis, Jurgis Grube (ISSP UL)
Printed by "Latgales Druka"
ISBN: 978-9984-45-171-5; UDK 539 Fu 506
Institute of Solid State Physics, University of Latvia
8 Kengaraga Street, LV-1063, Riga, Latvija
Phone: +371-67187816
Fax: +371-67132778
e-mail: issp@cfi.lu.lv
web: http://www.cfi.lv

Riga, 2010

PARTNERS

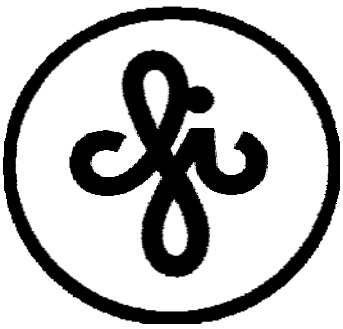

EXHIBITORS

Armgate, CSM Instruments, FANEX, Raith, Saint-Tech, Thorlabs

March 16

16:00	**Registration**
17:00 19:00	**Welcome party**

Plenary - 40 min
Invited - 30 min
Oral - 20 min

Theory and modelling
Nanostructuring and composites
Technologies and devices
Ferroelectrics and related materials
Spectroscopy and optical properties
Perspective materials
Bionanotechnologies
Information

March 17

8:00	**Registration**	
9:00	**Opening**	
9:20	M. Van de Voorde - Plenary	
10:00	R. Tomellini - Inv	
10:30	M. Bundule - Inv	
10:50	**Technical information**	
11:00	**Coffee**	
11:20	R. Evarestov - Inv	
11:50	E. Kotomin - Inv	
12:20	V. Trepakov - Inv	
12:50	**Lunch 12:50 - 13:40**	
13:50	**Conference photo**	
	HALL 1	**HALL 2**
14:00	Y. Shunin	C.-G. Granqvist - Inv
14:30	M. Brik	F. Davin
14:50	G. Zvejnieks	R. de Leeuw
15:10	A. Bandura	V. Sammelselg
15:30	D. Bocharov	I. Ayala
15:50	**Coffee**	
16:10		L. Maksimov - Inv
16:20	S. Piskunov	
16:40	D. Gryaznov	M. Chiesa
17:00	R. Eglitis	J. Butikova
17:20	D. Engers	A. Voitkans
17:50	**Poster overview**	
18:00 19:45	**Poster session & coffee**	

March 18

8:00	**Registration**	
8:20	**Technical information**	
	HALL 1	**HALL 2**
8:30	T. Ogawa - Inv	V. Skuratov - Inv
9:00	M. Tyunina	J. Piqueras
9:20	I. Shnaidshtein	J. Maniks
9:40	O. Malyshkina	W. Lojkowski
10:00	J. Banys	A. Salak
10:20	M. Dunce	M. Waegner
10:40	M. Rutkis	G. Chikvaidze
11:00	H.-J. Fitting	M. Krause
11:20	**Coffee**	
11:40	M. Romanova	M. Reinfelde
12:00	S. Tyutyunnikov	J. Teteris
12:20	M. Barczak	A. Ozols
12:40	Z. Irbe	J. Zavickis
13:00	K. Salma	G. Sakale
13:20	A. Stunda	G. Doke
13:40	**Lunch 13:40 - 14:40**	
14:40	A. Gavrilyuk - Inv	A. Trukhin - Inv
15:10	Y. Fujioka	V. Bogdanov
15:30	G. Bajars	S. Omelkov
15:50	J. Kleperis	J. Grube
16:10	M. Tomut	A. Fedotovs
16:30	M. Prabhu	M. Gokula Krishna
16:50	**Coffee**	
17:15 22:30	**Excursion & conference dinner**	

March 19

9:20	**Technical information**
9:30	L. Skuja - Inv
10:00	A. Kulkarni
10:20	A. Wisniewski
10:40	D. Zablotsky
11:00	G. Marcins
11:20	M. Chubarov
11:40	**Coffee**
12:00	Y. Zhukovskii - Plenary
12:40	**Closing**
13:00	**Goodbye refreshments**

ISSP UL International Supervisory Board Meeting - 18.03.10. 14:45 - 16:45

DURING THE CONFERENCE THE EXHIBITION OF SEVERAL COMPANIES WILL BE HELD

International Conference Functional Materials and Nanotechnologies
'FMNT – 2010'

PROGRAM

Tuesday, March 16

16:00 – 17:00	**REGISTRATION**
17:00 – 19:00	**WELCOME PARTY**

Wednesday, March 17

08:00 – 09:00	**REGISTRATION**
HALL 1	**OPENING**

Chairman of the conference: A. Sternbergs

09:00 - 09:10	J. Ekmanis	The president of the Latvian Academy of Sciences	
09:10 - 09:20	M. Auzinsh	The rector of the University of Latvia	
09:20 - 10:00	M. Van de Voorde	Research, development and technology (R&D&T) roadmaps 2020 for nanomaterials	PL - 1
10:00 -10:30	R. Tomellini	European research and development of novel materials for the knowledge society	INV - 1
10:30-10:50	M. Bundule	European research area initiatives – support instruments for material sciences	INV - 2

10:50 – 11:00	**Technical Information**
11:00 – 11:20	**Coffee**

11:20 - 11:50	R. Evarestov	Symmetry and models of BN and TiO_2 nanotubes	INV - 3
11:50 - 12:20	E. Kotomin	Oxygen incorporation reaction into mixed conducting ABO_3 - type perovskites for fuel cell applications	INV - 4
12:20 - 12:50	V. Trepakov	Amazing dielectric properties and structure of manganese-doped $SrTiO_3$ crystals	INV - 5

12:50 – 13:40	**Lunch**
13:40 – 13:50	**CONFERENCE PHOTO**
HALL 1	**THEORY AND MODELING**

Chairperson: E. Kotomin

14:00 - 14:30	Y. Shunin	Resistance simulations for junctions of SW and MW carbon nanotubes with various metal substrates	OR - 1
14:30 - 14:50	M. Brik	*Ab-initio* modeling of optical and electronic properties of pure and rare-earth ions doped wide-gap crystals under varying hydrostatic pressure	OR - 2
14:50 - 15:10	G. Zvejnieks	Modeling of Au-Ni surface alloy instability	OR - 3
15:10 - 15:30	A. Bandura	LCAO calculations of (001) surface oxygen vacancy structure in Y-doped $BaZrO_3$	OR - 4
15:30 - 15:50	D. Bocharov	First principles calculations on oxygen impurities incorporated in the vacancies of UN(001) substrate	OR - 5

15:50 - 16:10	**Coffee**

Wednesday, March 17

HALL 1	THEORY AND MODELING		
Chairperson: M. Kirm			
16:20 - 16:40	S. Piskunov	First-principles modeling of oxygen interaction with ABO_3-type perovskite surfaces	OR - 6
16:40 - 17:00	D. Gryaznov	Electronic, phonon and magnetic structure of pure and Sr-doped $LaCoO_3$	OR - 7
17:00 - 17:20	R. Eglitis	*Ab initio* calculations of $SrTiO_3$, $BaTiO_3$, $PbTiO_3$, and $CaTiO_3$ (001) and (011) surfaces	OR - 8
17:20 – 17:40	D. Engers	Temperature development of chemically ordered nanoregions in relaxor ferroelectric $Pb(Mg_{1/3}Nb_{2/3})O_3$ (PMN)	OR - 9
17:50 – 18:00	I. Muzikante	**POSTER OVERVIEW**	

HALL 2	TECHNOLOGIES AND DEVICES		
Chairperson: L. Maksimov			
14:00 - 14:30	C.-G. Grankqvist	Progress in chromogenic materials and devices: new data om thermochromic VO_2-based materials and electrochromic nickel-tungsten-oxide films	INV - 6
14:30 - 14:50	F. Davin	Advanced mechanical surface testing for thin coatings by nanoindentation, scratch and tribology investigation	OR - 10
14:50 - 15:10	R. de Leeuw	Nanopipette applications in bionanoscience	OR - 11
15:10 - 15:30	V. Sammelselg	Nanoscopy and – technology using scanning dual beam techniques	OR - 12
15:30 - 15:50	I. Ayala	Atomic layer deposition (ALD), enhanced thin films	OR - 13
15:50 - 16:10	**Coffee**		
Chairperson: C.-G. Granqvist			
16:10 - 16:40	L. Maksimov	Combined light scattering and acoustic methods for the study of glass macro- and nanostructure	INV - 7
16:40 - 17:00	M. Chiesa	Application of frequency domain thermoreflectance	OR - 14
17:00 - 17:20	J. Butikova	Aspects of SEM analysis of ablated tiles in ASDEX upgrade tokamak	OR - 15
17:20 – 17:40	A. Voitkans	Reflection high energy electron diffraction as a tool for nanoparticle deposition studies	OR - 16

HALL 1	
Chairperson: I. Muzikante	
17:50 – 18:00	**POSTER OVERVIEW**
18:00 – 19:45	**POSTER SESSION & Coffee**

DURING THE CONFERENCE THE EXHIBITION OF COMPANIES – SAINT-TECH, FANEX, CSM INSTRUMENTS, ARMGATE, THORLABS – WILL BE HELD

Thursday, March 18

08:00 – 08:20	**REGISTRATION**		
HALL 1	**FERROELECTRICS AND RELATED MATERIALS**		
Chairperson: A. Wisniewski			
08: 20 -08:30	**Technical Information**		
08:30 – 09:00	T. Ogawa	Domain switching and rotation in alkali bismuth titanate lead-free piezoelectric ceramics	INV - 8
09:00 - 09:20	M. Tyunina	Enhanced relaxor behaviour in epitaxial films of lead magnesium niobate	OR - 17
09:20 - 09:40	I. Shnaidshtein	First application of the thermal noise method for studying ferroelectrics thin films	OR - 18
09:40 – 10:00	O. Malyshkina	Influence of natural aging on the polarization profile in PZT - based ceramics	OR - 19
10:00 - 10:20	J. Banys	Broadband dielectric spectroscopy of ferroelectric $(1-x)Al_{0.9}Li_{0.1}NbO_3$ - $xBi_{0.5}K_{0.5}TiO_3$ ceramics	OR - 20
10:20 – 10:40	M. Dunce	Description of relaxor state in $Na_{1/2}Bi_{1/2}TiO_3$-$SrTiO_3$-$PbTiO_3$ system of solid solutions	OR - 21
10:40 – 11:00	M. Rutkis	Computer modeling of chromoprhore/polymer composite polarization: para- , antiferro- and ferroelectric behavior	OR - 22
11:00 – 11:20	H.-J. Fitting	Fast electron switching in dielectrics	OR - 23
11:20 – 11:40	**Coffee**		
HALL 1	**BIONANOTECHNOLOGIES**		
Chairperson: L. Berzina-Cimdina			
11:40 – 12:00	M. Romanova	Silicon based nanoparticles usage as adjuvants for treatment of viral infections	OR - 24
12:00 – 12:20	S. Tyutyunnikov	Experiments on application of high power microwave radiation to biomedicine using micro- and nanoparticles	OR - 25
12:20 – 12:40	M. Barczak	Synthesis, structure and adsorption properties of ordered mesoporous organo-silicas functionalized with different groups	OR - 26
12:40 – 13:00	Z. Irbe	Modification of setting properties of α-tricalcium phosphate cements	OR - 27
13:00 – 13:20	K. Salma	Preparation and sintering behaviour of β-tricalcium phosphate	OR - 28
13:20 - 13:40	A. Stunda	Structure of phosphate based bioactive glasses	OR - 29
13:40 – 14:40	**Lunch**		
HALL 1	**PERSPECTIVE MATERIALS I**		
Chairperson: V. Trepakov			
14:40 – 15:10	A. Gavrilyuk	Multifunctional hydrogen nanosized materials:WO_3, MoO_3, V_2O_5	INV - 10
15:10 – 15:30	Y. Fujioka	Structural study of nanocrystalline tungsten trioxide	OR - 48
15:30 – 15:50	G. Bajars	Study of structure and electrochemical characteristics of $LiFePO_4$/C as cathode material for lithium batteries	OR - 49
15:50 – 16:10	J. Kleperis	Oriented nanostructures for solar-hydrogen technologies	OR - 50
16:10 – 16:30	M. Tomut	Carbon materials for high-power heavy ions accelerators	OR - 51
16:30 – 16:50	M. Prabhu	Synthesis and characterization of pure titania nanocrystallites by sol-gel method	OR - 52
16:50 – 17:10	**Coffee**		

Thursday, March 18

HALL 2 — **NANOSTRUCTURING AND COMPOSITES**

Chairperson: E. Nommiste

08:30 – 09:00	V. Skuratov	The formation and modification of nanostructures in dielectric matrices using swift heavy ions	INV - 9
09:00 - 09:20	J. Piqueras	Defects and nanochannels in doped zinc oxide nanorods grown by thermal methods	OR - 30
09:20 - 09:40	J. Maniks	Nanostructuring and hardening of LiF crystals irradiated with 3-15 MeV Au ions	OR - 31
09:40 – 10:00	W. Lojkowski	Investigation of luminescence of zirconia nanopowders during change of oxygen content in the gas over the sample	OR - 32
10:00 - 10:20	A. Salak	Anion exchange in Zn-Al layered double hydroxides: in situ XRD study	OR - 33
10:20 – 10:40	M. Waegner	Top-down fabrication of ordered PZT nanodot arrays by nanosphere lithography	OR - 34
10:40 – 11:00	G. Chikvaidze	The influence of nonstoichiometric silicon carbide nanopowder on the reducing efficiency of silicon for solar cells	OR - 35
11:00 – 11:20	M. Krause	Experimental investigation of swift heavy ion-induced damage in highly ordered graphite	OR - 36

11:20 – 11:40 — **Coffee**

Chairperson: J. Piqueras

11:40 – 12:00	M. Reinfelde	Surface hologram recording in amorphous As-S-Se films by 0.6328μm laser	OR - 37
12:00 – 12:20	J. Teteris	Photoinduced mass transfer in disordered materials	OR - 38
12:20 – 12:40	A. Ozols	Effect of light polarization on holographic recording in glasy azocompounds and chalcogenides	OR - 39
12:40 – 13:00	J. Zavickis	The polyisoprene – nanostructured carbon composite as flexible pressure sensor material – properties and practical applications	OR - 40
13:00 – 13:20	G. Sakale	The investigation of organic solvent vapour sensing mechanism on polymer-nanostructured carbon composite	OR - 41
13:20 - 13:40	G. Doke	Synthesis and up-conversion luminescence in erbium doped $NaLaF_4$	OR - 42

13:40 – 14:40 — **Lunch**

HALL 2 — **SPECTROSCOPY AND OPTICAL PROPERTIES**

Chairperson: A. Kuzmin

14:40 – 15:10	A. Trukhin	Luminescence of dense, octahedral structured crystalline silicon dioxide (stishovite)	INV - 11
15:10 – 15:30	V. Bogdanov	Observation of α- relaxation in glasses at vicinity of T_g by ultrasonic and Mandel'shtam-Brillouin methods	OR - 43
15:30 – 15:50	S. Omelkov	The properties of luminescence of nominally pure $LiBaAlF_6$ single crystals	OR - 44
15:50 – 16:10	J. Grube	Up-conversion luminescence in erbium and ytterbium doped silicate glass ceramics	OR - 45
16:10 – 16:30	A. Fedotovs	Paramagnetic probes for studies of crystallization in the oxyfluoride glass ceramics	OR - 46
16:30 – 16:50	M. Gokula Krishna	Synthesis and characterization of pure and Sm doped TiO_2 nanocrystals by solid state reaction method	OR - 47

16:50 – 17:10 — **Coffee**

17:15 – 22:30 — **EXCURSION AND CONFERENCE DINNER**

Friday, March 19

HALL 1	PERSPECTIVE MATERIALS II		
Chairperson: W. Lojkowski			
09:20 – 9:30	**Technical Information**		
09:30 – 10:00	L. Skuja	Defects in the bulk and on the surfaces of amorphous silicon dioxide	INV - 12
10:00 - 10:20	A. Kulkarni	Adding functionality to cotton by stimuli sensitive microparticles	OR - 53
10:20 - 10:40	A. Wisnievski	Effect of particle size and pressure on magnetic properties of manganite and cobaltite nanoparticles	OR - 54
10:40 - 11:00	D. Zablotsky	Formation of microconvection in periodic concentration grating of magnetic nanoparticles	OR - 55
11:00 - 11:20	G. Marcins	Structure and characteristics of laser crystallized thin amorphous Si films	OR - 56
11:20 – 11:40	M. Chubarov	Thermoactivated spectroscopy of defects levels in GaN thin films	OR - 57
11:40 -12:00	**Coffee**		

Chairman of the conference: A. Sternbergs

12:00 - 12:40	Y. Zhukovskii	Growth mechanism for CNT bundle upon both flat and nano-structured Ni catalyst: *ab initio* simulations	PL - 2
12:40 – 13:00	**CLOSING**		
13:00 – 14:00	**GOODBYE REFRESHMENTS**		

Wednesday, March 17

Chairperson: I. Muzikante

18:00 – 19:45	**POSTER SESSION**	
M. Tyunina	Substrate induced relaxor behaviour in thin films of barium titanate	PO - 1
M. Tyunina	Ferroelectric domains in epitaxial and polycrystalline barium titanate films	PO - 2
M. Tyunina	Growth of perovskite-structure potassium tantalate films	PO - 3
M. Tyunina	Strongly inhomogeneous domain configuration in epitaxial lead zirconate titanate films	PO - 4
M. Tyunina	Ultrathin strontium titanate films by pulsed laser deposition	PO - 5
I. Smeltere	Electric properties of $Na_{0.5}K_{0.5}(Nb_{1-x}Sb_x)O_3$+0.5$MnO_2$ ceramics (x=0.04, 0.05 and 0.06)	PO - 6
I. Smeltere	Synthesis and characterization of lead-free 1-x$(K_{0.5}Na_{0.5})Nb_{1-y}Sb_yO_3$-x$BaTiO_3$	PO - 7
T.Ramoška	Microwave dielectric investigations of the 0.7$BaTiO_3$–0.3$(Ni,Zn)Fe_2O_4$ multiferroic composites	PO - 8
P. Keburis	Dielectric spectra of barium titanate doped with lanthanum magnesium titanate	PO - 9
K. Klemkaitė	Reconstitution effect of layered double hydroxide containing different cations	PO – 10
S. Rudys	Dieletric spectroscopy of xNBT–(1-x)LMT ceramics	PO - 11
A. Dziaugys	Phase transition dynamics in $Pb_5Ge_3O_{11}$ crystals	PO - 12
V.S. Lisitsin	Effect of annealing on polarized state stability in SBN crystals	PO - 13
M. Livinsh	Effects of axial pressure on the electrical properties of $Li_{0.06}Na_{0.94}NbO_3$ ceramic	PO - 14
B. Sorkin	Magnetic and vibronic theory of the influence of ferroelectricity on magnetic properties of Bi-based multiferroics	PO - 15
M. Ivanov	Dielectric and magnetic properties of carbon-coated nickel capsules in wide microwave frequency range	PO - 16
S. Bagdzevicius	Broadband dielectric investigation of sodium potassium niobate with 10% antimony substitution	PO - 17
K. Bormanis	Dielectric response in $(K_{0.5}Na_{0.5})(Nb_{1-x}Sb_x)O_3$+0.5mol%$MnO_2$ ceramics to weak sinusoidal fields of low and infra-low frequencies	PO - 18
K. Bormanis	The effect of bias field on dielectric response in lead ferrotantalate ceramics	PO - 19
K. Bormanis	Elastic properties of barium zirconate titanate ceramics	PO - 20
K. Bormanis	Dielectric properties and conductivity of ferroelectric $Li_xNa_{1-x}Ta_{0.1}Nb_{0.9}O_3$ solid solutions	PO - 21
K. Bormanis	Dielectric and elastic parameters of $Li_xNa_{1-x}Ta_{0.1}Nb_{0.9}O_3$ ferroelectric solid solution ceramics	PO - 22
K. Bormanis	Growth of lithium niobate single crystals from granulated charge	PO - 23
K. Bormanis	Physical properties and structure of niobium pentoxide ceramics treated by concentrated light flow	PO - 24
K. Bormanis	Kinetics of photorefractive light scattering in $LiNbO_3$:Cu[0.015 % mass] and $LiNbO_3$:Zn[0.5 % mass] single crystals	PO - 25

K. Bormanis	Modelling of cluster formation in optically nonlinear lithium niobate crystal	PO - 26
N. Mironova-Ulmane	Polarisation dependent Raman study of single-crystal nickel oxide	PO - 27
V. Koronovskyy	Investigation of the temperature-stimulated structure changes in thin garnet films by using of the electromagneto-optical method	PO - 28
A. Lusis	Application of metal coatings for functionalization of leached glass fabrics	PO - 29
S. Cornaja	Novel Pd supported catalysts for glyceric acid selective production	PO - 30
A. Dauletbekova	Nanosized defects on the surface of irradiated LiF crystals	PO - 31
V. Serga	Palladium nanocrystalline films produced by EPM. Phase composition and magnetic properties	PO - 32
A. Petruhins	Sulphide nanostructure fabrication using pulsed laser deposition	PO - 33
A. Voitkans	Laser induced ablation analysis of post-mortem tiles of ASDEX upgrade tokamak	PO - 34
E.P. Prokopev	Positronics and nanotechnologies: possibilities of studying nanoobjects in technically important materials and nanomaterials	PO - 35
L. Grinberga	Nanosized perovskites for photocatalytical water decomposition	PO - 36
J. Hodakovska	SPEEK and PANI based membranes for fuel cells	PO - 37
G. Vaivars	Anion exchange membrane based on alkali doped poly(2,5-benzimidazole) for alkaline membrane fuel cell	PO - 38
M. Vanags	Short duration voltage and current transients on water electrolyses cell	PO - 39
A. Dindune	Preparation and characterization of substituted by niobium $Li_{1.4}Ti_{1.9}P_3O_{12}$ ceramics	PO - 40
A. Zarins	Accumulation of radiolysis products and defects in nanopowders of lithium orthosilicate	PO - 41
A. Vitins	Tritium release properties of beryllium products for fusion devices	PO - 42
A. Mychko	Increased radiation hardness of CdZnTe by laser radiation	PO - 43
T. Puritis	Si, CdTe nanocrystals and surface structuring for solar cell applications	PO - 44
H.-J. Fitting	Si^+ ion beam mixing in SiO_2/Si structures	PO - 45
V. Zauls	Electron beam refining of solar silicon	PO - 46
V. Panibratskiy	Modelling the processes of electro-ray refining of silicon	PO - 47
P. Onufrijevs	Impact of laser radiation on microhardness of a semiconductor	PO - 48
J. Kozlova	Microscopic study of graphene and silicon/oxide/graphene/oxide structures	PO - 49
A. C. Peterlevitz	Diamond synthesis at room temperature by electrodeposition technique	PO - 50
R. Zabels	Indentation induced deformation behavior of ZnO	PO - 51
I. Mihailova	Obtaining $CuInSe_2$ heterostructures on nanostructured ZnO films	PO - 52
I.Kaulachs	Influence of thermal annealing on photosensitivity of GaOHPc:PCBM/P3HT:PCBM bulk heterojunction system	PO - 53

B. Polyakov	Manipulation of gold nanoparticles inside scanning electron microscope	PO – 54
V. Shints	Investigation of nanosized colloidal particles transfer through a porous layer	PO - 55
A. Mezulis	Creating concentration profiles of nanosized magnetic particles in non-uniform magnetic field	PO - 56
V. Vorohobovs	Functional nanocomposite material for visualization of irreversable impact of static magnetic field	PO - 57
P. Birjukovs	Characterization of nanodevices inside nanowire arrays using conductive afm and in-situ nanomanipulation techniques	PO - 58
R. Meija	Development and characterization of nanoelectromechanical switches	PO - 59
R. Poplausks	A nanoinjector based on nanoporous anodized aluminium oxide probes	PO - 60
I. Pastore	The preparation and application of ultra thin anodized aluminium oxide membranes	PO - 61
O. Shiman	Stimulated changes in bilayer Sb/Se film	PO - 62
U. Gertners	Multibeam holographic recording	PO - 63
A. Bulanovs	Investigations of As-S-Se thin films for use as inorganic photoresist for digital image-matrix holography	PO - 64
A. Gerbreders	The differnce of surface relief formation in As_2S_3-polymer and As_2S_3-DR1-polymer composites	PO - 65
I. Muzikante	Photoinduced surface relief gratings formation and properties of PMMA films with azobenzene derivative containing n, n-dicyclohexyl sulfonamide moiety	PO - 66
I. Reinholds	New compatibilisers for improvement of magneto-physical and deformation properties of polymer nanocomposites	PO - 67
S. Strode	Structure and properties of plasma synthesized ferrites as modifiers of polymer compositions	PO - 68
I. Elksnite	Development of liquid crystal polymer modified polyethylene composites and investigation of its elastic properties	PO - 69
A. Tokmakov	Molecular hyperpolarizabilities of indane derivatives measured by Hyper Rayleigh scattering	PO - 70
O. Strekalova	Silicon dioxide nanoparticles as a carrier of ascorbic acid	PO - 71
A. Pavlova	Fabrication of a conductive ceramic and its use in water treatment technology	PO - 72
V. Krilova	Ionization of carboxylic cation-exchanger and sorption of proteins	PO - 73
T. Dizhbite	Water soluble bioactive organic-inorganic Si- and Fe-containing hybrid materials based on lignosulphonate	PO - 74
M.Polakovs	EPR and Mössbauer spectra of iron ions in the hemoglobin	PO - 75
M. Kirm	UV-VUV spectroscopy of SiO_2 photonic crystal doped with HEuEDTA phosphor	PO - 76
L. Grigorjeva	Near-band luminescence of ZnO crystals in subnanosecond range	PO - 77
L. Grigorjeva	Photoluminescent and photocatalytic activity of nanosized zinc tungstate prepared by combustion synthesis	PO - 78
K. Smits	Up-conversion luminescence in ZrO_2 nanocrystals	PO - 79
T. Shalapska	The luminescence properties of lanthanides ions in $LiLn_{1-x}Ce_xP_4O_{12}$ polyphophates	PO - 80

D. Venkatesan	Characterization of pure and rare earth doped ZnO nanoparticles for optical applications	PO - 81
L. Dolgov	Sensitizing of Sm^{3+} fluorescence by silver dopant in the TiO_2 films	PO - 82
V. Korsaks	Luminescence of hexagonal boron nitride powder and nanotubes at different temperatures	PO - 83
D. Jakimovica	Photoluminescence of Al_2O_3 bulk and nanosize powders at low temperature	PO - 84
V. Pankratov	Luminescence and optical properties of semiconductor quantum dots in VUV spectral range	PO - 85
A.I. Popov	Silicon carbide nanowires: synthesis and luminescence properties	PO - 86
A.I. Popov	Surfactant-assisted synthesis of $Cd_{1-X}Co_XS$ nanocluster alloys and their structural, optical and magnetic properties	PO - 87
A.I. Popov	$CsPbCl_3$ nanocrystals dispersed in the $Rb_{0,8}Cs_{0,2}Cl$ matrix studied by far-infrared spectroscopy	PO - 88
A.I. Popov	Luminescence of $SrTiO_3$ single crystals excited under synchrotron radiation	PO - 89
L. Shirmane	Luminescence properties of YAG:Ce^{3+} nanocrystals in vacuum ultraviolet spectral range	PO - 90
A. I. Livshits	DFT simulation of guanine-quartet chiral structures	PO - 91
A. Gopejenko	*Ab initio* calculations of yttrium and vacancy point defects for ODS steels modeling	PO - 92
A. Kuzmin	First principles LCAO study of phonons in $NiWO_4$	PO - 93
A. Kuzmin	Electronic excitationS in $ZnWO_4$ and $ZnWO_4$:Ni using VUV synchrotron radiation	PO - 94
P. Merzlakovs	Analysis of void superlattice formation in CaF_2	PO - 95
R. I. Eglitis	*Ab initio* calculations of Nb-doped $SrTiO_3$	PO - 96
R.I. Eglitis	*Ab initio* calculations of MgF_2 (001) and (011) surfaces	PO - 97
E. Blokhin	*Ab initio* comparative study of phonons in different phases of $SrTiO_3$ perovskite	PO - 98
A. Kovalovs	Finite element modelling of thin polymer shell	PO - 99
J.Gabrusenoks	Lattice dynamics and phase transitions of AlF_3	PO - 100
J. Timoshenko	Molecular dynamics simulations of EXAFS in germanium	PO - 101
A. Kalinko	EXAFS study of $ZnWO_4$ on the W L_3 and Zn K edges	PO - 102
A. Anspoks	Probing NiO nanocrystals structure by EXAFS spectroscopy	PO - 103
I. Indrikova	Photoelectrical properties of indandione mono- and multistructured thin films	PO - 104
K. Pudzs	Energy structure and electro-optical properties of thin films of carbazole derivatives	PO - 105
B. Niparte	Photoinduced switching of the surface potential of host-guest films containing azobenzene derivatives	PO - 106

Abstracts of the plenary presentations

PL-1

RESEARCH, DEVELOPMENT AND TECHNOLOGY (R&D&T) ROADMAPS 2020 FOR NANOMATERIALS

M. Van de Voorde

Institute for Materials Science and Technology, University of Technology, Delft (NL)

e-mail: marcel.vandevoorde@xs4all.nl

The present status of nanomaterials R&D&T in the world will be reviewed and be demonstrated that a new strategy for Europe must be developed to ensure future impact on our economy and society, and success in this grand challenging new world.

It will be highlighted that **Fundamental research** is the backbone for future industrial success including new theories; design of third generation nanomaterials,; macro, mico-nano computer modelling, nanolifetime predictions …

Research-development-technology roadmaps: 2010 - 2020 are discussed for:

- Breakthroughs in communication and information
- Grand challenges in life science and medical applications
- Revolutionary nanomaterials with tailored functionalities for new generation energy sources/applications
- Role of nanomaterials in transportation and potentials new fuels
- ……..

Roadmaps 2010 – 2020 are shown giving the impact of nanoscience on environment i.e.

- Man-made environment
- Nuclear waste
- Global climate change
- Nanopotentials in safety (toxicology) and security
- ……

Guidelines for a prosperous Europe: modern economy and welfare for the society

- Initiate a European college of excellence for nano science/technology/industry and economy
- Create European nanoscience/nanotechnology centres of excellence
- Initiate "university – science/technology institutes -industry" partnerships
- Set up of a European Industrial Agency and reformulate European nanocorporate research
- Promote nanoindustrialisation: Technology parks, nanometrology and standardisation, …
- Prepare an international nanomaterials programme
- Initiate a strategy: European infrastructures for nanomaterials R&D&T
- Familiarisation of the society with the new culture of nanoscience/ technology" job creation – modern economy – international competitively - consumer protection
- **.....**

Model for a global nanolandscape

Nanoscience, technology and nanoindustrialisation is a complex topic for the world and cannot be subject anymore for one institute, nation or continent. The success rate will depend of joining brilliancies in the world. Models for collaboration between countries will be elaborated and mechanisms for execution proposed i.e. nanomaterials for energy in the frame of IEA (International Energy Agency), ….

PL-2

GROWTH MECHANISM FOR CNT BUNDLE UPON BOTH FLAT AND NANO-STRUCTURED Ni CATALYST: *AB INITIO* SIMULATIONS

Yu.F. Zhukovskii[1], S. Piskunov[1], E.A. Kotomin[1], S. Bellucci[2]

[1]*Institute of Solid State Physics, University of Latvia, Riga,*

[2]*INFN - Laboratori Nazionali di Frascati, Frascati (Rome), Italy*

e-mail: quantzh@latnet.lv

The chemical vapor deposition (CVD) growth of carbon nanotubes (CNTs) from the particles of metallic catalyst is a promising approach to control properties of nanotubes. The CNT growth is followed by the two important processes: (*i*) diffusion of C atoms upon the particle surface or across its interior (a rate-determining step) and (*ii*) nucleation of graphitic fragment as followed by further incorporation of carbon into the growing NT determining a chirality of nanotubes. Not only single-walled (SW) nanotubes (separated each from other) can be synthesized but also bundles of SW CNTs, which may contain hundreds of closely-packed nanotubes, as well as multi-walled (MW) CNTs [1].

We performed here *ab initio* simulations on 2D periodic models of the C/Ni(111) nano-interconnect, in order to understand the peculiarities of initial stage of growth for the bundle of SW CNTs upon (either flat or nanostructured) catalytic particles. The only limitation in this model is that the chiralities of nanotubes in the bundle are equivalent. Models of 2D supercells of the corresponding substrate are discussed. Appearance of the adsorbed carbon atoms follows from the dissociation of CVD hydrocarbon molecules, *e.g.*, CH_4: $(CH_4)_{ads} \rightarrow (CH)_{ads} + 3H_{ads}$ and $(CH)_{ads} \rightarrow C_{ads} + H_{ads.}$ Association of the adsorbed carbon atoms upon the catalyst surface precedes further swelling of the $(C_n)_{ads}$ islands after appearance of pentagonal defects within a honeycomb sheet [2] which is a more probable upon the catalyst surface containing either defects or nanoclusters (as in the case of the nanostructured substrate). The consequent growth of the capped CNTs is more effective upon the nanostructured Ni than a flat substrate (*cf.* values of CNT adhesion energy *per* boundary C atom for chiralities of armchair-type, 4.01 *vs*. 2.51 eV, and zigzag-type, 4.61 *vs*. 2.14 eV, respectively). The electronic charge transfer from the Ni catalyst towards the CNTs has been calculated for both chiralities (>1 *e per* C atom).

References

1. A. Loiseau, J. Gavillet, F. Ducastelle, J. Thibault, O. Stéphan, P. Bernier, S. Thair, *C.R. Physique*, 2003, 4**,** 975-991.

2. M. Fujita, R. Saito, G. Dresselhaus, and M.S. Dresselhaus, *Phys. Rev. B*, 1992, 45, 13834-13836.

Abstracts of the invited presentations

INV-1

EUROPEAN RESEARCH AND DEVELOPMENT OF NOVEL MATERIALS FOR THE KNOWLEDGE SOCIETY

R. Tomellini
European Commission - General Directorate for Research - Value-added Materials Unit
e-mail: renzo.tomellini@ec.europa.eu

The European Union (EU) and its Member States will be confronted in the coming decades with major challenges: the new industrial and trade situations, pressure on supplies and energy security, the climate change, the technological revolutions, the increased ageing of the population, the internal migrations, etc [1].

Within this frame, EU research and innovation have a big role to play as they can help delivering jobs, prosperity and quality of life for its citizens. The EU is striving to create a single European Research Area (ERA) that encourages knowledge transfer through networks of world-class European researchers. The Commission adopted a Communication on "*Better careers and more mobility: a European partnership for researchers*" [2] as one of the five ERA initiatives. It proposed a set of initiatives to ensure that researchers across the EU benefit from the right training and attractive career prospects and that barriers to their mobility are removed. Cooperation between European countries is further encouraged through cutting-edge infrastructure and joint policy-making for research. In addition, the EU must improve its record of translating scientific knowledge into patented processes and products for use in high-tech industries. The new European Institute for Innovation and Technology will support this process by promoting partnerships which link the three sides of the 'knowledge triangle': research, education and innovation.

Materials research plays a key role in supporting development of competitive and sustainable growth in Europe: the increasing complex needs of industry and society demand improved industrial processes and products with better quality, durability, specific functionalities and structural properties. They have also now to face with strategic objectives including cost effectiveness, global manufacturing and environmental legislation: it is essential for environmental sustainability to examine all aspects of a product's life cycle to make substantial reductions in the use of resources while minimising environmental and health concerns. At the same time, market trends make even harder to meet these objectives, as customers want greener, smaller, lighter and cheaper products.

A significant part of future goods and services are as yet unknown, but the main driving force behind their development will be Key Enabling Technologies (KETs), such as nanotechnology, micro- and nanoelectronics, biotechnology and advanced materials: mastering these technologies means being at the forefront of managing the shift to a low carbon, knowledge-based economy [3]. To this purpose, materials research requires a multi-disciplinary approach, integrating several basic disciplines (physics, chemistry, biology, nanosciences) with enabling and cross-cutting technologies.

New and improved materials represent therefore an *invisible revolution* that is becoming strategic and profitable, changing products and processes by great extents: new functionalities and/or improved properties can be introduced thus adding value to existing products/services. Searching for "leapfrog" industrial innovation, the engineered realization of *materials by design* will allow re-designing or re-conceiving products and/or processes under a really sustainable systemic approach: energy and primary raw materials consumption, added value, safety (REACH, …), less components, less production steps.

References

1. *http://ec.europa.eu/research/social-sciences/pdf/the-world-in-2025-report_en.pdf*
2. http://ec.europa.eu/euraxess/pdf/comm_pdf_com_2008_0317_f_en_communication.pdf
3. http://ec.europa.eu/enterprise/sectors/ict/files/communication_key_enabling_technologies_sec1257_en.pdf

INV-2

EUROPEAN RESEARCH AREA INITIATIVES – SUPPORT INSTRUMENTS FOR MATERIAL SCIENCES

M. Bundule

Latvian Academy of Sciences

e-mail: maija.bundule@lza.lv

INV-3

SYMMETRY AND MODELS OF BN AND TiO_2 NANOTUBES

R.A. Evarestov[1], Yu.F. Zhukovskii[2]

[1]*Department of Quantum Chemistry, St. Petersburg State University, 26 Universitetsky Prospect, Petrodvorets, 198504, Russia,*

[2]*Institute of Solid State Physics, University of Latvia, Latvia*

e-mail: re1973@re1973.spb.edu

The formalism of line groups for one-periodic (1D) nanostructures with rotohelical symmetry analyzed in this study has been applied for construction of both BN and TiO_2 nanotubes (NTs). They are formed by rolling up the stoichiometric two-periodic (2D) sheets cut from the energetically stable surfaces. For boron nitride, we consider graphene-like (0001) monolayer cut from BN crystal of the most stable hexagonal phase [1]. For titania, we consider either three (O-Ti-O) or six (O-Ti-O_O-Ti-O) (101) layers cut from TiO_2 crystal of stable anatase phase [2]. After optimization of geometry the latter keeps the centered rectangular symmetry of initial slab while the former is spontaneously reconstructed to the hexagonal fluorite-type (111) sheet. We have considered the two sets of BN NTs with optimized monolayer structure which possess the pairs of hexagonal (*n*,*n*) and (*n*,*0*) chiralities, as well as four sets of TiO_2 NTs with optimized three- and six-layer structures, which possess the two pairs of either fluorite (*n*,*n*) and (*n*,*0*) or anatase (*-n*,*n*) and (*n*,*n*) chiralities, respectively.

To analyze both structural and electronic properties of nanotubes, we have performed *ab initio* LCAO calculations on boron nitride and titania both slabs and nanotubes, using the hybrid Hartree-Fock/Kohn-Sham exchange-correlation functional. The band gaps and strain energies of these nanotubes have been computed as functions of NT diameter. As to other nanotube properties, the main contribution to the chemical bonding in boron nitride is provided by B(2*s*), B(2*p*), N(2*s*) and N(2*p*) orbitals [1], whereas in titania, the O(2*p*)-Ti(3*d*) bond hybridization is a more pronounced although the six-layer TiO_2 NT structures are found to be more stable chemically [2].

References

1. Yu.F. Zhukovskii, S. Piskunov, N. Pugno, B. Berzina, L. Trinkler, and S. Bellucci, *J. Phys. Chem. Solids,* 2009, 70, 796-803.

2. A.V. Bandura and R.A. Evarestov*, Surf. Sci.,* 2009, 603, L117-L120.

INV-4

OXYGEN INCORPORATION REACTION INTO MIXED CONDUCTING ABO_3-TYPE PEROVSKITES FOR FUEL CELL APPLICATIONS

E. A. Kotomin[1, 2], Yu. Mastrikov[1, 2], R. Merkle[1], J. Maier[1]

[1]*Max Planck Institute for Solid State Research, Heisenbergstr.1, Stuttgart, Germany,*

[2]*Institute of Solid State Physics, University of Latvia, Kengaraga str. 8, LV-1063, Riga*

e-mail: kotomin@latnet.lv

Mixed conducting perovskites have been applied as cathode materials in solid oxide fuel cells (SOFC) since the early 1980s, and $La_{1-x}Sr_xMnO_{3\pm\delta}$ (LSM) was the first material which found wide application. Under certain conditions and despite its low ionic conductivity, the cathode process can become limited rather by the *oxygen incorporation surface reaction* than by the bulk oxygen transport. The mechanism of the oxygen incorporation reaction at the perovskite surface cannot be resolved from experiments alone.

An extensive set of DFT calculations on $LaMnO_3$ slabs is used here as a basis for the identification of the most probable reaction mechanism. MnO_2[001] is found to be the most stable surface termination. Chemisorption leading to O_2^-, O_2^{2-} and O^- species atop surface Mn ions is exothermic, but due to the negative adsorption entropy and electrostatic repulsion the coverages are low (upper limit in the percent range). The energy barrier for oxygen vacancy jumps is significantly lower in the surface layer (0.67 eV) compared to the bulk (0.95 eV). Interestingly, the complementary O^--species show a much higher (2 eV) barrier for surface diffusion and thus are essentially immobile.

Reaction rates for a number of steps in the reaction network were estimated, in order to identify the most probable reaction mechanism. Under typical SOFC conditions, a mechanism comprising the dissociation of adsorbed O_2^- or O_2^{2-} at the perfect surface is found to exhibit the fastest rate, but still the subsequent approach of $V_O^{\cdot}$ to O^- could be the rate-determining step. Thus, it is not only the concentration of oxygen vacancies which is important for fast oxygen incorporation, but the mobility is equally relevant. An "extrapolation" to complex $(La,Sr)(Co,Fe)O_{3-\delta}$ perovskites indicates that a slightly different mechanism is valid, and that the drastic increase of oxygen vacancy concentration is responsible for the higher reaction rates observed.

INV-5

AMAZING DIELECTRIC PROPERTIES AND STRUCTURE OF MANGANESE- DOPED $SrTiO_3$ CRYSTALS

V. Trepakov[1, 2], A. Badalyan[2], M. Savinov[1], A. Dejneka[1], L. Jastrabik[1], V. Zelezny[1], D. Nuzhnyy[1], I. Gregora[1], J. Petzelt[1], P. Galinetto[3], A. Skvortsov[2]

[1]*Institute of Physics AS CR, Czech Republic,*

[2]*Ioffe Physical-Technical Institute, Russia,*

[3]*GNISM and Dipartimento di Fisica "A. Volta", University Pavia, Italy*

e-mail: trevl@fzu.cz

Intriguing properties of Mn- doped $SrTiO_3$ (STO:Mn) are the subject of burning interest and debates today. Recent studies of STO:Mn revealed a series of very attractive properties such as strong dielectric relaxation, polar state emergence, high dielectric tunability, magneto-dielectric tunability etc. Nature of these effects, character and role of Mn- centres in STO are the subject of controversy being attributed to presence of polaronic type defects or Mn^{2+}(Sr) off-centres. Because the recognized amazing Mn-doping effects have been reported for ceramics only, the question is whether the reported intriguing properties are intrinsic features or originate from heterogeneous chemistry of STO:Mn ceramics.

To solve this uncertainty, we report on detail board band dielectric (10 Hz – 110 MHz, 90 – 150 GHz), spectroscopy, IR reflectivity (20-3300 cm^{-1}), Raman scattering, optical absorption and EPR spectroscopy experiments with high quality STO:Mn single crystals from Furuuchi Chemical Corporation. We found that the solubility of Mn impurities in STO is very low and the dielectric properties of STO:Mn crystals significantly differ from those in ceramics looking at the first glance not consistently enough. As a result, manifestations and the nature of Mn-doping dielectric effects in STO appear to be more complex and multiform than it was believed. The offered mechanisms of amazing STO:Mn properties consider the presence of inhomogeneities and peculiar nanostructure essentially inherent to STO:Mn crystals. Important role belongs to specific features of Mn- centers structure, charge transfer processes, localized hole- and polaronic centers formation.

INV-6

PROGRESS IN CHROMOGENIC MATERIALS AND DEVICES: NEW DATA ON THERMOCHROMIC VO_2-BASED MATERIALS AND ELECTROCHROMIC NICKEL-TUNGSTEN-OXIDE FILMS

C.G. Granqvist, S.V. Green, S.Y. Li, N.R. Mlyuka, G.A. Niklasson

Department of Engineering Sciences, The Ångström Laboratory, Uppsala University, P O Box 534, SE-75121 Uppsala, Sweden

e-mail: claes-goran.granqvist@angstrom.uu.se

Chromogenic materials change their properties under the action of an external stimulus. We first present new experimental data on thermochromic VO_2-based films and computed data on VO_2-based nanoparticles. In particular it is shown that a lower luminous absorptance can be obtained than with earlier known materials. Then we turn to electrochromic thin films and present new results on Ni-W-oxide-based films. The focus here is on enhanced values of the coloration efficiency. The final part discusses how thermochromics and electrochromics can be combined in order to achieve superior fenestration for energy efficient buildings.

INV-7

COMBINED LIGHT SCATTERING AND ACOUSTIC METHODS FOR THE STUDY OF GLASS MACRO- AND NANOSTRUCTURE

L. Maksimov[1], A. Anan'ev[1], V. Bogdanov[2], O. Yanush[3]

[1]*Research and Technological Institute of Optical Material Science,*

[2]*Saint Petersburg State University,*

[3]*Saint Petersburg State Technological University of Plant Polymers Saint Petersburg, Russia*

e-mail: maksimov@interglass.spb.su

The study is aimed at consideration of the approach to glass structure characterization based on the combination of Rayleigh and Mandel'shtam-Brillouin scattering (RMBS) spectroscopy and temperature dependent acoustic data and the results of specially processed Raman scattering (RS) spectra of inorganic glasses. RMBS contains information about both macroscopic parameters of a glass (elastic and elastooptic coefficients) and Rayleigh scattering losses caused by nano-scaled inhomogeneities "frozen-in' in the process of glass melt cooling [1,2]. Usage of electrochemical data, temperature dependences of ultrasonic velocity in glass melts and the Schroeder-Macedo formalism makes it possible to separate contributions of "frozen-in" concentration and density nanoinhomogeneities into Rayleigh scattering intensity. Novelty of RS application to glass study lies in the accurate measurement of RS bands intensities and processing of RS spectra series by the Walles-Katz and chemometrics techniques. Unchangeable spectral forms found in some glass forming systems are ascribed to the constant stoichiometry groupings the fluctuation concentrations of which determine Rayleigh scattering intensity in glasses.

References

1. J.Schroeder, *Light Scattering of Glass. Treatise on Material Science and Technology, 12, Glass 1, − New York, N.Y. Academic Press* 1977, 157-222.

2. V.Bogdanov et al., *Journal of Physics: Conference Series,* 2007, 93**,** 012033

INV-8

DOMAIN SWITCHING AND ROTATION IN ALKALI BISMUTH TITANATE LEAD-FREE PIEZOELECTRIC CERAMICS

T. Ogawa[1], M. Furukawa[2], T. Tsukada[2]

[1]*Department of Electrical and Electronic Engineering, Shizuoka Institute of Science and Technology, Japan,*

[2]*Materials and Process Development Centre, TDK Corporation, Japan*

e-mail: ogawa@ee.sist.ac.jp

Material research regarding lead free piezoelectric ceramics has been paid much attention because of global environmental considerations. The key practical issue is the difficulty to realized large piezoelectricity such as coupling factors and piezoelectric strain constants. A coupling factor (k) of is closely related to the orientation degree of ferroelectric domains through the DC poling process. In this study, the poling characteristics, especially DC poling field (E) dependence of dielectric and piezoelectric properties were investigated to evaluate the domains in bismuth titanate

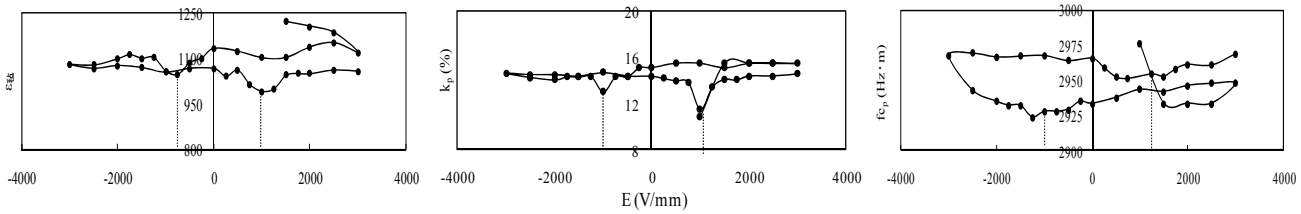

Fig. 1 DC poling field (E) dependence of dielectric constant (ε_r), planar coupling factor (k_p) and the frequency constant (f_{cp}) in 0.93($Na_{0.5}Bi_{0.5}$)TiO_3-0.07$BaTiO_3$ lead-free ceramics. Domain clamping accompanied with domain switching was observed at a specific E (dotted lines in figures).

lead-free ceramics in comparison with alkali niobate ceramics [1]. The domain switching was confirmed by the E to realize minimum dielectric constant ε_r, minimum k and maximum frequency constant (f_c) in Fig. 1, because of domain clamping. On the other hand, the domain rotation occurred at the E to obtain maximum ε_r and minimum f_c. These phenomena are observed in PZT ceramics as well as the lead-free ceramics.

This work was partially supported by a Grant-in-Aid for Scientific Research C (No. 21560340) from the Ministry of Education, Culture, Sports, Science and Technology, a Research Foundation Grant 2009 jointly sponsored by Academia and Industry of Fukuroi City, and the Murata Science Foundation 2009.

References

1. T. Ogawa, M. Furukawa, T. Tsukada, *Jpn. J. Appl. Phys.*, 2009, 48, 09KD07-1-5.

INV-9

THE FORMATION AND MODIFICATION OF NANOSTRUCTURES IN DIELECTRIC MATRICES USING SWIFT HEAVY IONS

V. Skuratov[1], I. Antonova[2]

[1]*Joint Institute for Nuclear Research, Dubna, Russia,*

[2]*Institute of Semiconductor Physics, SB RAS, Novosibirsk, Russia*

e-mail: skuratov@jinr.ru

High energy heavy ion beams are the unique tool for nanostructuring insulating solids in a controllable manner. Huge energy deposition in nanometer volume surrounding ion trajectory often leads to structural rearrangements not achievable by other methods. This report is a brief review of recent experimental studies of:

1) swift heavy ion irradiation effects on the structural and photoluminescence properties of silicon nanocrystallites embedded in a dielectric *(*SiO_2*)* matrix;
2) low-dimensional properties of the ordered arrays of Si nanocrystals in SiO_2;
3) irradiation induced shaping of the metallic or semiconductor nanoparticle and formation of metallic nanowires;
4) formation of low-dimensional structures on the surface of radiation-resistant insulators (Al_2O_3, $MgAl_2O_4$, ZrO_2) by single energetic ions.

INV-10

MULTIFUNCTIONAL HYDROGEN NANOSIZED MATERIALS: WO_3, MoO_3, V_2O_5.

A. Gavrilyuk

A.F. Ioffe Physical-Technical Institute of Russian Academy of Sciences, Sankt-Petersburg, Russia

e-mail: gavrilyuk@ioffe.mail.ru

The presentation concerns interesting effects in hydrogen nanosized materials: WO_3, MoO_3, V_2O_5.

Less-common properties of nanosized WO_3 thin films are highlighted, which make it possible either to achieve or to enhance photolysis in silver and cuprous halide films via the use of halide–WO_3 double-layer structures. First the WO_3 film provides photoinduced detachment of hydrogen atoms from organic molecules adsorbed on the oxide surface. The hydrogen atoms, being transferred into WO_3, turn into electrons and protons which migrate to the halide film forming sensitizing centers on the halide surface being illuminated simultaneously with the illumination of the WO_3 surface. This in turn gives rise to photolysis in the halide films. The nanosized WO_3 film makes it possible to trigger two famous surface photochemical reactions, first proton-coupled electron transfer between the hydrogen-donor molecules and the oxide surface, and then the photolysis of the halide, which radically changes the optical parameters of both the WO_3 and the halide films. The mechanism and the peculiarities of the process are discussed.

In the optical density spectra of nanosized MoO_3 films, the great difference was observed depending on the conditions of the illumination. The results obtained have been described with the help of the model, according to which, three kinds of centers arise due to hydrogen atoms in the series of transition metal oxide films: two paramagnetic centers $Mo^{5+}{}_b$ and $Mo^{5+}{}_s$ (bulk and surface), and one diamagnetic surface center [$Mo^{5+}{}_s$ $Mo^{5+}{}_s$] consisting of two $Mo^{5+}{}_s$ paired cations.

It is reported on the mechanism of the photo-induced hydrogen transfer between selected organic molecules and the surface of highly disordered V_2O_5 films at room and low temperatures, and the dramatic rearrangement in the oxide energy bands caused by the photoinjection of hydrogen: the part of the fundamental absorption edge attributed to electron transitions between π and π^* orbitals being eliminated, which yields giant changes in the optical parameters. The giant shift of the fundamental absorption edge in the V_2O_5 films exhibits differences at different temperatures. It has been also shown that the V^{4+} cations arising in material can exist in two states either as single V^{4+} cations or paired $V^{4+}V^{4+}$ dimers.

INV-11

LUMINESCENCE OF DENSE, OCTAHEDRAL STRUCTURED CRYSTALLINE SILICON DIOXIDE (STISHOVITE)

A.N. Trukhin[1], K. Smits[1], A. Sarakovskis[1], G. Chikvaidze[1], T.I. Dyuzheva[2], L.M. Lityagina[2]

[1]*Institute of Solid State Physics, University of Latvia, LV-1063, Riga, Latvia,*

[2]*L.F.Verechshagin Institute of High pressure Physics of RAS, Troitsk, Russia*

e-mail: truhins@cfi.lu.lv

It is obtained, that luminescence of stishovite single-crystals exists in as grown, non-irradiated samples. Three excimer pulsed lasers (KrF, 248 nm; ArF, 193 nm; F_2, 157 nm) were used for photoluminescence (PL) excitation Fig.1. Two PL bands were observed. One, in the UV range with maximum at 4.7±0.1 eV with FWHM equal to 0.95±0.1 eV, mainly seen under ArF laser. Another, in the blue range with maximum at 3±0.2 eV with FWHM equal to 0.8±0.2 eV, seen under all three lasers. The UV band main fast component of decay is with decay time constant τ= 1.3±0.1 ns in the range 16 - 150 K. The blue band possesses fast and slow component. The fast component of the blue band decay is ranging from 0.5 ns to 4 ns. The slow components of the blue band exhibits decay well corresponding to exponent with time constant equal to 17±1 μs within temperature range 16-200 K. The deviations from exponential decay were observes as well and explained by influence of nearest interstitial OH groups on the luminescence center. The UV band is not observed for F_2 laser excitation. For the case of KrF laser only a structure-less tail up to 4.6 eV was observed. Both the UV and the blue bands also were detected in recombination process. For UV band it is lasting in μs range of time, obeying to power law $\sim t^{-2}$. For blue band the decay is lasting to ms range of time with power law decay $\sim t^{-1}$. For the case of x-ray excitation we have strong drop down of luminescence intensity at 100 K which does not take place in the case of PL intensity. The activation energies for both cases are different as well. Average value of that is 0.03±0.01 eV for the case of x-ray and it is 0.15±0.05 eV for the case of PL. So the processes of thermal quenching are different for these kinds of excitation and, probably, are related to interaction of the luminescence center with OH groups. The nature of luminescence excited in the transparency range of stishovite is ascribed to a defect existing in the crystal after growth. Similarity of the stishovite luminescence with that of oxygen-deficient silica glass and induced by radiation luminescence of α-quartz crystal presumes similar nature of centers in those materials.

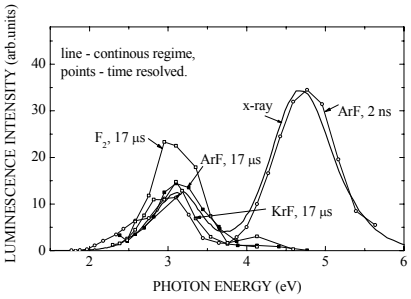

Fig.1 Luminescence spectra of dense crystalline silicon dioxide (stishovite) at 80 K, x-ray, ArF (193 nm), KrF (248 nm) and F_2 (157 nm) lasers excited.

INV-12

DEFECTS IN THE BULK AND ON THE SURFACES OF AMORPHOUS SILICON DIOXIDE

L. Skuja[1, 2], K. Kajihara[2, 3], M. Hirano[2], H. Hosono[2, 4]

[1]*Institute of Solid State Physics, University of Latvia, Kengaraga iela 8, LV1063 Riga, Latvia,*

[2]*Transparent Electro-Active Materials Project, ERATO-SORST, Japan Science and Technology Agency, in Frontier Collaborative Research Center, Mail Box S2-13, Tokyo Institute of Technology, 4259 Nagatsuta, Midori-ku, Yokohama 226-8503, Japan,*

[3]*Department of Applied Chemistry, Graduate School of Urban Environmental Sciences, Tokyo Metropolitan University, 1-1 Minami-Osawa, Hachioji 192-0397, Japan,*

[4]*Materials and Structures Laboratory & Frontier Collaborative Research Center, Tokyo Institute of Technology, 4259 Nagatsuta, Midori-ku, Yokohama 226-8503, Japan*

e-mail: skuja@latnet.lv

Due to its outstanding optical, dielectric and chemical properties, amorphous SiO_2 is one of technologically the most important amorphous oxide materials, widely used in fiber optic waveguides, silicon microelectronic chips and laser/UV optics. It is available in wide variety of nanosized forms as particles (aerogels, materials produced by sputtering), thin oxide films on silicon, nanowires, grown by oxidizing Si crystal or porous Si materials, self-organized nanotubes (MCM type materials), photonic crystals obtained by fiber drawing, etc. The properties of the nanomaterials are often dominated by their large surface and by the point defects and dangling bonds located on it. Given the large internal surfaces of amorphous SiO_2, there exists a deep similarity between the bulk and surface dangling bond-type defects in this material. The purposes of the present talk are: (i) to give a brief insight in the presently well-confirmed defects on the surfaces and bulk of SiO_2, and to characterize their similarities and differences, (ii) to report several recent experimental advances related to the optical properties of oxygen dangling bonds in deep ultraviolet region and their generation mechanisms by vacuum-ultraviolet F_2 laser photons. Dangling oxygen bonds are easily created by photolysis of silanol (Si-OH) groups and belong to the most optically and chemically active defect centers in SiO_2.

Abstracts of the oral presentations

OR-1

RESISTANCE SIMULATIONS FOR JUNCTIONS OF SW AND MW CARBON NANOTUBES WITH VARIOUS METAL SUBSTRATES

Yu.N. Shunin[1], Yu.F. Zhukovskii[2], S. Bellucci[3], N. Burlutskaya[1]

[1]*Information Systems Management Institute, Latvia,*

[2]*Institute of Solid State Physics, University of Latvia,*

[3]*INFN - Laboratori Nazionali di Frascati, Frascati (Rome), Italy*

e-mail: shunin@isma.lv

Basic attention is paid now to applications for carbon nanotubes (CNTs) of various morphology (which possess the unique physical properties) in nanoelectronics, *e.g.*, contacts of CNTs with other conducting elements of a nanocircuit, which can be considered as promising candidates for interconnects in a high-speed electronics. In this study, simulations of conductivity and resistivity are performed using the multiple scattering theory and effective media cluster approach for coherent potentials (CPA-EMA formalism) [1]. The main problems of the current stage of researches on resistance in CNT junctions with metal particles appear due to the influence of chirality effects in interconnects of SW and MW CNT with the fitting metals (Me = Ni, Cu, Ag, Pd, Pt, Au) for predefined CNT geometry. The main goal of this study is the implementation of advanced simulation models for construction of the nanocircuits containing CNTs and their junctions with metallic contacts. Using the model of *'effective bonds'* developed in current study in the framework of CPA-EMA formalism based on both scattering theory and Landauer theory, we can predict the resistivity properties for both SW and MW CNT-Me interconnects (see, Figs.1, 2). We have also developed the model of the inter-wall interaction inside the MW CNTs, thus estimating the transparency coefficient as the indicator of possible 'radial current' losses.

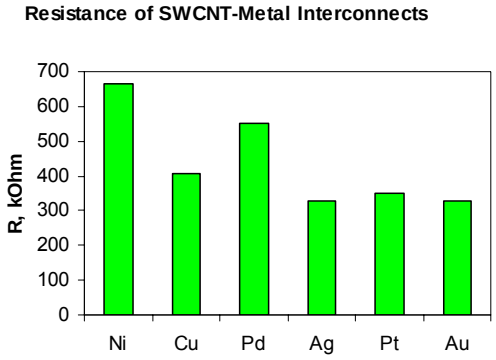

Fig.1 Resistance of various zigzag-type SWCNT-Me interconnects for the CNT diameter ~1 nm

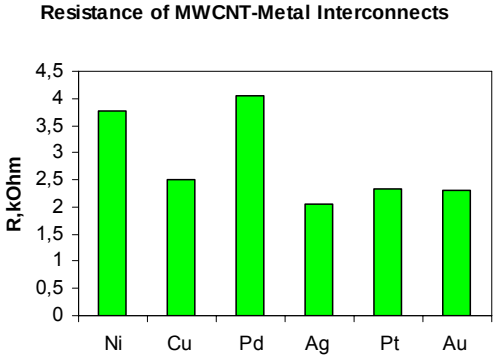

Fig.2 Resistance of various MWCNT-Me interconnects for the CNT

References

1. Yu.N. Shunin, Yu.F. Zhukovskii, S. Bellucci, *Computer Modelling and New Technologies*, 2008, 12, 2, 66-75.

OR-2

AB-INITIO MODELING OF OPTICAL AND ELECTRONIC PROPERTIES OF PURE AND RARE-EARTH IONS DOPED WIDE-GAP CRYSTALS UNDER VARYING HYDROSTATIC PRESSURE

M.G. Brik, I. Sildos, V. Kiisk, J. Kikas

Institute of Physics, University of Tartu, Riia 142, Tartu 51014, Estonia

e-mail: brik@fi.tartu.ee

In the present work we report on first-principles studies of the structural, electronic, optical and elastic properties of several groups of compounds: anatase and rutile TiO_2 (pure and Sm^{3+}-doped) [1]; $YAlO_3$ (pure and doped with different rare-earth ions) [2]; ternary semiconductors $CuXS_2$ (X=Al, Ga, In) [3], spinels $ZnGa_2O_4$ and $ZnAl_2S_4$. The CASTEP module of the Materials Studio package was used in all calculations. After having optimised the corresponding crystal structures, the band structure, total and partial densities of states, absorption spectra, dependencies of the refractive index on the wavelength, elastic constants were calculated and compared with available experimental data. Special attention has been paid to location of impurity's electronic states with respect to the band structure of the host. In addition, studies of pressure effects on the structural and electronic properties of materials were also performed; in particular, dependence of the unit cell volume on pressure was fitted to the Murnaghan equation of state to extract the values of the bulk moduli and their pressure derivatives, as shown, for example, in Fig. 1.

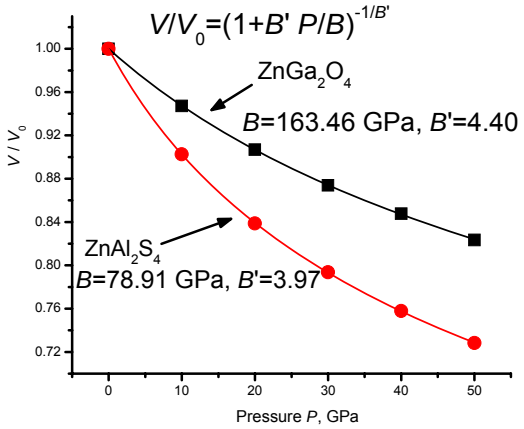

Fig.1 Relative volume change V/V_0 as a function of pressure (symbols) and fits to the Murnaghan equation (solid lines) for $ZnAl_2S_4$ and $ZnGa_2O_4$. Equation and parameters of fit are shown in the figure.

Acknowledgment: We thank Prof. Ü. Lille (Tallinn University of Technology) for allowing to use Materials Studio package.

References

1. M.G. Brik, I. Sildos, V. Kiisk (submitted)

2. M.G. Brik, *ECS Transactions*, 2009, 25, 25-37.

3. M.G. Brik, *J. Phys.: Condens. Matter*, 2009, 21, 485502.

OR-3

MODELING OF Au-Ni SURFACE ALLOY INSTABILITY

G. Zvejnieks[1], E.E. Tornau[2]

[1]*Institute of Solid State Physics, University of Latvia,*

[2]*Semiconductor Physics Institute, Lithuania*

e-mail: guntars@latnet.lv

Advances in surface growth technologies allows alloy formation out of two thermodynamically bulk-immiscible metals just in the surface layer, e.g., the Au-Ni surface alloy on Ni(111). However, it was found unstable at industrially relevant high CO pressures due to nickel carbonyl formation reaction [1].

The problem of phase separation in Au-Ni surface alloy at high CO pressures was studied in a simplified model [2], where the role of CO were neglected assuming that at high pressures the CO concentration on surface is saturated. This hinders the possibility to model experimentally observed Au-Ni alloy step flow rate dependence on CO pressure/concentration.

We propose the kinetic Monte Carlo model for Au-Ni separation in Au/Ni(111) surface alloy by taking into account CO adsorption and carbonyl formation reaction. We estimate both Au-Au, Ni-Ni and Au-Ni pair (v(Au-Au)=-0.08 eV, v(Ni-Ni)=-0.39 and v(Au-Ni)=-0.25) as well as trio interaction constants using *ab initio* calculations. The pair interactions satisfy the inequality $|v(Au-Au)|+|v(Ni-Ni)|<2|v(Au-Ni)|$, that ensures an increased Au concentration on step edge after relaxation, while being very close to the phase separation condition. We study the step flow rate dependence on trio Au-Au-Au in a line interaction which is one of the sensitive parameters (along with CO pressure and reaction rate) governing the process of nickel carbonyl formation.

References

1. E.K. Vestergaard et al, *Phys. Rev. Lett.*, 2005, 95, 126101.

2. V.P. Zhdanov et al, *Surf. Sci. Lett.*, 2006, 600, L260.

OR-4

LCAO CALCULATIONS OF (001) SURFACE OXYGEN VACANCY STRUCTURE IN Y-DOPED $BaZrO_3$

A. Bandura, R. Evarestov, D. Kuruch

Department of Quantum Chemistry, St. Petersburg State University, Russia

e-mail: andrei@ab1955.spb.edu

Y-doped $BaZrO_3$-based oxides are demonstrated to combine high stability with high proton conductivity. Trivalent Y^{3+} dopant can be incorporated into the $BaZrO_3$ by aliovalent substitution at Zr sites with forming of charge compensating oxygen vacancies. We study the formation of oxygen vacancy on (001) surface of Y-doped cubic $BaZrO_3$ using periodic PBE0 LCAO calculations via the CRYSTAL06 [1] computer code. The Stuttgart small-core pseudopotentials [2] have been used to reproduce the core-valence interactions of Ba, Zr and Y atoms. All-electron 8-411G(*d*) basis set is applied to O atoms, and it is retained at the lattice point of the expelled oxygen atom.

We model ZrO_2-terminated surface of cubic $BaZrO_3$ by the symmetrical 2D slab consisting of alternating 4 BaO and 5 ZrO_2 layers. To create vacancy, the surface oxygen atom is removed and two neighbouring Zr atoms are replaced by Y atoms. Using 2×2 and 3×3 surface supercells, two models have been constructed: (1) with a vacancy on one side of slab only; (2) with the vacancies on the both sides of slab (the inversion symmetry provides the equivalence of the both surfaces in this case). The different locations of dopant atoms near the vacancy are examined. Coordinates of all atoms were optimized, except the positions of middle-plane atoms in model (2). The vacancy formation energy E_{form} is calculated by the equation:

$E_{form} = (1/n)$ [E(Y-doped slab with O vacancies) + $2nE(ZrO_2) - E$(slab) – $nE(Y_2O_3)$], where n = 1 or 2 for models (1) and (2), respectively. The monoclinic ZrO_2 and cubic Y_2O_3 bulk crystal structure was fully optimized to calculate the energies $E(ZrO_2)$ and $E(Y_2O_3)$. The relaxation of the surface atoms is investigated and geometry of the most favorable surface vacancy-dopant configurations is established. Electronic properties of defective surfaces are analyzed basing on the calculated band structure and DOS. Both models in consideration produce close results. This justifies that the 9-layer slab chosen is sufficient to model the defective surface of $BaZrO_3$ crystal.

The authors are grateful for the support of RBRF (grant 08-03-00438-a).

References

1. R. Dovesi, et al., CRYSTAL06 User's Manual, University of Torino, Torino, 2006.

2. W. Kuechle, M. Dolg, H. Stoll, H. Preuss, *J. Chem. Phys.*, 1994, 100, 7535.

OR-5

FIRST PRINCIPLES CALCULATIONS ON OXYGEN IMPURITIES INCORPORATED IN THE VACANCIES OF UN(001) SUBSTRATE

D. Bocharov[1, 2, 3], D. Gryaznov[1], Y. F. Zhukovskii[1], E. A. Kotomin[1]

[1]*Institute for Solid State Physics, University of Latvia, Kengaraga 8, Riga LV-1063,*

[2]*Faculty of Computing, University of Latvia, Raina blvd. 19, Riga LV-1586,*

[3]*Faculty of Physics and Mathematics, University of Latvia, Zellu 8, Riga LV-1002*

e-mail: bocharov@latnet.lv

UN nitride fuel samples synthesized for reactors contain considerable amount of O impurities, which greatly affect the fuel properties in contrast to "traditional" UO_2 oxide where the problem with possible oxidation is absent. Thus, it is important to understand the mechanism of oxygen adsorption upon the uranium nitride and further penetration of O inside the substrate. In this study, we present results for the oxygen incorporation in uranium and nitrogen vacancies disposed on both the UN(001) surface as well as the subsurface and mirror planes inside the corresponding slab. We also analyze the total energy gain of this process.

To simulate the UN(001) surface, we construct various 3D slab models [1] as well as perform their DFT plane wave calculations using the formalism of projected augmented-wave (PAW) as implemented in the VASP computer code. The energy balance for O incorporation can be described using formula $I = E_{def} - (E_{vac} + E_O)$, where E_{def} is a negative total energy of defective supercell (with O impurity occupying either U or N vacancy), E_{vac} an energy of supercell containing a vacancy, and E_O that for O atom at infinity. Negativity of I value means that this process is energetically favourable. For O incorporation in U vacancy, I depends on the slab thickness, vacancy position and vacancy periodicity (2×2 and 3×3 supercell) changing within the limits of -2.7 to -5.4 eV. As to O incorporation in N vacancy, it is found to be energetically favorable: for different slab thickness, incorporation site and distribution periodicity I changes from -9.5 to -10.0 eV. Possibilities of further oxygen atom diffusion between the adjacent vacancies inside the UN(001) slab are discussed too.

References:

1. R.A. Evarestov, A.V. Bandura, M.V. Losev, E.A. Kotomin, Yu.F. Zhukovskii, and D. Bocharov, *J. Comput. Chem.*, 2008, 29, 2079-2087.

OR-6

FIRST-PRINCIPLES MODELING OF OXYGEN INTERACTION WITH ABO_3-TYPE PEROVSKITE SURFACES

S. Piskunov[1], E.A. Kotomin[1], Yu. Zhukovskii[1], V. Alexandrov[2]

[1]*Institute of Solid State Physics, University of Latvia, Riga,*

[2]*Department of Chemical Engineering and Materials Science and NEAT ORU, University of California, Davis, USA*

e-mail: piskunov@lanet.lv

Adsorption of gas-phase oxygen on the ABO_3-type perovskite surfaces is important for sensors, capacitors, photoelectrodes, photocatalysis, and fuel cell applications. The difficulties in distinguishing between adsorbed and lattice oxygen (unless the adsorbed species carry a net spin) result in a significant lack of experimental information about the oxygen adsorption processes occurring on perovskite surfaces. Furthermore, the results of *theoretical* simulations of oxygen adsorption on ABO_3 perovskites are very scarce in the literature.

Large scale parallel first-principles calculations based on density functional theory (DFT) employing two very different computer codes and approaches were used to study the energetics, geometry of fully relaxed structure, and the electronic charge redistribution for adsorbed atomic and molecular oxygen on defect-free unreconstructed $SrTiO_3(001)$ surfaces, both SrO- and TiO_2-terminated. The B3PW functional, used in the CRYSTAL code with atomic basis set, contains a ‘‘hybrid’’ of the DFT exchange and correlation functionals with exact non-local Hartree–Fock (HF) exchange. In its turn, the Generalized Gradient Approximation (PBE-GGA) was used in the plane-wave computer code VASP.

We performed calculations of two-dimensional 7 plane slabs with unit cells large enough for the adsorbed species to be treated as isolated. In particular, both types of calculations agree that the atomic oxygen is chemisorbed in the bridge position between the two adjacent metal and oxygen surface ions on both SrO- and TiO_2-terminated surface (>2.0 eV with respect to a free O atom) and migrates along the (001) axis with the activation energy ca. 1 eV. The surface O vacancies are much more mobile and thus control encounter with the adsorbed O atoms and oxygen penetration to the surface which is the limiting step for many applications to be discussed.

OR-7

ELECTRONIC, PHONON AND MAGNETIC STRUCTURE OF PURE AND Sr-DOPED $LaCoO_3$

D. Gryaznov[1, 2], R.A. Evarestov[3], E.A. Kotomin[1, 2], J. Maier[1]

[1]*Max Planck Institute for Solid State Research, Germany,*

[2]*Institute of Solid State Physics, University of Latvia,*

[3]*St. Petersburg State University, Russia*

e-mail: d.gryaznov@fkf.mpg.de

Mixed ionic-electronic conductor $(La,Sr)(Co,Fe)O_3$ is a promising cathode material for fuel-cell applications. Its main counter part, $LaCoO_3$, is a perovskite-type material with unusual properties which are presently a subject of many debates (e.g., [1]). In the present study we addressed its complex electronic and magnetic properties for cubic and rhombohedral $LaCoO_3$ phases using several DFT approaches. Namely, we applied the hybrid PBE0 functional and the so-called DFT+U method as implemented in LCAO code Crystal and plane wave code VASP, respectively. In our calculations, the Hubbard U-parameter was varied in order to analyze its impact on the calculated properties of $LaCoO_3$. We observed a stabilization of rhomobohedral non-magnetic phase only when the hybrid functional is used, in agreement with experimental findings. On the other hand, the ferromagnetic structure is more energetically favourable for the cubic phase of $LaCoO_3$ if the DFT+U method is used and $U < 2.0$ eV. Moreover, a standard DFT approach could be used.

The results are also supported by calculations of phonon modes obtained by using the frozen-phonon approach available in both codes. Classification of phonon states was done with the help of the site symmetry approach and induced representations of space groups. In addition, the formation energy of different super-structures when cubic $LaCoO_3$ is doped with Sr at different concentrations was calculated, and corresponding order-disorder transition temperatures were identified within the concentration wave theory.

References

1. G .Maris, Y. Ren, V. Volotchaev, C. Zobel, T. Lorenz, T. T. M. Palstra, Phys. Rev. B, 2003 67, 224423;

2. M. Zhuang, W. Zhang, N. Ming, Phys. Rev. B 57, 1998, 17, 10705

OR-8

AB INITIO CALCULATIONS OF $SrTiO_3$, $BaTiO_3$, $PbTiO_3$ AND $CaTiO_3$ (001) AND (011) SURFACES

R. I. Eglitis

Institute of Solid State Physics, University of Latvia

e-mail: reglitis@yahoo.com

While the (001) surfaces of $SrTiO_3$, $BaTiO_3$, $PbTiO_3$ and $CaTiO_3$ have been extensively studied, much less is known about the (011) surfaces [1-3]. On the (001) surfaces, we consider both AO (A=Sr, Ba, Pb or Ca) and TiO_2 terminations. In the former case, the surface AO layer is found to relax inward for all four materials with the sole exception of SrO-terminated $SrTiO_3$ (001) surface first layer O atom, while outward relaxations of all atoms in the second layer are found for both kinds of (001) terminations and for all four materials. The surface relaxation energies of BaO and TiO_2 terminations on $BaTiO_3$ (001) are found to be comparable, as are those of PbO and TiO_2 on $PbTiO_3$, as well as those of SrO and TiO_2 on $SrTiO_3$. In the first two cases the relaxation energy is slightly larger for TiO_2 termination, while in the last case it is larger for the SrO termination.

As for the (011) surfaces, we consider three types of surfaces, terminating on a TiO_2 layer, a Ba (Pb, Sr or Ca) layer and O layer. The surface relaxation energies for $BaTiO_3$, $PbTiO_3$, $CaTiO_3$ and $SrTiO_3$ (011) surfaces for all terminations are considerably larger than for (001) surfaces. Among the (011) surfaces, the relaxation energy is much larger for the TiO-terminated surface than for the Ba- or Pb-terminated surfaces for the $BaTiO_3$ and $PbTiO_3$ perovskites, but the relaxation energy for the Sr-terminated surface is larger than for the TiO-terminated surface in the case of $SrTiO_3$. We predict a considerable increase of the Ti-O chemical bond covalency near the $ATiO_3$ (011) surfaces as compared to both the bulk and the (001) surfaces.

References

1. R. I. Eglitis and D. Vanderbilt, *Physical Review B*, 2007, 76, 155439.

2. R. I. Eglitis and D. Vanderbilt, *Physical Review B*, 2008, 77, 195408.

3. R. I. Eglitis and D. Vanderbilt, *Physical Review B*, 2008, 78, 155420.

OR-9

TEMPERATURE DEVELOPMENT OF CHEMICALLY ORDERED NANOREGIONS IN RELAXOR FERROELECTRIC $Pb(Mg_{1/3}Nb_{2/3})O_3$ (PMN)

E. Klotins[1], A.I. Popov[1], V. Pankratov[1], L. Shirmane[1], D. Engers[2]

[1]*Institute of Solid State Physics, University of Latvia,*

[2]*Faculty of Physics and Mathematics, University of Latvia*

e-mail: klotins@cfi.lu.lv

The nature of regions with a special order is a central issue in understanding the complex structure of heterogeneous materials and especially ABO_3 perovskite based relaxor ferroelectrics $Pb(B_xB'_{1-x})O_3$ distinguished by local symmetry breaking and charge neutrality violation. Diffuse neutron scattering in PMN [1] supports the concept of polar nanoregions as presumably initiated by short-range chemical ordering of Mg and Nb cations which are located randomly in the B sites. A first principles study of chemically ordered supercells in PMN [2] reveal the crucial role of structural relaxation in the development of local symmetry breaking and gives an inspiring background for the statistical analysis as the objective of this work. The analysis is based on empirically modified effective Hamiltonian build of first principles superlattice parameters [2] and on the presumptions about invariance under permutations, pseudorandom distribution of polarization, and dipole-dipole interaction between 8x8x8 15-atom supercells. Instead of artificial "local fields" [3] the symmetry breaking emerges here exclusively as a natural consequence of first principles lattice dynamics. Both the polarization switching at reduced temperatures and the weak but definitive polarization of supercells at high temperatures are found in resemblance with diffuse neutron scattering results [1]. Another development goes beyond the linear theory and highlights the impact of intrinsic localized excitations [4] in the appearance of polar nanoregions vital for further understanding of the subject.

References

1. P. Gehring, et al., *Phys. Rev.B,* 2009, 79, 224109

2. S.A. Prosandeev,et al., *Phys. Rev. B, 2004,* 70 134110

3. B.P.Burton, et al., *Phase Transitions,* 2006, 79, 91-121

4. E. Klotins, *Physica E*, 2010, 42, 614-617

OR-10

ADVANCED MECHANICAL SURFACE TESTING FOR THIN COATINGS BY NANOINDENTATION, SCRATCH AND TRIBOLOGY INVESTIGATION

F. Davin

CSM Instruments, Switzerland

e-mail: francois.davin@csm-instruments.com

Thin films and coatings are becoming more and more evident and finding function in many different industrial applications. In order to simulate (and if possible extend) the service life of a particular system and to improve efficiency, it is important to characterize the material properties within the system. A variety of different instruments, techniques and methods are here presented for the principal characterization of the surface mechanical properties of various ranges: Nano Scratch, Nanoindentation and instrumentation for tribological studies.

Nanoindentation testing is achieved by pressing an indenter, usually a diamond of known geometry, into the test surface. During this indentation, penetration depth and applied load are monitored both during the insertion and withdrawal of the indenter. Using such a method called instrumented indentation, material hardness, elastic modulus, strain-hardening exponent, fracture toughness and viscoelastic behaviors of the surface can all be characterized.

Scratch testing is a versatile tool to evaluate the adherence, stress and strain between a coating and a substrate as a diamond stylus is passed over the surface with some normal load applied.

Tribological tests allow the study of friction, wear and lubrication and relate the interaction of two surfaces that are in interaction through a sliding motion.

OR-11

NANOPIPETTE APPLICATIONS IN BIONANOSCIENCE

R. de Leeuw[1], V. Shakel[2]

[1]*Park Systems Corp., Suwon, Korea,*

[2]*SIA Saint-Tech, Riga, Latvia*

e-mail: rdeleeuw@stinstruments.com

Nanopipettes, characterized by the nanoscale size of the pore at the tip, are of great interest because of their unique physicochemical properties and potential for various biomedical and biological applications. They find their primal use in SICM [1] (scanning ion conductance microscopy), a non-invasive form of the scanning probe microscopy family, which is capable of imaging live cells at high spatial resolution under physiological conditions. In combination with patch clamp, high resolution imaging together with electrophysiological studies on single ion channels are reported [2]. The nanopipette can be used to do local delivery of molecules to the cell surface [3] and its inner compartments [4] and can be extended to the study of live cell response to targeted chemical or drug stimulation. Recently, studies reporting label-free biosensing with functionalized probes show that non-labelled target molecules present in a liquid environment can be effectively detected using nanopipettes [5].

References

1. Hansma, P.K., Drake, B., Marti, O.,Gould, S.A. and Prater, C.B., *Science*, 1989, 243, 641-643.

2. Gorelik, J. et al., *Biophysics J.*, 2002, 83(6):3296-3303.

3. Bruckbauer, A, et al., *Biophysics J.*, 2007, 93:3120-3131.

4. Laforge, F.O., Carpino, J., Rotenberg, S.A., Mirkin, M.V., *Proc. Natl. Acad. Sci USA.*, 2007, 104:11895-11900.

5. Umehara S et al., *Proc. Natl. Acad. Sci USA*, 2009 24;106(12):4611-6

OR-12

NANOSCOPY AND –TECHNOLOGY USING SCANNING DUAL BEAM TECHNIQUES

V. Sammelselg[1, 2]

[1]*Institute of Physics University of Tartu, Estonia,*

[2]*Institute of Chemistry, University of Tartu, Estonia*

e-mail: vaino.sammelselg@ut.ee

The birth and development of nanotechnology is much initiated by the creation and development of new types of microscopes, and techniques based on these new equipment. In the 60-80s of former century the scanning electron microscopy and in 70-80s the focused ion beam technology were developed very intensively, but combined SEM-FIB equipment appeared in labs only in the end of 90s. Development of sub-nanometric electron and nanometric ion beams in the beginning of this century allowed creating real nanotechnological dual beam equipment that are able to characterize not only surface but also depths of the samples in nanometric scale, and help to create their 3D tomographic models. In addition, different nanolithographical techniques that can be realised on the equipment allow create new nanostructures on the surface of a sample or into it.

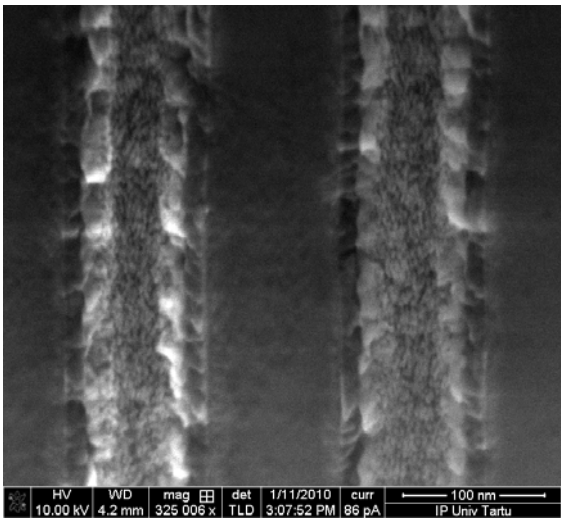

Fig.1 Visualization of thin metal oxide film grown to the inner walls of high aspect hollows. The structure is cut by FIB and studied in HR-SEM mode.

In the presentation the first results of usage of our new equipment Helios 600 NanoLab (FEI) for different nanotechnological studies will be given. Also brief comparison of the equipment with scanning probe microscopes will be done.

OR-13

ATOMIC LAYER DEPOSITION (ALD), ENCHANCED THIN FILMS

I. Ayala[1], N. Isomäki[1], I. Javaitis[2]

[1]*Beneq Oy, P.O Box 262, FI-01511 Vantaa, Finland,*

[2]*Armgate SIA, Liliju str. 20., Marupe, Latvia*

e-mail: israel.ayala@beneq.com

Atomic Layer Deposition (ALD) is a thin film deposition method with many unique features. ALD is done in gas phase and it is based on alternate saturating surface reactions. ALD is chemical vapor deposition (CVD) like coating method, but as distinct from CVD, in ALD process the precursor vapors are pulsed alternately into the reaction chamber. Precursors are pulsed one at a time and separated by purging periods. Each pulsing step saturates the surface with a monocular layer of precursor. As result of pulsing there is a unique self-limiting film growth mechanism with a number of advantageous features, such as conformality and uniformity [1].

ALD films deliver very unique features, such as capability to produce highly conformal pin-hole free films on complex structures and excellent adhesion to most surfaces. ALD's capability to produce these enhanced thin film coatings is often highly appreciated by researchers and industrial applications. Relatively low deposition temperatures and vacuum level in mbar range are also considered positive. The material selection is very wide, including numerous oxide and nitride materials as well as combinations and multilayer structures of these materials. Examples of these new ALD applications include barrier, anti-corrosion, wear resistant, optical and hard coatings aiming to improve the properties of existing products. ALD has been used for several years in semiconductor and display research and industry, and its industrial application scope is constantly growing.

References

1. Ritala M., Leskelä M., Atomic Layer Deposition, Handbook of Thin Film Materials, Vol. 1, Chapter 2., 2001.

OR-14

APPLICATION OF FREQUENCY DOMAIN THERMOREFLECTANCE

A. Schmidt[1, 2], R. Cheaito[1], M. Chiesa[1]

[1]*Masdar Institute of Science and Technology, Abu Dhabi UAE,*

[2]*Boston University, Boston, MA, USA*

e-mail: mchiesa@masdar.ac.ae

Photothermal phenomena have been successfully employed in the development of non-contact measuring techniques for the characterization of thin films or nano-structures. Frequency-domain methods based on a modulated laser heating source and time-domain methods built on a time delay between pulses from a pulsed laser heating source constitute two important classes of non-contact measuring methods. We present the versatility of a recently introduced frequency domain thermoreflectance (FDTR) method that combines the advantages of the two classes of measuring methods above mentioned 0. FDTR employs the same spot geometry and analysis approach as the time domain thermoreflectance (TDTR), but the frequency is the independent experimental parameter. By varying the modulation frequency one obtains a frequency domain measurement that yields the same parameters as TDTR with similar or improved sensitivity. This is illustrated in Fig. 1 for fused Silica. Both methods yield a thermal conductivity in accordance with the literature value. We present the versatility of the FDTR method by 1) determining the composition of layered media and their thickness and 2) characterizing metallic thin films on low conductivity substrates.

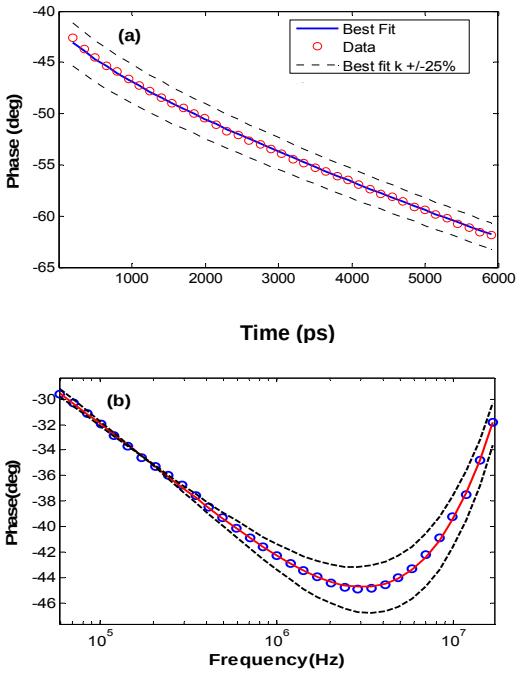

Fig.1 (a) TDTR @ 5MHZ (b) FDTR

References

1. A. J. Schmidt, R. Cheaito, M. *Chiesa Rev. Scie. Inst*, 2009, 80, 1-6.

OR-15

ASPECTS OF SEM ANALYSIS OF ABLATED TILES IN ASDEX UPGRADE TOKAMAK

J. Butikova[1], D. Jakovlevs[2], I. Tale[1]

[1]*Institute of Solid State Physics, University of Latvia,*

[2]*Riga Technical University*

e-mail: but@latnet.lv

The initial stages of the ablation crater formation in the graphite and tungsten-coated graphite tile from the ASDEX (Axial Symmetry Divertor EXperiment) Upgrade fusion reactor chamber were investigated using SEM imaging as a function of fluence and incident laser shot number.

SEM images of the both samples show that the interaction of intense light pulse with the surface together with formation of plasma results in development of dust particles on the surface of material. In the graphite tile, the dimension of the dust particles decreases with the increase of the crater depth. The bottom of the crater replicates the initial structure of the material.

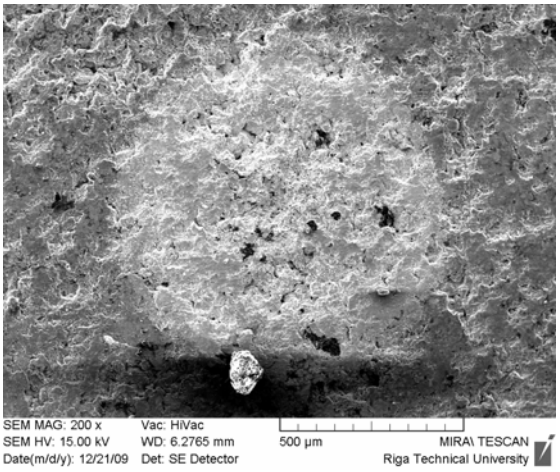

Fig.1 SEM image of a tungsten-coated sample exposed to 6 mJ laser pulse. A dust particle formed after the 3rd pulse

Laser ablation of the tungsten-coated sample results in creation of the dark spots, which expand as the number of the ablation pulses increase. This indicates that the part of tungsten layer is removed from the sample.

At high intensities of the laser pulse, a specific track around the edge of the crater was observed. This is most probably caused by the edge diffraction occurring during the ablation process [1].

References

1. B.Polyakov, G.Marcins, M.Chubarov, A.Kuzmin, V.Klykov, I.Tale, *Latv J.Phys.Techn.Sci*., 2009, 3, 50-54.

OR-16

REFLECTION HIGH ENERGY ELECTRON DIFFRACTION AS A TOOL FOR NANOPARTICLE DEPOSITION STUDIES

A. Voitkans[1, 2], A. Kleibert[2, 3], K.-H. Meiwes-Broer[2]

[1]*Institute of Solid State Physics, University of Latvia,*

[2]*Institute of Physics, University of Rostock, Germany,*

[3]*Swiss Light Source, Paul Scherrer Institut, Switzerland*

e-mail: andris.voitkans@lais.lv

Investigations on supported clusters have been an important direction in the field of nanotechnologies. Numerous methods have been developed for generation of nanostructures on surfaces, but deposition of preformed clusters provides almost any selection for the substrate and cluster material composition. Here the control of the magnetic, electronic and catalytic properties is of grate interest for future applications.

In this contribution we present *in situ* investigations on the orientation and structure of Fe nanoparticles deposited onto a W(110) surface. Our study is carried out reflection high energy electron diffraction (RHEED) [1]. Compared to X-ray based techniques RHEED has several advantages: (i) the wavelength of the probe can be easily adjusted, (ii) electrons have a much higher cross section and (iii) *in situ* experiments are feasible. Also the relative low costs of the experimental setup makes it suitable for daily work in laboratory conditions, as it does not require synchrotron radiation like in modern XPS and XRD studies. Our experiments prove that RHEED is a valuable tool for *in situ* investigations in cluster deposition experiments.

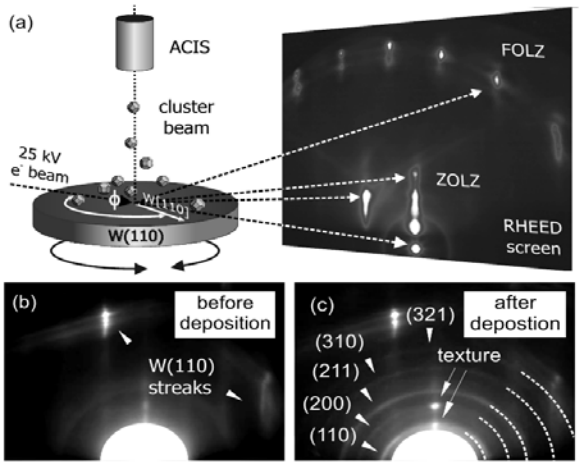

Fig. 1 (a) Experimental setup for in situ electron diffraction studies in a nanoparticle deposition experiment. The depicted diffraction pattern shows the zeroth (ZOLZ) and first order Laue zone (FOLZ) of the bare W(110) crystal surface. (b) Enlarged central section of a W(110) RHEED pattern before nanoparticle deposition. (c) Diffraction pattern after deposition of Fe nanoparticles with a diameter D = 20 nm.

References

1. A. Kleibert, A. Voitkans, and K.-H. Meiwes-Broer, PSS B, accepted.

OR-17

ENHANCED RELAXOR BEHAVIOUR IN EPITAXIAL FILMS OF LEAD MAGNESIUM NIOBATE

M. Tyunina, J. Levoska

Microelectronics and Materials Physics Laboratories, University of Oulu, Finland

e-mail: marinat@ee.oulu.fi

Large dielectric permittivity and effective piezoelectric coefficient exhibited by perovskite-type relaxor ferroelectrics, or relaxors (REs), sustain device oriented research of these materials. Compared to bulk ceramic or single-crystal REs, thin RE films are attractive for miniature devices but are much less studied and understood. Recently, the intrinsic low-frequency dielectric properties of epitaxial films of RE $PbMg_{1/3}Nb_{2/3}O_3$ (PMN) have been experimentally assessed and shown to noticeably differ from those of single-crystal PMN. In the films compared to bulk PMN, enhancement of RE behaviour has been evidenced by a profound increase of the empirical scaling factor. In order to clarify possible mechanism driving epitaxial films towards "stronger" RE state, the low-frequency dielectric properties of epitaxial PMN films are analyzed in more detail.

The response is interpreted as that of a composite consisting of "matrix" and "dipoles". Temperature dependence of the measured effective permittivity is explained by growth of the "dipolar" volume fraction on cooling. The "dipolar" relaxation time spectra are found to contain large fractions of fast relaxators which increase with decreasing film thickness. This is shown to explain the enhanced relaxor behaviour in the films. The peculiar fast "dipoles" are suggested to be influenced by film-substrate coupling.

OR-18

FIRST APPLICATION OF THE THERMAL NOISE METHOD FOR STUDYING FERROELECTRICS THIN FILMS

I. Shnaidshtein, P. Bednyakov

Lomonosov Moscow State University, Russia

e-mail: shnaidshtein@phys.msu.ru

In recent years the interest for ferroelectric thin films steadily increases. But there are a number of problems during their research. In particular, measurement of initial dielectric susceptibilities of thin films requires applying of the very small electric field. When the classical bridge method is used, the restrictions on reductions of measuring electric field appears.

We used a thermal noise method for the decision of this problem. The original automated experimental setup has been created for study of temperature dependences of dielectric properties. We carried out a number of comparative measurements for demonstration of advantages of a thermal noise method against a bridge method.

In our presentation the experimental data on barium titanate crystal grown by different technologies are discussed. We have bulk crystals of different quality, polycrystalline and epitaxial thin films. We carried out experimental investigation of each sample using both a classical bridge method and a thermal noise method.

The most interesting results are received when we compare the data obtained for epitaxial films. In this case there is significant difference in temperature and frequency dependencies of the dielectric susceptibility obtained by various methods.

This work is supported by Russian Foundation for Basic Research (project of №08-02-01010).

OR-19

INFLUENCE OF NATURAL AGING ON THE POLARIZATION PROFILE IN PZT-BASED CERAMICS

O.V. Malyshkina[1], A.A. Movchikova[1], E.V. Barabanova[1], A. Belousov[1], I.A. Embil[2], S.I. Pugachev[2]

[1]*Tver State University, Tver, Russia,*

[2]*State Marine Technical University of St. Petersburg, St.- Peterburg, Russia*

e-mail: Olga.Malyshkina@mail.ru

In parallel with the increase in the development of thin-film functional materials there also has been a rise in the application of bulk piezoceramics in medical instruments, hydroacoustics and other ultrasonic devices. In this view it is of special interest to possess information on how long do polarized ceramics conserve their initial state.

In the present work the effect of natural aging on the polarization state of PZT and PZT(75%) +BZT(25%) (PBZT) has been studied. The polarization profile was examined with the thermal square wave method (TSWM) [1, 2]. It is shown that during the natural aging process the polarization value in the centre of the samples is smaller than at the depth of 0.25 of the sample thickness for both types of ceramics, although no asymmetry is observed in the general shape of polarization profile. At the same time there is a tendency for PZT samples to increase their polarization at the expense of the migrational polarization contribution, in contrast to its decrease in PBZT. Apparently this is related to the introduction of barium titanate (BT) into the PBZT composition. Thus the results of the present study indicate that PZT is more stable with respect to aging in comparison with BT.

This work was performed within the Federal Target Program "Research and Research-Pedagogical Personnel of Innovation Russia for 2009-2013" and supported by the Russian Foundation for Basic Research, project no. 08-02-97502-r_centre_a.

References

1. O.V. Malyshkina, A.A. Movchikova, G. Suchaneck, *Physics of the Solid State*, 2007, 49, 2144–2147

2. O.V. Malyshkina, A.A. Movchikova, *Physics of the Solid State*, 2009, 51, 1381–1384.

OR-20

BROADBAND DIELECTRIC SPECTROSCOPY OF FERROELECTRIC $(1-x)Al_{0.9}Li_{0.1}NbO_3 - xBi_{0.5}K_{0.5}TiO_3$ CERAMICS

J. Pozingis[1], J. Banys[1], J. Macutkevic[2], R. Adomavicius[2], A. Krotkus[2], D.C. Lupascu[3]

[1]*Department of Radiophysics, Vilnius University, Sauletekio9, Vilnius, Lithuania,*

[2]*Institute of Semiconductor Physics, Gostauto 11, Vilnius, Lithuania,*

[3]*Institute for Materials Science, University Duisburg-Essen, Essen, Germany*

e-mail: jan@pfi.lt

Lead based relaxor ferroelectric single crystals and ceramics with the perovskite structure, like PMN, PZN, PLZT and PMN-PT have been widely studied and met promising applications e.g., as very efficient piezoelectric materials. Nowadays, is generally accepted that diffusive and frequency dependent dielectric anomaly in relaxors is caused of dynamics of polar nanoregions, with appears near the Burns temperature (T_B). Due a toxicity of lead one very important topic is searching of lead free relaxor ceramics and crystals, which exhibit piezoelectric properties similar to PMN-PT. On the other hand the investigations of broadband dynamics of polar nanoregions are rather, because it is very difficult to perform dielectric investigations of relaxors in frequency range 1 GHz – 1 THz near and below T_B. In this work we presented dielectric properties of $(1-x)Al_{0,9}Li_{0,1}NbO_3 - xBi_{0,5}K_{0,5}TiO_3$ (ALNBKT) ceramics in very wide frequency (20 Hz – 2 THz) and temperature ranges (500 K – 20 K). The dielectric dispersion of investigated ceramics appears in microwave and THz frequency range at high temperatures. On cooling the dielectric dispersion becomes broader and it splits into two parts below the dielectric permittivity maximum temperature at 1 kHz. The low frequency dielectric dispersion part anomalously slows down and at low temperatures its part appears without our frequency range. However, the high frequency part remains at microwave and THz frequencies. The distribution of relaxation times has been calculated from the dielectric spectra. The longest relaxation times diverge according to the Vogel-Fulcher law, while the most probable relaxation time diverges according to the Arhenius law. Such dielectric behaviour is typical for ferroelectric relaxors. At very low temperatures (below 100 K) the relaxation dielectric dispersion almost vanishes in THz range. Here the resonant soft mode was observed. The microscopic origin of polar nanoregions in lead free $(1-x)Al_{0,9}Li_{0,1}NbO_3 - xBi_{0,5}K_{0,5}TiO_3$ relaxors is discussed.

OR-21

DESCRIPTION OF RELAXOR STATE IN $Na_{1/2}Bi_{1/2}TiO_3$-$SrTiO_3$-$PbTiO_3$ SYSTEM OF SOLID SOLUTIONS

M. Dunce, E. Birks, M. Antonova, M. Kundzinsh

Institute of Solid State Physics, University of Latvia, Latvia

e-mail: marija.dunce@lais.lv

The dielectric properties of ferroelectric relaxors are traditionally described, assuming:

- temperature dependence of static dielectric permittivity, which is characterized by its continuous increasing, if temperature is decreased;
- continuous distribution function of relaxation times $g(\ln\tau)$ in range between τ_{min} and $\tau_{cut\text{-}off}$, where temperature dependence of $\tau_{cut\text{-}off}$ follows Vogel-Fulcher law, diverging at a definite temperature $T_f<T_m$ (T_m – temperature of maximum of dielectric permittivity).

This interpretation is based on relaxation of polar microregions in multiwell potential in presence of external electric field. The divergence of relaxation times or freezing is explained as result of unlimited increasing of interaction between these microregions. Among behaviour, inherent for such concept, there are appearance of maximum in temperature dependence of dielectric permittivity and its temperature shift, depending on frequency of measuring field. Since such the relaxation mechanism does not contribute to dielectric permittivity at $T<T_f$, other mechanisms are needed to explain the experimentally stated relaxation at low temperatures.

In this work it is shown that the behaviour of relaxation is the same both above, and below T_f. From such a point of view it follows that real freezing in ferroelectric relaxors does not occur, instead continuous increasing of $\tau_{cut\text{-}off}$ is expected, if temperature decreases in all temperature range below maximum of dielectric permittivity. Temperature dependence of the parameters, describing relaxation, introduced earlier for low temperature region [1], contains information about static dielectric permittivity and $\tau_{cut\text{-}off}$. As well as previously developed models, this concept for the present time does not explain the nature of distribution of relaxation times.

References

1. Cheng Z.-Y., Katiyar R.S., Yao X., Guo A., *Phys.Rev. B*, 1996, 55, 8165

OR-22

COMPUTER MODELING OF CHROMOPRHORE/POLYMER COMPOSITE POLARIZATION: PARA- , ANTIFERRO- AND FERROELECTRIC BEHAVIOR

M. Rutkis, A. Jurgis

Institute of Solid State Physics, University of Latvia, Riga, Latvia

e-mail: martins.rutkis@cfi.lu.lv

Over last two decades there is a stable interest to make use of organic molecular materials in a wide variety of NLO applications. One of the possibilities to create a material for these applications, like EO modulators, is to disperse NLO active chromophores in polymer matrix ("host/guest") or to attach them to polymer backbone ("grafted"). To act in an NLO material chromophores must be acentrically aligned, what is generally achieved by applying an external electrical poling field. Calculating, from first principles, the extent of the alignment and via this NLO efficiency of material has proven to be challenging. One approach to solve this problem is pure analytic statistical mechanics treatment [2], what could be enhanced by Monte Carlo (MC) statistical mechanical modelling [3]. Disadvantage of these statistical mechanical methods is impossibility to get some insight in poling (relaxation) dynamics. Observation of the time evolution of a system is possible by fully atomistic molecular modelling employing classical force field molecular dynamic (MD) methods [4]. Unfortunately, in case when polymer and chromophores are represented at atomistic level, MD approach requires huge amount of computations. One of the solutions is to reproduce the motion of the molecules of interest (chromophores) using Langevin dynamics (LD). This method simulates the effect of molecular collisions and the resulting dissipation of energy that occur in real host, without explicitly including host molecules. In this contribution, we would like to present results of our LD simulations of the systems modelling "host/guest" and "grafted" NLO polymers. Chromophore load, dipole moment and poling field impact on alignment and relaxation dynamics as well as polarization loops of systems will be presented.

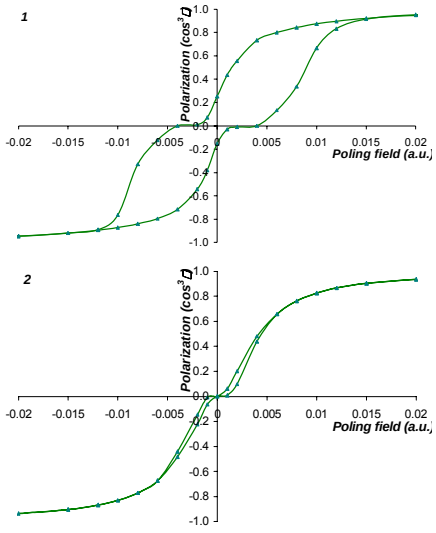

Fig.1 LD simulation of polarization:
1 - Ferroelectric behavior of "host/guest" NLO polymer;
2 - Paraelectric behavior of "grafted" NLO polymer.

References:
1. L. R. Dalton, *J. Phys.: Condens. Matter 15, R897–R934, (2003)*
2. A. Piekara, *Proc. R. Soc. London, A 1939, 172, 360.*
3. R. D. Nielsen, H. L. Rommel, and B. H. Robinson, *J. Phys. Chem. B 2004, 108, 8659-8667*
4. M. R Leahy-Hoppa, P. D. Cunningham, J. A. French, L. M. Hayden, *J. Phys. Chem. A 2006, 110, 5792.*

OR-23

FAST ELECTRON SWITCHING IN DIELECTRICS

H.-J. Fitting

Institute of Physics, University of Rostock, Universitaetsplatz 3, D-18051 Rostock, Germany

e-mail: hans-joachim.fitting@uni-rostock.de

First investigations of time-dependent transport are made for secondary electrons (SE) relaxation and attenuation by means of Monte Carlo simulations, [1]. These MC calculations of ballistic electron scattering in dielectrics are based on interactions with optical and acoustic phonons as well as on impact ionization of valence band electrons, i.e. the creation of so-called tertiary electrons (TE) and cascading. The strongest cooling of SE occurs over femtoseconds and is given by the latter process of cascading whereas the electron-phonon scattering leads to slower attenuation, see Fig.1.

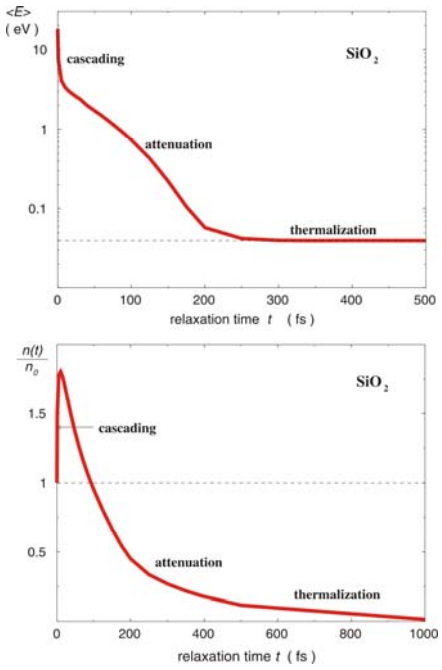

Fig.1 Mean energy <E> and rate $n(t)/n_0$ of SE in silica.

The electron beam induced selfconsistent charge transport and secondary electron emission in insulators are described by means of an electron-hole flight-drift model (FDM) implemented by an iterative computer simulation, [2,3]. Ballistic secondary electrons and holes, their attenuation and drift, as well as their recombination, trapping, and field- and temperature-dependent Poole-Frenkel detrapping are included, [3]. As a main result the time dependent spatial distributions of currents $j(x,t)$, charges $\sigma(x,t)$, field $F(x,t)$, as well as, the secondary electron emission rate $\sigma(t)$ and the surface potential $V_0(t)$ are obtained. Whereas the switching-on of the secondary electron emission proceeds over milli-seconds due to selfconsistent charging the switching-off process occurs much faster, even over femto-seconds and is described more detailed in Ref. [4]. Thus a rapid electron beam switching becomes possible with formation of ultra-short electron beam pulses offering an application in stroboscopic electron spectroscopy and microscopy.

References

1. E. Schreiber, H.-J. Fitting, *J. Electron Spectroscopy & Rel. Phenomena*, 2002, 124, 25 – 37.

2. X. Meyza, D.Goeuriot, C.Guerret-Piécourt, D.Tréheux, H.-J.Fitting, *J. Appl. Phys.*, 2003, 8, 5384.

3. N. Cornet, et.all, *J. Appl. Phys.*, 2008, 103, 064110.

4. H.-J. Fitting, M. Touzin, *J. Appl. Phys.,* 2010 submitted.

OR-24

SILICON BASED NANOPARTICLES USAGE AS ADJUVANTS FOR TREATMENT OF VIRAL INFECTIONS

Yu. Dekhtyar[1], A. Kachanovska[1], A. Patmalnieks[2], P. Pumpens[3], R. Renhofa[3],
M. Romanova[1], D. Skrastina[3]

[1]*Riga Technical University, Biomedical engineering and nanotechnologies institute, Latvia,*

[2]*Univeristy of Latvia,*

[3]*Biomedical research and study centre, Latvia*

e-mail: marina.romanova@inbox.lv

Immunomodulation is a new kind of viral infection treatment where molecular agents that are injected inside patient organism stimulate immune system to respond effectively to a viral infection. It is important to deliver immune response-modulating (IM) agents exactly to target cells thus reducing their overall concentration in organism of the patient, which could otherwise lead to side effects. It is possible to use nanocarriers (adjuvants) that are able to pack many IM agents for this purpose. Possible use of Si-n, Si-p and SiO2 nanoparticles as adjuvants was studied in this work. Four different types of virus-like particles (VLP) were used as IM agents. The systems Si based nanoparticle – VLP were created. The systems were studied by means of spectrophotometry as well as by electron and fluorescent microscopy. The study showed that Si-n, Si-p and SiO2 nanoparticles can be used as nanocarriers for corresponding VLP. VLP packing properties depend on the surface charge of both VLP and nanoparticle. Vaccination of animals with the SiO2 nanoparticle – Hepatitis B virus VLP system resulted in twelve-time increase in antibody synthesis.

References

1. Virus particle explorer, Human Hepatitis B Viral Capsid, http://viperdb.scripps.edu

2. Chen He-sheng, Sun Zhen-ya, Xue Li-hui, , *Journal of Wuhan University of Technology--Materials Science Edition*, 2004, 19, 4.

3. C.Sealy, *Nanotoday*, 2006, 1, 2.

OR-25

EXPERIMENTS ON APPLICATION OF HIGH POWER MICROWAVE RADIATION TO BIOMEDICINE USING MICRO- AND NANOPARTICLES

S.I. Tyutyunnikov[1], S.P. Besedin[2], A.K. Kaminsky[1], O.V. Komova[1], E.A. Krasavin[1], I.A. Krjachko[1], E.A. Perelstein[1], S.N. Sedykh[1], V.N. Shaljapin[1], N.L. Shmakova[1]

[1]*Joint Institute for Nuclear Research, Dubna, Moscow region, Russia,*

[2]*Russian Scientific Center "Kurchatov Institute", Moscow, Russia*

e-mail: tsi@sunse.jinr.ru

High pulsed power microwave radiation gives new possibilities in the biomedicine, particularly to cancer cell damage study. Cooperative influence of microwaves and conducting micro- or nanoparticles provides local and selective action of microwaves on cancer cells. First results of JINR successful experiment are reported on cancer cells killing with the help of high power microwaves propagating through the thin gold layer. The microwave source was the JINR free electron maser with the power of 20 MW and frequency of 30 GHz. The microwave fluence was about 1 J/cm^2 during cell irradiation, number of pulses was 300 -1000. In the culture medium there are the cancer cells located on an object glass near the golden layer. The cell disruption was observed through 30-60 minutes after irradiation. The cells leaved the glass in the form of large conglomerates. Through 12 hours there were no irradiated cancer cells on the object glass. The preliminary studies of processes leading to cancer cell damages were performed to estimate the perspective of such technique.

OR-26

SYNTHESIS, STRUCTURE AND ADSORPTION PROPERTIES OF ORDERED MESOPOROUS ORGANOSILICAS FUNCTIONALIZED WITH DIFFERENT GROUPS

M. Barczak, D. Pietras-Ożga, S. Pikus

Maria Curie-Sklodowska University, Maria Curie-Skłodowska Sq. 3, 20-031 Lublin, POLAND

e-mail: mbarczak@umcs.pl

Ordered mesoporous organosilicas are very attractive materials due to their high surface areas, large volumes of ordered mesopores and diverse morphology what makes them attractive potential catalysts and adsorbents. From the other hand the possibility of introduction of the organic groups into the ordered structure of the final material during the synthesis is an invaluable advantage of the sol-gel processing of organosilicas. In the present work channel-like mesoporous organosilicas (SBA-15) were synthesized via co-condensation of tetraethyl orthosilicate (TEOS) with alkoxysilanes bearing terminal thiol-, vinyl-, phenyl- and cyano- groups in the presence of Pluronic P123 triblock copolymer.

Obtained SBA-15 materials were characterized by infrared spectroscopy, powder X-ray diffraction, thermogravimetry and nitrogen sorption measurements. The resulted materials exhibit well-ordered mesoporous structure, high values of specific surface areas and pore volumes and a high content of vinyl and phenyl surface groups introduced during co-condensation. The sizes of ordered mesopores are in the range of 6-10nm. It was establish that even small amount of alkoxysilanes substantially changes the properties of the final materials so cocondensation can be used not only to introduce the surface functional groups but also to modify the structural-adsorption characteristics of the resulted materials.

This work has been supported by Polish Ministry of Higher Education and Science under Grant No. N N204 111135. BASF is also acknowledged for providing free samples.

OR-27

MODIFICATION OF SETTING PROPERTIES OF α-TRICALCIUM PHOSPHATE CEMENTS

Z. Irbe, L. Vecbiskena, L. Berzina-Cimdina

Riga Technical University, Riga Biomaterials Innovation and Development Centre

e-mail: zilgma.irbe@rtu.com

Calcium phosphate bone cements are widely investigated biomaterials for bone repair in non-load bearing sites. Advantages of calcium phosphate bone cements are bioactivity, biocompatibility and hardening *in situ*. The hardening properties of calcium phosphate cements are highly important for clinical application. There are works focused on the use of citrate and pyrophosphate ions as setting retarders for brushite-tetracalcium phosphate and β-tricalcium phosphate-phosphoric acid cements [1, 2]. In this work the hardening process α-tricalcium phosphate (α-TCP) cements is investigated, modified by two additives – citrate ions and pyrophosphate ions.

The cement was considered set, when it could bear the weight of 267g indentor needle with 1mm diameter. Phase composition and morphology of cements was determined using X-ray diffractometry, Fourier-transform infrared spectrometry and scanning electron microscopy.

Presence of phosphate ions is necessary for setting of α-TCP cements. The setting time is dependent both on phosphate ion concentration and initial pH of liquid component. The influence of citrate and pyrophosphate ion additives on setting properties strongly depends on pH of the liquid phase. Cement with 0.5 M of phosphate ions in liquid phase and with initial pH 7 set in 8 min without additives, in 15 min with addition of 0.01 M pyrophosphate ions and in 13 min with addition of 0.1 M citrate ions. By using suitable additives α-TCP cements with controllable setting properties and with initial pH of liquid component near physiological pH can be obtained.

References

1. S.V.Dorozhkin, *J.Mater.Sci*., 2008, 43, 3028-3057.

2. M.Bohner, H.P.Merkle, P.van Landuyt, G.Trophardy, J.Lemaitre, *J.Mater.Sci.Mater.Med*., 2000, 11, 111-116.

OR-28

PREPARATION AND SINTERING BEHAVIOUR OF β-TRICALCIUM PHOSPHATE

K. Salma, N. Borodajenko, L. Pluduma, V. Zalite, L. Berzina-Cimdina
Riga Biomaterials Innovation and Development Centre, Riga Technical University, Latvia
e-mail: kristine.salma@rtu.lv

The sintering behavior of β-tricalcium phosphate [β-TCP, $Ca_3(PO_4)_2$] was investigate. β-Tricalcium phosphate powders were synthesized by modified wet chemical method – precipitation from aqueous medium by slow addition of orthophosphoric acid solution to a calcium hydroxide suspension [1]. The ending pH value of the suspension was stabilized in the range of 5-7 at ambient temperature. Synthesized powders were uniaxially pressed in cylindrical tablets and sintered at temperatures ranging from 700 to 1300°C for 1 h.

The morphology and microstructure, functional group analysis, phase composition and transformation, thermal stability of synthesized and sintered samples were investigate by XRD, FT-IR, FE-SEM, DTA and optical dilatometry.

The study shows that the ending pH of precipitation medium considerably influences the composition of synthesized powder, especially hydrogen phosphate (HPO_4^{2-}) ions content and the hydroxyapatite or calcium pyrophosphate phase formation after sintering. The phase composition significantly affects the physical characteristics of synthesized β-TCP powders, especially microstructure and thermal stability. The highly thermally stable (up to 1300ºC) β-TCP bioceramic can be successfully synthesized by room synthesis temperature and acidic ending pH 5.

References

1. K.Salma, N.Borodajenko, A.Plata, L.Berzina-Cimdina, A.Stunda, *14-th Nordic-Baltic Conference on Biomedical Engineering and Medical Physics, the IFMBE Proceedings Series*, 2008, 68-71.

OR-29

STRUCTURE OF PHOSPHATE BASED BIOACTIVE GLASSES

A. Stunda, L. Berzina-Cimdina

RTU Riga Biomaterials Innovation and Development Centre, Riga, Latvia

e-mail: agnese.stunda@rtu.lv

Phosphate based bioactive glasses and glass-ceramics are very promising materials for biomedical applications. Calcium phosphates glasses are closer to chemical composition of human bone than silicate glasses and are better soluble than hydroxyapatite ceramics. Glass solubility (and bioactivity) depends on glass structure. The aim of this research was to summarize literature about structures of phosphate based glasses and glass ceramics and their solubility. Then, against this background, predict solubility of synthesised samples and to single out glasses with high and low solubility for further biomedical research.

There is a number of works that determine glass structure by ^{31}P NMR analysis [1, 2, 3]. The structure of glass can be represented using Q^n terminology, where n represents the number of bridging oxygen atoms per PO_4^{3-} tetrahedron. The number of bridging oxygen atoms depends on M_2O (or MO) and P_2O_5 ratio in composition [2, 3]. The bridging oxygen theory explains that as more bridging oxygens, as longer chains and cross linking starts, though as more bridging oxygens, as better chemical durability. Inverted glasses with Q^0 and Q^1 structure (orthophosphates PO^{4-} and pyrophosphates $P_2O_7^{4-}$) are the most soluble, Q^2 – (metaphosphates PO_3^-) are less soluble, and ultraphosphates with Q^3 structure have 3-dimensional network and are the most inert structures and are not discussed in literature as bioactive material.

It should be taken into consideration that bivalent cation oppose to monovalent cation are ionic cross-links between chains, though monovalent cation increases solubility comparing to bivalent one [2, 3]. Monovalent cations are usually alkaline; this means that they tend to hydrolyse – this is another reason of increasing solubility [3].

Analysed samples contain β-$Ca_3(PO_4)_2$, $Ca_{10}Na(PO_4)_7$, $Ca_2P_2O_7$ and also $Na_4(Nb_8P_4O_{32})$, $NaNbO_3$ in various proportions; solubility of these phases can be put in a decreasing order: $Ca_{10}Na(PO_4)_7$ > β-$Ca_3(PO_4)_2$ > $Ca_2P_2O_7$ > $NaNbO_3$ > $Na_4(Nb_8P_4O_{32})$. The main advantage of this is that niobium which should increase mechanical strength of glass is not in almost insoluble phases.

References

1. T.Kasuga, *Acta Biomaterialia,* 2005, 1, 55-64.

2. Marikani et al, *Journal of Non-Crystalline Solids,* 2008, 354, 3929-3934.

3. H.A.ElBatal, *Ceramics International,* 2009, 35, 1195-1204.

OR-30

DEFECTS AND NANOCHANNELS IN DOPED ZINC OXIDE NANORODS GROWN BY THERMAL METHODS

Y. Ortega[1, 2], Ch. Dieker[1], W. Jäger[1], P. Fernández[2], J. Piqueras[2]

[1]*Microanalysis of Materials, Christian-Albrechts-University of Kiel, Germany,*

[2]*Department of Materials Physics, Universidad Complutense de Madrid, Spain*

e-mail: piqueras@fis.ucm.es

The study of low dimensional ZnO structures is a subject of increasing interest due to their potential applications in fields such as nanoelectronics, optical nanodevices, gas sensing, catalysis and others. In this work, Sn and Al doped ZnO nanorods have been grown by a thermal evaporation-deposition method and their defect structure has been investigated by transmission electron microscopy. The nanorods have been also characterized by X-ray diffraction, scanning electron microscopy, energy dispersive spectroscopy and cathodoluminescence.

Mixtures of ZnO and SnO_2 powders or of ZnO and Al_2O_3 powders were used as precursors of the Sn doped and the Al doped nanorods, respectively. In the ZnO:Sn rods, empty channels and rows of voids along the growth axis appear associated to small Sn precipitates, which suggests that Sn diffusion is the mechanism of formation of channels and other hollow regions. Some of the rods have a tubular structure composed of ZnO and partially filled with Sn. Under the electron beam (of the TEM), dilatation of the Sn column in the ZnO tube is observed. The partially Sn filled, core-shell Sn/ZnO structure obtained in the rods is a nanoscale metal-semiconductor contact and by melting of the Sn core has nanothermal and nanoelectrical applications.

Al doped nanorods grow with a complex hierarchical network structure. Transmission electron microscopy suggests that the network growth is related to the formation of nanodrops on the surface of single nanorods.

References

1. Y. Ortega, P. Fernández and J. Piqueras, *J. Cryst. Growth*, 2009, 311, 3231.

2. Y.Ortega, P.Fernández, J.Piqueras, *Nanotechnology*, 2007, 18, 115606.

3. Y. Ortega, P. Fernández and J. Piqueras, *J. Appl. Phys.*, 2009, 105, 054315.

OR-31

NANOSTRUCTURING AND HARDENING OF LiF CRYSTALS IRRADIATED WITH 3-15 MeV Au IONS

J. Maniks[1], I. Manika[1], R. Grants[1], R. Zabels[1], K. Schwartz[2], M. Sorokin[3]

[1]*Institute of Solid State Physics, University of Latvia,*

[2]*GSI, Darmstadt, Germany,*

[3]*Russian Research Centre "Kurchatov Institute", Moscow, Russia*

e-mail: manik@latnet.lv

The change of structure and micromechanical properties of LiF single crystals irradiated with 3-15 MeV Au ions at 10^{12} - 10^{14} ions/cm^2 has been studied using AFM and nanoindentation techniques. The nanoindentation shows remarkable (up to 160%) ion-induced increase of hardness typical for the aggregation stage of radiation defects. The thickness of hardened layer coincides with the range of Au ions in LiF calculated using SRIM 2008. In contrast to GeV ions, which deposit their energy mainly by inelastic interactions with target electrons, thereby causing excitation and ionization processes, the MeV ions deposit a significant fraction of their energy by elastic collisions with the target atoms. The depth profile of hardness correlates with that for total energy loss (Fig.1) thus indicating that both the elastic and electronic mechanism contribute the hardening. AFM studies revealed generation of dislocations and nanostructuring in irradiated layer where columnar grains with a cross-section of 100-150 nm were observed. The annealing experiments showed an increase of the thermal stability of ion-induced modifications with increasing the fluence and beam current density. Accordingly, formation of colloids and other thermally stable aggregates is promoted under conditions of high ion fluence and flux as it was established earlier by optical absorption spectroscopy [1].

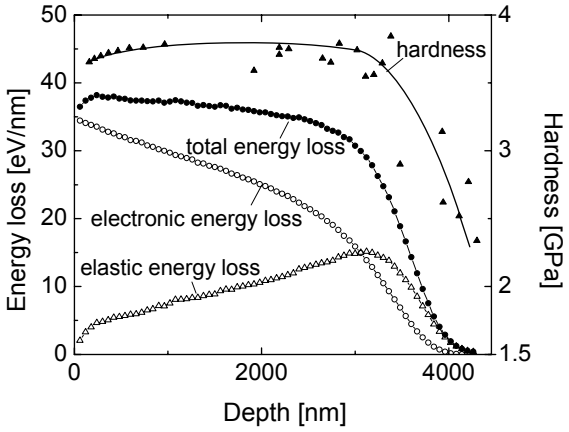

Fig.1 Depth profiles of hardness and energy loss of ions in LiF crystal.irradiated with 15 MeV Au ions at a fluence of 5×10^{13} cm^{-2}

References

1. A.Lushchik, Ch. Lushchik, K.Schwartz *et.al. Phys.Rev*. B, 2007, 76, 054114.

OR-32

INVESTIGATION OF LUMINESCENCE OF ZIRCONIA NANOPOWDERS DURING CHANGE OF OXYGEN CONTENT IN THE GAS OVER THE SAMPLE

W. Łojkowski[1], K. Gałązka[1], T. Chudoba[1], A. Opalińska[1], J.D. Fidelus[1], K. Smits[2], L. Grigorjeva[2], D. Millers[2], E. Wolska[3], M. Godlewski[3]

[1]*Institute of High Pressure Physics, Polish Academy of Sciences,*

[2]*Institute of Solid State Physics, University of Latvia,*

[3]*Institute of Physics, Polish Academy of Sciences*

e-mail: wl@unipress.waw.pl

Our previous studies showed that the intensity of photoluminescence of nanocrystalline zirconia increases when the material is annealed in an oxygen poor atmosphere in the temperature range 300 -360^{o}C. This effect can be exploited in an oxygen sensor. Till now all the luminescence tests have been carried out after cooling the sample to room temperature, however the dependence of luminescence on temperature gave strong evidence that luminescence of zirconia can be measured at higher temperatures as well. Thus, the device was developed where the sample can be heated up to 300^{o}C while the atmosphere over the sample is changed and luminescence can be measured in real time. The oxygen content effect on luminescence was confirmed in an experiment where the annealing temperature was 200^{o}C and the excitation source was a pulsed semiconductor laser emitting light at 405 nm. This discovery opens the way to make oxygen sensors with better performance than presently available. These phenomena strongly depend on the sample preparation method. The observed effects must be connected with changes in surface layers of the nanoparticles. This work was supported under the project ERANET – OXYNANOSEN and Project of the Polish Ministry for Science and High Education DONANO and Project 1126 of Latvian Council of Science

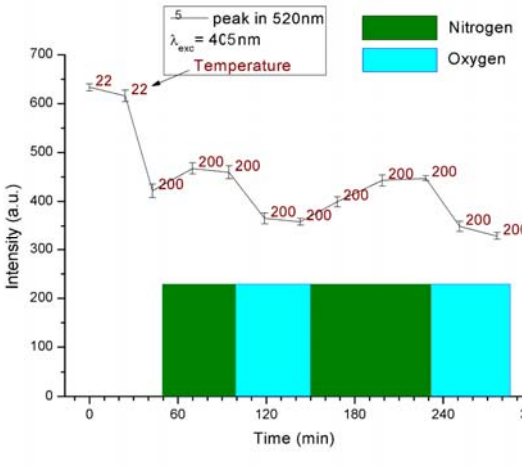

Fig.1 Effect of changing the atmosphere over nano-ZrO2 from oxygen to nitrogen and back to oxygen atmosphere sample on its luminescence intensity.

OR-33

ANION EXCHANGE IN Zn-Al LAYERED DOUBLE HYDROXIDES: IN SITU XRD STUDY

A.N. Salak, J. Tedim, A.I. Kuznetsova, M.L. Zheludkevich, M.G.S. Ferreira
Department of Ceramics and Glass Engineering/CICECO, University of Aveiro, Portugal
e-mail: salak@ua.pt

Layered double hydroxides (LDHs) are of great interest for (Nano)Materials Science and Technology due to their unique anion-exchanging capacity. Ability to control the release of active species under certain circumstances makes LDHs promising for corrosion protection. The anticorrosion effect of LDHs loaded with both inorganic and organic inhibitors has been proved [1-3].

Crystallinity is an important property with respect to application of LDHs as *nano-containers* for the corrosion inhibitors. The observed low intensity and broadening of the characteristic XRD reflections gave rise to doubt of crystallinity of the appropriate LDH compositions - Zn-Al-pyrovanadate [3]. Broad diffraction peaks were also observed for other Zn-Al-vanadates [1]. Overlapping peaks originated from the different LDH phases, loss of crystallinity, and small crystallite size were reported as possible reasons of the broadening.

In this work, *in situ* XRD was used to clarify mechanism of the anion exchange in Zn-Al LDHs. It has been found that the observed broadening of the peaks reflects indeed a smaller average crystallite size of the LDH Zn-Al-pyrovanadate in comparison with the respective precursor nitrate LDH. Substitution vanadate↔nitrate in Zn-Al LDHs results in *irreversible* decrease of the average size of crystallites. There is fragmentation rather than dissolution/recrystallization during the anion-exchange process. Strength of the effect is determined by the exchange conditions: concentration of substituting anions in solution, activation and direction of the exchange.

References

1. S.P.V. Mahajanam and R.G. Buchheit, *Corrosion*, 2008, 64, 230-240.

2. S.K. Poznyak, J. Tedim, L.M. Rodrigues, A.N. Salak, M.L. Zheludkevich, L.F.P. Dick and M.G.S. Ferreira, *ACS Appl. Mater. Interfaces*, 2009, 1, 2353-2362.

3. M.L. Zheludkevich, S.K. Poznyak, L.M. Rodrigues, D. Raps, T. Hack, L.F. Dick, T. Nunes, M.G.S. Ferreira, *Corrosion Science*, 2010, 52, 602-611.

OR-34

TOP-DOWN FABRICATION OF ORDERED PZT NANODOT ARRAYS BY NANOSPHERE LITHOGRAPHY

M. Waegner, G. Suchaneck, G. Gerlach

TU Dresden, Solid State Electronics Lab, 01062 Dresden, Germany

e-mail: martin.waegner@mailbox.tu-dresden.de

Nanosphere lithography (NSL) is a low-cost, versatile method for patterning and generation of nanostructures down to a few tens of nanometers. NSL utilizes monodisperse polystyrene latex nanospheres self-assembled into a hexagonal-closed-packed monolayer and deposited onto a substrate. Combining related techniques known from semiconductor and microelectromechanical system (MEMS) fabrication, various ordered arrays of nanoparticles, nanotubes and template structures can be prepared. Recently, arrays of ferroelectric nanostructures were manufactured by pulsed laser deposition of $BaTiO_3$ nanodots through a NSL-derived lift-off type monolayer mask [1] (bottom-up approach). Perovskite oxide nanodots showing piezoelectricity and ferroelectricity have numerous microelectronic device applications such as arrays of submicron ferroelectric cells for mass-storage applications, nano-sensor arrays, nano-tip field emitters, photonic crystals devices, nonlinear optical device, MEMS etc.

In this work, we describe the top-down fabrication of ordered $Pb(Zr,Ti)O_3$ (PZT) nanodot arrays by means of NSL. A monolayer of a well-ordered hexagonal array of latex spheres with a diameter < 1 μm was deposited onto the PZT thin film. To adjust a desired sphere size in the range of 300 to 800 nm, the latex sphere monolayer was treated by low-pressure plasma etching in an argon-oxygen atmosphere at low RF power. The remaining template serves then as a mask for PZT ion beam etching.

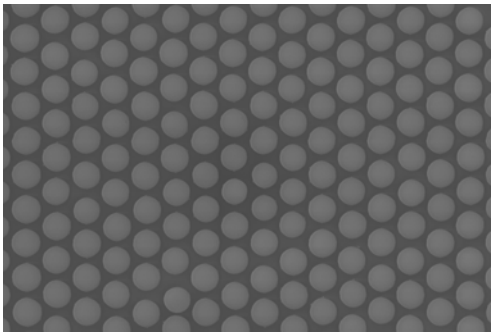

Fig. 1: SEM picture of a PS nanosphere mask. The white bar has a size of 2 μm.

References

1. W. Ma, C. Harnagea, D. Hesse, U. Gösele, *Appl. Phys. Lett.*, 2003, 83, 3770-3772.

OR-35

THE INFLUENCE OF NONSTOICHIOMETRIC SILICON CARBIDE NANOPOWDER ON THE REDUCING EFFICIENCY OF SILICON FOR SOLAR CELLS

G. Chikvaidze[1], V. Zauls[1], M. Gadzyra[2], V. Osokin[3], V. Panibratskiy[3], V. Solonenko[4]

[1]*Institute of Solid State Physics, University of Latvia,*

[2]*Institute of Problems for Material Sciences of the National Academy of Sciences of Ukraine,*

[3]*The State Scientific Research Institute "Helium", Vinnitsa, Ukraine,*

[4]*State Pedagogical University of Vinnitsa, Ukraine*

e-mail: georgc@cfi.lu.lv

A vacuum process is proposed for the reduction of silicon from its oxide using an electron beam melting method. Nonstoichiometric carbide of silicon was used as the reducer. Nonstoichiometric silicon carbide nano-powder synthesized by the authors, which contains in its structure carbon planar clusters, is an active reducer of silicon oxide.

Silicon carbide has significantly higher purity than other carbon materials which are used in traditional technologies for obtaining metallurgical silicon. The purity of carbon in structure of silicon carbide makes it one of the most prospective reducers of silicon oxide due to sp^3-hybridization of atoms. The deviation of stoichiometry in silicon carbide supports its meta-stability and results in a lowering of the temperature of the silicon oxide reduction process.

The processing of nonstoichiometric silicon carbide nano-powder with quartzite in an induction furnace with flowing argon results in the formation of metallurgical silicon with increased purity. After chemical purification and electron-beam melting, high purity silicon was obtained. Further increase in purity of reduced silicon was achieved by quick crystallization of the melt, which leads to the formation of a highly dispersed structures and localization of impurities on grain boundaries. After grinding such structures, the effectiveness of chemical purification is improved. The alloying of purified silicon powder in an induction furnace assists in obtaining a spongy material for final remelting and refining in an electron-beam furnace, and the production of silicon of solar purity.

OR-36

EXPERIMENTAL INVESTIGATION OF SWIFT HEAVY ION-INDUCED DAMAGE IN HIGHLY ORDERED GRAPHITE

M. Krause[1, 2], M. Tomut[2, 3], A. Sankarakumar[4, 5], W. Egger[6], L. Ravelli[6], C. Trautmann[2], R. Neumann[2], W. Ensinger[1]

[1]*Technische Universität Darmstadt, Germany,*

[2]*GSI Helmholtzentrum für Schwerionenforschung GmbH, Darmstadt, Germany,*

[3]*NIMP, Bucharest, Romania,*

[4]*IHFG, University of Stuttgart, Germany,*

[5]*MSD, IGCAR, Kalpakkam, India,*

[6]*Universität der Bundeswehr, München, Germany*

e-mail: m.krause@gsi.de

Fine grained isotropic R6650 grade graphite (SGL Carbon) will be the material of choice for beam catchers and rare isotope production target at the future large scale heavy-ion accelerator facility FAIR (Facility for Antiproton and Ion Research, Darmstadt, Germany)[1]. For this application graphite has unique properties such as high thermal conductivity and good thermal shock resistance. However radiation induced defect formation induces microstructural und thermo-mechanical changes of the material and will therefore ultimately limit the lifetime of these components.

We are investigating ion-induced effects in highly oriented pyrolytic graphite (HOPG, ZYB grade, NT-MDT) which serves as a model graphitic material due to its well defined structure. Irradiation experiments were carried out at room temperature with different swift heavy ions (Xe...U) of energies between 0.1 and 2.6 GeV and fluences ranging from 5×10^{11} to 8.4×10^{13} ions/cm^2.

Damage characterization with Raman spectroscopy and scanning electron microscopy (SEM) indicate irradiation induced disordering effects and crystallite size reduction. The use of positron annihilation spectroscopy (PAS) provides information about vacancy clusters resulting from the microstructural evolution of defects produced within the ion track.

References

1. M. Winkler et al., *Nuc Inst Meth .B*., 2008, 266, 4183-4187.

OR-37

SURFACE RELIEF GRATING RECORDING IN AMORPHOUS As-S-Se FILMS BY 0.6328 μm LASER

M. Reinfelde, J. Teteris

Institute of Solid State Physics, University of Latvia, Latvia

e-mail: mara.reinfelde@cfi.lu.lv

In this research we have studied the influence of He-Ne λ=0.6328 μm laser light illumination on formation and properties of surface relief gratings (SRG) in amorphous As-S-Se films at different recording conditions. Light exposition necessary for achieving maximum values of diffraction efficiencies (DE) of relief HG is high – up to 10^4 J/cm^2. A value of DE and relief depth strongly depends on recording light beam polarisation and grating period. An absorption coefficient for amorphous As-S-Se film at λ=0.6328 μm is of $\alpha \sim 10^3 cm^{-1}$ Therefore it is important to clear up the influence of light penetration inside the sample during the holographic recording of surface gratings. As we conclude from our previous measurements, at symmetric two beam one side (transmission scheme) recording, that one could affect relief depth – even up to 0,5μm for gratings of period Λ=2.6μm. More complicated situation arises when recording beams comes from opposite sides (reflection scheme). Essential role at formation of surface relief the inner reflection and diffraction began to play. As it one can see from added picture, sophisticated relief structure develops. Geometrical parameters of such structures strongly depend on sample orientation corresponding to recording system.

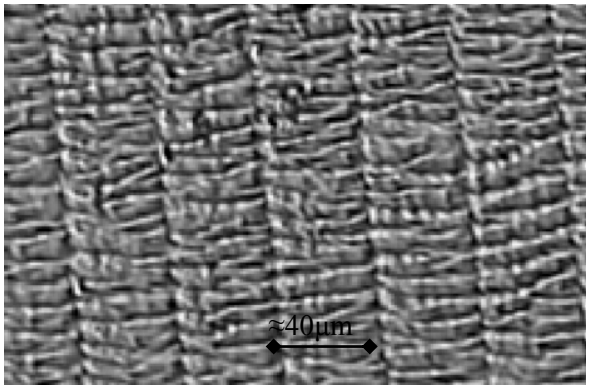

Fig. Optical microscope picture of relief structure on ≈3μm thick As-S-Se film recorded with He-Ne laser at reflection geometry. At least three grating types are possible to detach.

OR-38

PHOTOINDUCED MASS TRANSFER IN DISORDERED MATERIALS

J. Teteris, U. Gertners, M. Reinfelde

Institute of Solid State Physics, University of Latvia, Latvia

e-mail: teteris@latnet.lv

An interaction between laser light beam with high intensity gradient and disordered materials (amorphous chalcogenide and organic polymer films, organic and water liquid solutions) was studied. The single light beam focusing and two coherent beam interference were used for light intensity modulation with high gradient. Under intensive illumination the formation of relief structures on the surface of amorphous films and concentration redistribution of dissolved substances in liquids due to lateral mass transport regarding the light propagation direction have been observed [1, 2]. The possibility to apply this phenomenon in surface nanopatterning, chemistry for separation of substances and other branches has been discussed.

The influence of the amorphous film thickness, recording laser wavelength (266 nm, 325 nm, 441.6 nm, 532 nm, and 632.8 nm), grating period, light intensity and polarization state on the relief formation process in amorphous inorganic and organic films was studied. It was shown that the efficiency of the surface-relief formation strongly depends on the recording light polarization state (two *p*-linear, *s*-linear, identical circular or orthogonal circular polarized beams). The relief grating profile on amorphous films was analyzed by means of atomic force microscope (AFM).

The mechanism of the direct recording of surface-relief on amorphous chalcogenide and organic polymer films based on the photo-induced anisotropic plasticity of amorphous films and the optical gradient force induced mass transfer has been discussed.

References

1. U.Gertners, J.Teteris, *Journ. Optoelectronics and Advanced Materials*, 2009, 11, 1963-1966.

2. U.Gertners, J.Teteris, *Optical Materials*, 2010, doi: 10.1016/j.optmat.2010.01.008.

OR-39

EFFECT OF LIGHT POLARIZATION ON HOLOGRAPHIC RECORDING IN GLASY AZOCOMPOUNDS AND CHALCOGENIDES

A. Ozols, V. Kokars, P. Augustovs, I. Uiska, K. Traskovskis, D. Saharov
Faculty of Material Science and Applied Chemistry, Riga Technical University
Azenes iela 14/24, LV-1007, Riga, Latvia
e-mail: aozols@latnet.lv

Effect of recording and readout light polarization on holographic grating recording in glassy molecular azobenzene films 8a, 11,16 and glassy chalcogenide a- $As_{40}S_{15}Se_{45}$ films has been experimentally studied at 633 and 532 nm with *s-s, p-p,* CE-1 and CE-2 circular-elliptic (differing by light electric field rotation directions) recording beam polarizations.The polarization changes in the diffraction process were studied as well. Azocompounds exhibited much higher self-diffraction efficiency (SDE) and diffraction efficiency whereas chalcogenides were more sensitive .Their recording efficiency polarization dependences also were different and spectrally-dependent. SDE up to 45% was achieved in 8a with *p-p* and up to 2.8% in a- $As_{40}S_{15}Se_{45}$ with CE-2 polarized recording beams at 633 nm. Linear *p-p* polarizations were the most efficient at 633 nm whereas CE-1 polarizations were the best at 532 nm in azocompounds .It was found that light polarization changes in the process of diffraction depended on chemical composition, wavelength and exposure time. Vector gratings with SDE up to 25% were recorded in 8a rotating a linear polarization by 90^0. No light polarization changes were found in chalcogenide films. Coherent self-enhancement of gratings was observed only in azocompounds for *s-p* and both CE polarizations in 8a at 532 nm, and for *s-p* polarizations at 633 nm. The evidence is found for *trans-cis* photoisomerization holographic recording mechanism at both 532 and 633 nm.

OR-40

THE POLYISOPRENE – NANOSTRUCTURED CARBON COMPOSITE AS FLEXIBLE PRESSURE SENSOR MATERIAL – PROPERTIES AND PRACTICAL APPLICATIONS

J. Zavickis[1], M. Knite[1], K. Ozols[1], A. Linarts[1], G. Malefan[2]

[1]*Institute of Technical Physics, Riga Technical University, Latvia,*

[2]*Institute of Sciences and Engineering for Toulon and the Var, University of Toulon and the Var, France*

e-mail: juriszavickis@inbox.lv

Polyisoprene - nanostructured carbon composite (PNCC) is often treated as a prospective multifunctional sensor material [1]. It has unique property to rapidly and reversibly change its electrical conductivity under applied external strain or pressure. More likely – under all types of external deformation it has a remarkable as well as reversible piezoresistive effect. To obtain PNCC, certain conditions must be taken into account, such as hyper elastic polymer matrix and high structure conductive carbon filler must be chosen. The previous research approved that unique properties are provided only after the composite is vulcanized [2].

In our work we present latest result on designing, preparing and obtaining the PNCC with necessary properties, as well our efforts on practical application of such material. The dependence of PNCC sensing properties on vulcanization time, pressure as well as filler type and concentration is evaluated. The completely-hyper elastic multi layer structural design is proposed to be used as a sensing element.

References

1. M. Knite, K. Ozols, J. Zavickis, V. Tupureina, I. Klemenoks, R. Orlovs,, *Journal of Nanoscience and Nanotechnology*, 2009, 9,6, 3587-3592

2. J.Zavickis, G.Malefan, M.Knite, V.Teteris, Polyisoprene-nanostructured carbon black functional composite for pressure sensors, Proceedings of Scientific Conference of Young Scientists on Energy Issues (CYSENI 2008), Kaunas, Lithuania, May 28-29, 2009, ISSN 1822-7554

OR-41

THE INVESTIGATION OF ORGANIC SOLVENT VAPOUR SENSING MECHANISM ON POLYMER-NANOSTRUCTURED CARBON COMPOSITE

G. Sakale, M. Knite, V. Teteris

Riga Technical University, Institute of Technical Physics, Latvia

e-mail: gitasakale@inbox.lv

It is known from our previous research that determinative electric resistance change mechanism, which is responsible for polymer-carbon black composite organic solvent vapour (osv) sensing, is tunneling current decrease between carbon black aggregates in thin layers of matrix. Obtained results from in-situ electric resistance and the composite length change measurements (toluene vapour concentration ~ 500g/m^3) indicate that above mentioned is true only for relatively small vapour concentrations and for short exposure time. Conductive channel destruction starts to dominate in electric resistance change mechanism, when relative deformation of polyisoprene-nanostructured carbon composite (PNCC) is larger than 0,018.

The PNCC sensitivity has been tested to osv like: tetrahydrofuran, benzene, ethyl acetate, dichloroethane, toluene, acetone, chlorbenezene, p-xylene, o-xylene and propanol (sensitivity to vapour decrease in line). We observed no response to polar osv. It can be explained by polyisoprene and vapour molecule incompatibility due to very large difference in dielectric permeability values [1]. Changing the composite matrix material from non-polar polyisoprene to a polar polymer the composite sensitivity to polar osv can be improved.

References

1. G. Sakale, M. Knite, V. Teteris. Polyisoprene – nanostructured carbon composite material for volatile organic compound detection. Proceedings of the International Conference on Biomedical Electronics and Devices, Porto, Portugal, January 14-17, 2009, INSTICC Press, 117-122.

OR-42

SYNTHESIS AND UP-CONVERSION LUMINESCENCE IN ERBIUM DOPED $NaLaF_4$

G. Doke, A. Sarakovskis J. Grube, M. Springis

Institute of Solid State Physics, University of Latvia

e-mail: guna.doke@gmail.com

Rare-earth doped $NaYF_4$ is considered to be one of the most prospective up-conversion luminophors due to its low phonon energy and multisite nature of the crystalline lattice [1]. The isostructure and low phonon energy of $NaLaF_4$ suggest that this host doped with rare-earth ions is a prospective material to be used for up-conversion purposes [2].

In this work $NaLaF_4:Er^{3+}$ is synthesized. Its structure, traditional photoluminescence and up-conversion luminescence of the material are studied at different stages of synthesis by means of x-ray diffraction (XRD), stationary and time-resolved spectroscopy methods.

XRD measurements of the samples synthesized at different temperatures show gradual increase of $NaLaF_4$ content as the synthesis temperature grows. Up-conversion luminescence measurements of $NaLaF_4:Er^{3+}$ reveal the bands in the violet, green and red spectral regions related to the electronic transitions within Er^{3+} ($^2H_{9/2} \rightarrow {}^4I_{15/2}$, $^4S_{3/2} \rightarrow {}^4I_{15/2}$, $^4F_{9/2} \rightarrow {}^4I_{15/2}$, respectively). Several decay components are present in the temporal profiles of the up-conversion luminescence measured for the samples synthesized at different temperatures.

From the analysis of the experimental data it is concluded that during the synthesis of $NaLaF_4:Er^{3+}$ different oxygen-related defects are formed in the material. The formation of the defects is responsible for the shortening of Er^{3+} up-conversion luminescence lifetime.

The financial support of ESF project 2009/0202/1DP/1.1.1.2.0/09/APIA/VIAA/141 is greatly acknowledged.

References

1. J.F. Suyver, J. Grimm, M.K. van Veen, D. Biner, K.W. Krämer, H.U. Güdel, *Journal of Luminescence*, 2006, 117, 1, 1 – 12.

2. A. Sarakovskis, J. Grube, A. Mishnev, M. Springis, *Optical Materials*, 2009, 31, 10, 1517 – 1524.

OR-43

OBSERVATION OF α- RELAXATION IN GLASSES AT VICINITY OF T_g BY ULTRASONIC AND MANDEL'SHTAM-BRILLOUIN METHODS

V. Bogdanov[1], A. Golovnev[1], A. Pakhnin[1], S. Smerdin[2], V. Solovyev[1], A. Anan'ev[3], S. Nemilov[3]

[1]*Saint Petersburg State University, Russia,*

[2]*Omsk Railway Engineering University, Russia,*

[3]*Research and Technological Institute of Optical Material Science, Russia*

e-mail: v.n.bogdanov@mail.ru

Structural (α-) relaxation in glasses at temperatures close to the glass transition temperature T_g was studied by means of high temperature acoustics and Rayleigh and Mandel'shtam-Brillouin scattering (RMBS) spectroscopy. Ultrasonic (US) velocities (v) in glasses and their melts were measured with the specially designed high temperature (to 1400^0C) phase – pulse US interferometer. RMBS data were obtained via pressure scanned Fabry-Perot interferometer. It was found that a form of $v = v\ (T)$ at $T < T_g$ can be considered as a result of extrapolation of high frequency part of the curve corresponding to v values of high viscous melts measured at $T > T_g$ [1]. Hence, the fictive temperature T_f of glass can be found as intersection of high frequency limiting values of v in high-viscous melts and v in solid glasses. Annealing a glass at lower T_f leads to formation of more regular and more homogeneous structures (more low light scattering) with probably deeper or more uniform minimums of interatomic potentials. Variations of v and light scattering usually are reversible. Repeated thermal processing of glass is followed by careful controlling of elastic parameters and nano- and microinhomogeneity of glasses [2]. Annealing induced relaxation is caused by α- relaxation in a glass as it takes place in highly viscous fluids. It was found that time dependence of v in isothermal experiments was non-exponential due to both nonlinearity and existence of several ("fast" and "slow") relaxation processes: the latter fact was confirmed by "cross-over" experiments.

References

1. A.Golovnev, V.Bogdanov et al., *Influence of heat treatment of glasses on their elastic properties and light scattering.Abstracts of XXI International Congress on Glass ICG 2007, Strasbourg, July 1-6, 2007,* 28.

2. V.Bogdanov et al., *Journal of Physics: Conference Series,* 2007, 93**,** 012033.

OR-44

THE PROPERTIES OF LUMINESCENCE OF NOMINALLY PURE $LiBaAlF_6$ SINGLE CRYSTALS

S.I. Omelkov[1, 2], M. Kirm[2], E. Feldbach[2], V.A. Pustovarov[1], S.S. Lobanov[3], L.I. Isaenko[3]

[1]*Ural State Technical University, Yekaterinburg, Russia,*

[2]*Institute of Physics, University of Tartu, Estonia,*

[3]*Institute of Geology and Mineralogy SB RAS, Novosibirsk, Russia*

e-mail: omelkovs@mail.ru

Ternary fluorides offer wide material engineering capabilities which, combined with various rare-earth doping, allow creation of new optical materials for VUV region. $LiCaAlF_6$ (LiCAF) and $LiSrAlF_6$ (LiSAF) colquiriite crystals are studied as the transparent insulators in VUV region due to their large band gap (>11 eV), while doped with Cr^{3+}, they have been applied for tunable solid-state lasers in the near-IR region. The Ce^{3+} and Eu^{2+} activated LiCAF crystals were also studied as a promising scintillators and TLD. However, much less attention has been given to the luminescence properties of homologous $LiBaAlF_6$ (LiBAF) compound.

In this work, the relaxation of electronic excitations of nominally pure LiBAF single crystals were analyzed using luminescence spectroscopy and complimentary optical methods, and the luminescence properties of this crystal were compared with the LiCAF compound [1]. The intrinsic emission at 4.2 eV due to self-trapped excitons was identified. The fast (3 ns at T = 10 K) luminescence of recombination type emission center revealed at 3.0 eV. Both emissions degrade under electron beam irradiation, most probably due to the defects created which are blocking excitonic energy transfer channel. These defects are unstable and luminescence intensity is dynamically restored by thermal processes. In addition, the luminescence of an uncontrolled impurity peaked at 2.5 eV was found, and tentatively assigned to an oxygen-related emission center.

References

1. M Kirm, M True, S Vielhauer, G Zimmerer, N V Shiran, I Shpinkov, D Spassky, K Shimamura, N Ichinose, *Nucl. Instr. Meth. A*, 2005, 537**,** 291-294

OR-45

UP-CONVERSION LUMINESCENCE IN ERBIUM AND YTTERBIUM DOPED SILICATE GLASS CERAMICS

J. Grube, A. Sarakovskis, G. Doke, M. Springis

Institute of Solid State Physics, University of Latvia

e-mail: jurgis.grube@cfi.lu.lv

For many years rare-earth doped materials have been playing an outstanding role in many applications. In the past years much attention has been paid to the studies of up-conversion (UC) processes in the rare-earth doped phosphors related to the emission of higher-energy photons (VIS and UV) when excited by lower-energy photons (usually IR).

Oxyfluoride glass ceramics has attracted great scientific attention in the field of efficient UC phosphors. Having nanosized crystalline phase dispersed in the glassy matrix, the transparent oxyfluoride glass ceramics combines the efficiency of UC luminescence of the fluorides with the chemical and mechanical stability of the oxide matrix.

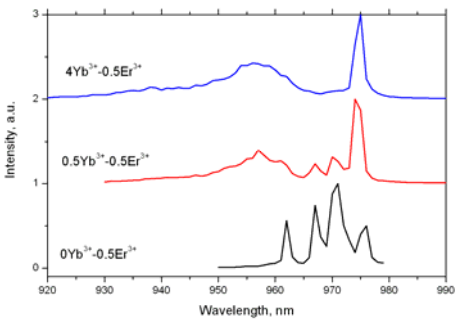

Fig. Excitation spectra of UC luminescence at 540nm with different Yb^{3+} concentration.

The aim of the current research was to study energy transfer mechanisms of UC luminescence in silicate glass ceramics containing LaF_3: Er^{3+},Yb^{3+} at different Yb^{3+} concentrations. For this purpose the transparent oxyfluoride silicate glass ceramics containing LaF_3:Er^{3+},Yb^{3+} crystallites was synthesized. UC luminescence spectra, excitation spectra (*Fig.*) and time-resolved luminescence show presence of both UC mechanisms: excited state absorption and energy transfer. Experiments revealed that energy transfer becomes dominant mechanism when Yb^{3+} concentration is increased.

The financial support of ESF project 2009/0202/1DP/1.1.1.2.0/09/APIA/VIAA/141 is greatly acknowledged.

OR-46

PARAMAGNETIC PROBES FOR STUDIES OF CRYSTALLIZATION IN THE OXYFLUORIDE GLASS CERAMICS

A. Fedotovs, D. Berzins, A. Sarakovskis, U. Rogulis

Institute of Solid State Physics, University of Latvia

e-mail: andris-f@navigator.lv

The use of transition elements as paramagnetic probes could help to investigate crystallization processes in the heat treated oxyfluoride glasses by means of magnetic resonances [1].

In this work, we used Mn^{2+} as a dopant in the oxyfluoride glasses. Electron paramagnetic resonance (EPR) measurements were carried out before and after heat treatment of the material. In both cases, a well pronounced hyperfine structure of the EPR spectra characteristic to the Mn^{2+} ion have been observed. EPR measurements were also studied for the separate fluoride counterparts of the oxyfluoride glass. EPR spectra for the LaF_3:Mn^{2+} powder shows that Mn^{2+} ion has a strong hyperfine interaction with surrounding fluorine nuclei.

We will discuss the obtained EPR results and consider possible further uses of such paramagnetic investigations for oxyfluoride glasses and ceramics.

The financial support of ESF project 2009/0202/1DP/1.1.1.2.0/09/APIA/VIAA/141 is greatly acknowledged.

References

1. R.W.A. Franco, J.F. Lima, C.J. Magona, J.P. Donoso, Y. Messaddeq, *J. Non-Cryst. Sol.*, 2006, 352, 3414–3422

OR-47

SYNTHESIS AND CHARACTERIZATION OF PURE AND Sm DOPED TiO_2 NANOCRYSTALS BY SOLID STATE REACTION METHOD

M. Gokula Krishna[1], M. Prabhu[1], K. Chandar[2], Dr. S. Jayavel[2]

[1]*Department of Mechanical Engineering, College of Engineering, Guindy, Anna University Chennai, Chennai – 25,*

[2]*Centre for Nanoscience and Technology, Anna University Chennai, Chennai – 25*

e-mail: mgkrishna_89@yahoo.co.in

Pure TiO_2 nanocrystals were prepared by simple solid state reaction from $TiOSO_4$ and Na_2CO_3 as precursors. Similarly, Samarium doped TiO_2 nanocrystals were synthesized from $TiOSO_4$, Na_2CO_3 and $Sm(NO_3)_3$ by simple solid state reaction with 0.5, 1, 1.5 mol% of $Sm(NO_3)_3$. The resulting powders were calcined at 200 ºC. The X – ray diffraction results showed the grain sizes of pure and Sm doped TiO_2 to be 14 nm and 11 nm respectively. The FTIR spectra showed the presence of Ti – O band stretching at 425cm^{-1} in both pure and doped samples. There was a sharp band at 3860 cm^{-1} which attributes to the octahedral vacancy sites. The UV – visible DRS spectroscopy showed the cut off at 352 nm for pure and 370 – 380 nm for doped samples respectively. The band gap of pure and doped TiO_2 was calculated and found to be decreased for Sm doped TiO_2. The PL spectra showed yellow band emissions. The SEM image showed the morphology to be spherical and EDS spectra confirmed the composition of pure and Sm doped TiO_2 nanocrystals.

References

1. Vaclav Stengl, Snejana Bakardjieva, Nataliya, *Materials Chemistry and Physics*, 2009,114, 217–226

2. E. Setiawati, K. Kawano, *Journal of Alloys and Compounds*, 2008, 451, 293–296

OR-48

STRUCTURAL STUDY OF NANOCRYSTALLINE TUNGSTEN TRIOXIDE

Y. Fujioka[1], J. Frantti[1], V. Lantto[2]

[1]*Aalto University School of Science and Technology, Department of Applied Physics,*

[2]*University of Oulu, Microelectronics and Materials Physics Laboratories*

e-mail: yukari.fujioka@tkk.fi

Tungsten trioxide (WO_3) undergoes numerous structural distortions as a function of temperature. Characteristic to the phase transitions are changes in oxygen octahedral tilting. Notably interesting is the lowest temperature phase having the *Pc* space group symmetry allowing ferroelectricity [1], which may occur at room temperature in the case of small particles. The critical size at which this may occur in the case of free particles is yet not known. Single phase, homogeneous small particle size WO_3 powders were prepared by solution techniques to study the effect of particle size on crystal symmetries down to 20 nm. The room temperature crystal symmetry was found to be *Pbcn* once the particle size diminished below 40 nm as was revealed by the x-ray diffraction. In bulk material this phase is stable above 623 K. This implies that if the free WO_3 particles undergo a phase transition to the *Pc* phase, the critical size is below 20 nm. Transmission electron microscopy studies were conducted to study the powder morphology and homogeneity. Also magnetic properties were studied down to 2 K.

References

1. P. Woodward et al., *J. Solid State Chem.*1997, 9, 131.

OR-49

STUDY OF STRUCTURE AND ELECTROCHEMICAL CHARACTERISTICS OF $LiFePO_4$/C AS CATHODE MATERIAL FOR LITHIUM BATTERIES

G. Bajars, J. Smits, G. Kucinskis, J. Kleperis

Institute of Solid State Physics, University of Latvia

e-mail: gunars.bajars@gmail.com

Recently increased attention has been dedicated to $LiFePO_4$ as a promising cathode material in lithium-ion batteries for use in consumer electronics and electric vehicles because of the environmental compatibility and low manufacturing cost. In addition, $LiFePO_4$ has a relatively large theoretical capacity of 170 mAh/g, good thermal stability and little hygroscopicity [1, 2]. The main problem restricting the practical application of $LiFePO_4$ is its low electronic conductivity and poor rate capability. One way to solve the above mentioned problems is to increase the surface area of the cathode by the use of thin film technology [3, 4].

In our present work $LiFePO_4$ was synthesized from Li_2CO_3, $FeC_2O_4 \cdot 2H_2O$ and $NH_4H_2PO_4$ with different carbon content. $LiFePO_4$/C thin films prepared under various sputtering conditions were characterized by x-ray diffraction, scanning electron microscope and Raman spectroscopy. The deposited thin films were tested as cathode materials for lithium ion batteries by electrochemical impedance spectroscopy and cyclic voltammetry. The electrochemical characteristics of $LiFePO_4$/C thin films are related to conditions of preparation, structure, surface morphology and carbon content.

References

1. M.Takahashi, S.Tobishima, K.Takei, Y.Sakurai, *Solid State Ionics,* 2002, 148, 283-289.

2. F.Gao, Z.Tang, *Electrochimica Acta,* 2008, 53, 5071-5075.

3. K.-F.Chiu, P.Y.Chen, *Surface & Coatings Technology,* 2008, 203, 872-875.

4. J.Xie, N.Imanishi, T.Zhang, A.Hirano, Y.Takeda, O.Yamamoto, *Electrochimica Acta,* 2009, 54, 4631-4637.

OR-50

ORIENTED NANOSTRUCTURES FOR SOLAR-HYDROGEN TECHNOLOGIES

J. Kleperis, M. Vanags, J. Hodakovska, J. Klavins
Institute of solid State Physics, University of Latvia
e-mail: kleperis@latnet.lv

Recently oriented nanomaterials have demonstrated great potential for next-generation energy-conversion and -storage devices [1,2]. Such oriented nanostructures can be applied in thermal and photovoltaics solar energy harvesting, in rechargeable batteries, supercapacitors, thermoelectrics, hydrogen technologies. Some common fundamental challenge for such structures are maximal surface activity, controlled pore directions and optimized transport of electrons and ions.

In this report, we highlight the synthesis and application of oriented carbon based nanostructure coatings in solar thermocolectors. Direct coating method using acetilene flame allowed to prepare smoth black films on specially prepared metal substrate. To achieve preferred orientation of carbon nanoparticles, angle between flame and substrate was adjusted and magnetic field used. Preliminary results will be reported on steel and cuprum metals coated with carbon based nanoparticles.

Next results about integrated semiconductor catalyst and electron-proton conducting membranes will be discussed. An idea for membrane reactor which utilizes solar energy to drive chemical reactions using carbon dioxide from atmosphere and water from Earth to produce useful chemicals is intenting many researchers around all the World [2]. Although such an efficient and integrated membrane reactor has not yet been demonstrated, research is going on to design oriented nanoporous arrays with desired architecture, catalys and conductivity properties.

References

1. On Solar Hydrogen and Nanotechnology, L. Vayssieres (Ed.), Interscience Wiley, 2010, 696 pages.
2. Jun Liu et all., Oriented Nanostructures for Energy Conversion and Storage, ChemSusChem, v. 1, is. 8-9 (2008), p. 676 – 697.

OR-51

CARBON MATERIALS FOR HIGH-POWER HEAVY IONS ACCELERATORS

M. Tomut[1, 2], M. Krause[1, 3], W. Ensinger[3], C. Trautmann[1]

[1]*GSI Helmholtzentrum für Schwerionenforschung GmbH, Darmstadt, Germany,*

[2]*NIMP, Bucharest, Romania,*

[3]*Technische Universität Darmstadt, Germany*

e-mail: m.tomut@gsi.de

The development of high-power heavy-ions accelerators like FAIR, LHC and FRIB poses new challenges to materials that have traditionally served in the nuclear field. Key components: targets, beam dumps, collimators, strippers have to perform in severe radiation conditions and have to resist irradiation-induced degradation of properties that control shock and fatigue.

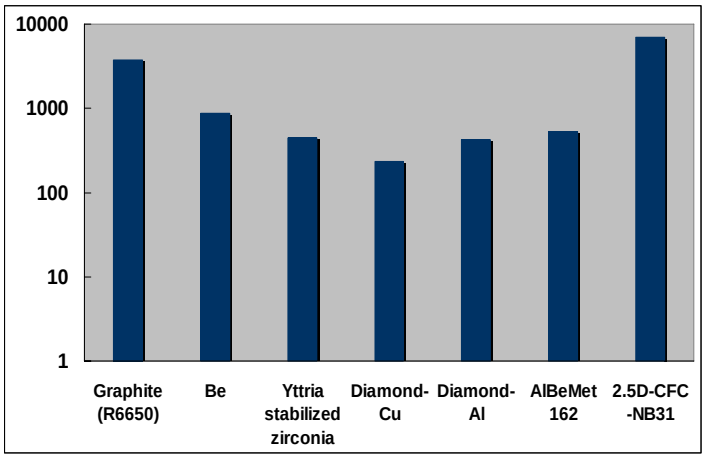

Fig.1 Figure of merit for resistance of candidate materials for high-power accelerators to ion beam-induced thermal stress

To allow for an extended utilization of these components at high beam intensity, in the pulsed operating regime, new materials more resilient to pressure waves are desirable. Figure 1 shows a comparison of candidate target materials based on a figure of merit describing the resistance to thermal shocks induced by ^{238}U beam. This parameter compares the bending strength of the material to a parameter proportional to the thermal stress induced by the ion beam energy deposition. Carbon materials remain the best choice for high temperature, high thermal stress and high dose applications.

A discussion of problems specific to various irradiation environments, recent experimental results of ion-induced radiation damage studies in carbon materials and a quest for new advanced material solutions are presented.

OR-52

SYNTHESIS AND CHARACTERIZATION OF PURE TITANIA NANOCRYSTALLITES BY SOL-GEL METHOD

M. Prabhu[1], M. Gokula Krishna[1], R. Sankar[2], S. Jayavel[3]

[1]*Department of Mechanical Engineering, College of Engineering, Guindy, Anna University Chennai, Chennai – 25,*

[2]*Crystal Growth Centre, Anna University Chennai, Chennai – 25,*

[3]*Centre for Nano Science and Technology, Anna University Chennai, Chennai – 25*

e-mail: prabhu280389@gmail.com

Pure titania nanocrystallites were synthesized from aqueous hyrolysis of $TiCl_4$ and precipitation by NaOH at 450 ºC, 550 ºC, 650 ºC. The nanocrystallites were characterized using X – ray diffraction revealed the sizes to be 7 nm, 11 nm, 18 nm.. The FTIR spectroscopy showed an absorption band between 3000 - 3500 cm^{-1} in the sample prepared at 450 ºC, 550 ºC which is the presence of –OH group and this disappeared at 650 ºC. The absorption band at 3700 – 3800 cm^{-1} confirms the presence of octahedral vacancies in the form oxygen vacancy levels at surface sites. The samples were characterized using UV – Vis DRS showed the cut – off wavelength at 352 nm. The band gap energy was calculated to be 2.92 eV, 2.95 eV, and 3.01 eV for Titania nanocrystals at three temperatures. Photoluminescence spectra showed emissions at 450 nm, 468 nm, and 473 nm with blue band emission. The SEM analysis was performed which is revealed the spherical morphology of the nanocrystals. The EDS spectra explained the composition of pure TiO_2 nanocrystals.

References

1. Xuanyong Liua, Xiaobing Zhaoa, Ricky K.Y. Fub, Joan P.Y. Hob, Chuanxian Dinga, Paul K. Chub, *Biomaterials*, 2005, 26, 6143–6150.

2. C. Garzella, E. Comini, E. Tempesti, C. Frigeri, G. Sberveglieri, *Sensors and Actuators B*, 2000, 68, 189 –196.

OR-53

ADDING FUNCTIONALITY TO COTTON BY USING STIMULI SENSITIVE MICROPARTICLES

A. Kulkarni, M. M.C.G. Warmoeskerken, D. Jocic

Engineering of Fibrous Smart Materials (EFSM), Faculty of Engineering Technology (CTW), University of Twente, Enschede, The Netherlands

e-mail: a.n.kulkarni@ctw.utwente.nl

Intelligent or responsive textile materials are being extensively investigated in the last decade, since they are considered cutting-edge materials with a number of applications in bio-medicine and protective apparel. A promising strategy to develop responsive textiles is functional finishing by incorporation of surface modifying systems (SMS) based on stimuli-responsive polymeric gels of micro or nano size [1]. The SMS based on poly (N-isopropylacrylamide) (poly-NiPAAm) and chitosan (CS) microparticles (PNCS) was synthesized using surfactant free emulsion method [2]. PNCS were characterized by various methods (SEM, DLS, UV-Vis) to obtain information on their morphology and pH/temperature responsiveness (200-300 nm; LCST at 33-34ºC; LCST decreases with decrease in pH). The PNCS microparticles were incorporated to textile material (cotton) by simple pad-dry-cure method using 1,2,3,4-butanetetracarboxylic acid (BTCA) as crosslinking agent. The morphology and surface chemical properties of thus modified cotton were studied (SEM, FTIR-ATR, XPS). The results confirm that the newly developed textile material shows good temperature/pH response in terms of water uptake by showing transitional region between 28 and 32ºC.

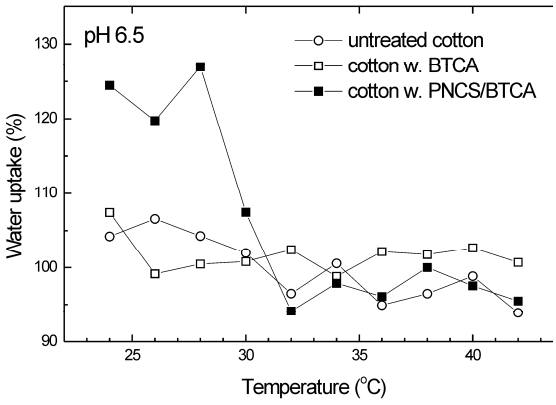

Fig. 1 Water uptake of modified cotton studied at various temperatures.

The authors are thankful for financial support provided by Marie Curie Excellence Grant (EXT) project ADVANBIOTEX (MEXT-CT-2006-042641), funded by the EU's Sixth Framework Programme.

References

1. D. Jocic, A. Tourrette, P. Glampedaki, M.M.C.G. Warmoeskerken, *Materials Technology*, 2009, 24(1), 14-23.

2. C.F. Lee, C.J. Wen, W.Y. Chiu, *J. Polym. Sci. A: Polym. Chem.*, 2003, 41, 2053-2063.

OR-54

EFFECT OF PARTICLE SIZE AND PRESSURE ON MAGNETIC PROPERTIES OF MANGANITE AND COBALTITE NANOPARTICLES

A. Wisniewski[1], V. Markovich[2], I. Fita[2, 3], R. Puzniak[1]

[1]*Institute of Physics, Polish Academy of Sciences, Warsaw, Poland,*

[2]*Department of Physics, Ben-Gurion University of the Negev, Beer-Sheva, Israel,*

[3]*Donetsk Institute for Physics and Technology, Donetsk, Ukraine*

e-mail: wisni@ifpan.edu.pl

When the size of the magnetic nanoparticles is reduced to few nanometers, some of their basic magnetic properties, e.g., the spontaneous magnetization, the Curie temperature, T_C, the coercivity, and even the type of magnetic ordering are strongly influenced by the particle size and may differ significantly from the bulk properties.

The magnetic studies of nanocrystaline manganites $La_{1-x}MnO_{3+\delta}$ were performed for particles with average particle size of 20, 25, and 30 nm ($T_C \approx 220$, 268, and 268 K, respectively). The relative volume of ferromagnetic (FM) phase increases with increasing particle size and approaches a value of about 93% for nanoparticles with average size of 30 nm. It was found that an applied pressure enhances the T_C of all $La_{1-x}MnO_{3+\delta}$ nanoparticles, with a pressure coefficient of $dT_C/dP \approx 1.9$ Kkbar^{-1} for 20 nm nanoparticles. The pressure coefficient is found to be in accordance with the double-exchange driven ferromagnetism.

The x-ray and magnetization measurements for $LaCoO_3$ nanoparticles with different size showed that with increasing the surface-to-volume ratio the lattice parameters of $LaCoO_3$ nanoparticles expand distinctly due to a surface effect and FM moment increases simultaneously. The observed correlation between FM phase and lattice parameters indicates that ferromagnetism of $LaCoO_3$ results from the intermediate spin state (IS) of Co ions, induced by an expansion of the unit-cell and/or Co-O bonds. On the other hand, an applied hydrostatic pressure suppresses strongly the FM phase, leading to its full disappearance at 10 kbar. It was shown that ferromagnetism in $LaCoO_3$ is attributed to ferromagnetically coupled IS Co^{3+} ions which appear/disappear with expanding/compressing the lattice and/or Co-O bonds. In general, this indicates that ferromagnetism in these nanoparticles is controlled by their size.

OR-55

FORMATION OF MICROCONVECTION IN PERIODIC CONCENTRATION GRATING OF MAGNETIC NANOPARTICLES

D. Zablotsky, E. Blums

Institute of Physics of University of Latvia, 32 Miera str., LV-2169 Salaspils, Latvia

e-mail: Dmitrijs.Zablockis@gmail.com

Microeffects concerning the transfer of heat and colloidal particles attract the scientific attention by their cooperative nature. Ferrofluids are colloidal suspensions of magnetic nanoparticles and as such they posses superparamagnetic properties and an additional control parameter - the magnetic field. We will consider a periodic concentration grating induced in a thin layer of ferrofluid by interfering laser beams of high intensity under the action of externally applied uniform magnetic field. As soon as the optical grating is focused within the layer, the ferrofluid is locally heated and the corresponding concentration grating starts to develop due to the strong Soret effect characteristic for colloidal solutions. When diffusion and thermodiffusion reach equilibrium, the beams are switched off and the temperature nonhomogeneities immediately relax. The relaxation of the concentration grating takes much longer due to vastly different timescales. It is suspected ([1], [2]) that microconvective instability may develop at this stage causing enhanced mixing and significant increase of the experimentally measured effective diffusion coefficient. The results of numerical simulations of the microconvection will be presented for different values of the dimensionless parameters.

Fig.1 Numerically calculated microconvective rolls in concentration grating

References

1. A. Mezulis, E. Blums, *Magnetohydrodynamics*, 2005, 41, 4, 341–348.

2. M. Igonin, Magnetohydrodynamics, 2004, 40, 1, 53–64.

OR-56

STRUCTURE AND CHARACTERISTICS OF LASER CRYSTALLIZED THIN AMORPHOUS Si FILMS

G. Marcins, M. Chubarov, J. Butikova, I. Tale, B. Polyakov, R. Kalendarjov, A. Muhin
Institute of Solid State Physics, University of Latvia, LV-1063 Riga, Latvia
e-mail: gmarcins@gmail.com

Polycrystalline silicon (p-Si) is a very attractive material for thin film electronic devices such as integral circuits due to its resemblance to crystalline silicon (c-Si) electronic properties. One way to obtain p-Si is by crystallization of amorphous silicon (a-Si), using pulse UV laser radiation. It is relatively fast and flexible method to obtain large-grained poly-silicon [1, 2], and it allows to crystallize selected parts of the sample. However laser crystallization process can be influenced by many parameters and each case needs to be studied individually.

In current work silicon wafer was used as a substrate. Its surface was oxidized and 390 nm SiO2 layer was made. On top of it were deposited Si3N4 and a-Si layers of 100 and 220 nm respectively. The crystallization was performed using III harmonic Nd:YAG pulse laser (τ = 135 ps). After treatment some samples were annealed for 30 min in hydrogen atmosphere at 600 ^{o}C.

Raman spectroscopy is a standard characterization method in the field of thin film silicon. Therefore Raman spectroscopy measurements were performed on both untreated and laser crystallized samples. Results suggest that samples were successfully crystallized after threshold energy of ~200 mJ/cm^2 was reached.

Electric properties of a-Si and p-Si were studied using Hall and I-V measurements. Obtained data shows significant decrease in resistivity of 10^4 and increase in carrier mobility. After annealing in hydrogen the sheet resistivity becomes less sensitive to changes in crystallization energy level and stabilizes to 1.1 MOhm.

Scanning Electron microscopy was used to study surface. From the samples crystallized in air, obtained results shoes that at high energy levels surface modification starts and dielectric droplets of ~60 nm are formed. After etching samples in HF solution these droplets can be easily removed, suggesting that they consist of SiO_2.

References

1. P. Lengsfeld, “Successive laser crystallization of doped and undoped a-Si:H”, Ph thesis, Berlin (2001).
2. B. Nayak, M. Gupta, *Applied Physics A*, 2007, 89, 3, 663-666.

OR-57

THERMOACTIVATED SPECTROSCOPY OF DEFECT LEVELS IN GaN THIN FILMS

M. Chubarov, G. Marcins, I. Tale, L. Dimitrocenko

Institute of Solid State Physics, University of Latvia

e-mail: mikhail.chubarov@gmail.com

Usually, GaN is grown on a sapphire substrate. In this case dislocations, point defects, point defect clusters can appear in high concentration due to lattice mismatch between GaN and a sapphire. The defects can seriously affect optical and electrical properties of the material [1]. Experimental and theoretical research shows that V_{Ga} (Gallium vacancy) acts as a deep compensating defects level for n-type GaN [2 – 5]. Theoretical calculations show that O_N (Oxygen donors) and V_{Ga} form complexes, that are energetically favorable than single defects [3]. Also, long lasting photostimulated luminescence (PSL) in donor – acceptor pair (DAP) region is observed. This fact is explained by different distance between donors and acceptors [6]. For a better understanding of the material properties containing such defects a number of investigation techniques should be applied. In our research GaN samples were grown on a sapphire substrate using a MOCVD (Metal-Organic Chemical Vapor Deposition) technology. For the investigation of the defect properties TSL (thermally stimulated luminescence), TSC (thermally stimulated currents), FGT (fractional glow technique) [7] and ESL (electrically stimulated luminescence) were applied. In the temperature region 10 – 300 K TSL is observed. We found that at low temperatures (10 K – 140 K) during thermal stimulation of the charge carriers trapped on the defect levels, charge carriers tunnel between the neighbor defects and recombine yielding characteristic luminescence of DAP at 1.8 eV (685 nm). The voltage, applied during the TSL measurement did not influence the intensity of the luminescence. This argument allows to conclude, that the defects involved in the TSL formation are positioned deep in the band gap that the charge carriers preferably tunnel between the defects.

References

1. J.Y. Shi, L.P. Yu, Y.Z. Wang, G.Y. Zang, H. Zang, *Appl.Phys.Lett.*, 2002 80, 2293

2. T.L. Tansley and R.J. Egan, *Phys. Rev. B*, 1992, 45, 10942

3. N. Nepal, M. L. Nakarmi, J. Y. Lin, and H. X. Jiang, *Appl.Phys.Lett.*, 2006, 89, 092107

4. K. B. Nam, M. L. Nakarmi, J. Y. Lin, and H. X. Jiang, *Appl. Phys. Lett.*, 2005, 86, 222108

5. K. Saarinen, T. et. all, *Phys. Rev. Lett.*, 1997, 79, 3030

6. D. G. Thomas, J. J. Hopfield, and W. M. Augustiniak, *Phys. Rev.* 1965, 140, A202

7. I. A. Tale, *Phys. Stat. Sol. A*, 1981, 66, 65

Abstracts of the poster presentations

PO-1

SUBSTRATE INDUCED RELAXOR BEHAVIOUR IN THIN FILMS OF BARIUM TITANATE

M. Tyunina[1], J. Levoska[1], M. Plekh[1], J. Narkilahti[1], B. Malic[2], M. Kosec[2]

[1]*Microelectronics and Materials Physics Laboratories, University of Oulu, Finland,*

[2]*Department of Electroceramics, Jozef Stefan Institute, Slovenia*

e-mail: marinat@ee.oulu.fi

The best studied perovskite-structure ferroelectric barium titanate ($BaTiO_3$, or BTO) is known to experience cubic paraelectric to tetragonal ferroelectric phase transition at about 403 K with two consequent structural transitions in ferroelectric states. In contrast to bulk BTO, thin epitaxial films of BTO have been found to exhibit relaxorlike behaviour in the broad temperature range below 450 K. This contradicts to both theoretically predicted phase diagrams of epitaxial BTO films and bulk behaviour. Similar experimental observations made in different laboratories suggest technologically independent fundamental origin of such an unusual behaviour. To clarify its possible mechanism, thin BTO films with different microstructure were prepared and their dielectric response was experimentally studied and analyzed.

Randomly oriented polycrystalline BTO films (poly-grain) with equi-axed 10 – 100 nm large grains were prepared by chemical solution deposition. Epitaxial strain-free BTO films (epi) were grown by in situ pulsed laser deposition using an oxide bottom electrode layer and single-crystal substrates. Randomly oriented poly-crystalline BTO films (poly) with columnar grains were pulsed laser deposited onto Pt-coated sapphire substrates.

Relaxorlike frequency dispersion of the dielectric permittivity and loss factor was clearly seen in epi-films. In poly-grain films, all bulk-type transitions were found. In poly-films, the dielectric peak was smeared over the range 100 – 500 K. The broad peak in losses around 200 K resembled relaxorlike one. The observations indicated film-substrate coupling as a factor possibly influencing relaxorlike features.

PO-2

FERROELECTRIC DOMAINS IN EPITAXIAL AND POLYCRYSTALLINE BARIUM TITANATE FILMS

M. Plekh[1], J. Levoska[1], J. Narkilahti[1], M. Tyunina[1], B. Malic[2], M. Kosec[2]

[1]*Microelectronics and Materials Physics Laboratories, University of Oulu, Finland,*

[2]*Department of Electroceramics, Jozef Stefan Institute, Slovenia*

e-mail: marinat@ee.oulu.fi

Perovskite-structure BaTiO3 (BTO) is known to have tetragonal ferroelectric phase at room temperature. Also in epitaxial BTO films without crystallographic strain, room-temperature ferroelectric phase is predicted using phenomenological and *ab initio* approaches. Experimental studies of epitaxial BTO films, however, have indicated relaxorlike behaviour different from the theoretically predicted. The possible reason can be related to small film thickness or to film-substrate coupling. To investigate such possibilities, the room-temperature ferroelectric domains in epitaxial and polycrystalline BTO films are investigated using piezo-response force microscopy (PFM) and compared.

Randomly oriented polycrystalline BTO films (poly-BTO, 600 nm thick) were prepared by chemical solution deposition onto the polished alumina substrates. For dielectric measurements, 3 μm-air-gapped capacitors were patterned using magnetron sputtered Cr/Au electrodes. PFM measurements were performed by applying ac voltage on the said capacitor and measuring in-plane piezoresponse in the gap. Epitaxial strain-free BTO films (epi-BTO) were grown by in situ pulsed laser deposition using $La_{0.5}Sr_{0.5}CoO_3$ bottom electrode layer and single-crystal substrates. PFM characterization of the films was carried out in both out-of-plane and in-plane directions.

In poly-BTO, ferroelectric domains were detected inside the grains. The grains were single-domain. In epi-BTO, PFM studies showed absence of ferroelectric domains, in agreement with macroscopic relaxorlike response. The results discard effect of thickness on relaxorlike properties of BTO films.

PO-3

GROWTH OF PEROVSKITE-STRUCTURE POTASSIUM TANTALATE FILMS

J. Narkilahti, M. Plekh, M. Tyunina

Microelectronics and Materials Physics Laboratories, University of Oulu, Finland

e-mail: marinat@ee.oulu.fi

Growth and properties of epitaxial films perovskite-structure quantum paraelectrics such as $SrTiO_3$ (STO) and $KTaO_3$ (KTO) have recently become of great fundamental interest. This is due to possible predicted strain-induced onset of ferroelectricity n such films [1]. Experimental evidence of strain induced ferroelectric transition has not been obtained so far. Here we focus on studies of KTO films.

It is known that in KTO, formation of unwanted pyrochlore-structure phase is a common technological obstacle. Previously it has been shown that perovskite formation can be enhanced using strong over-stoichiometric content of K [2]. In our work, KTO films were grown by in situ pulsed laser deposition using stoichiometric KTO ceramic target. Deposition parameters such as ambient oxygen pressure, laser fluence, substrate temperature, and number of shots (and hence thickness of the film) were varied. Influence of these parameters on crystal structure of KTO films was systematically analyzed.

KTO films were deposited directly on STO and MgO single-crystal substrates and also using $SrRuO_3$ and $LaScCoO_3$ as bottom electrode layers. The room-temperature crystal structure of the films was studied by x-ray diffraction. Under optimized deposition conditions, strained perovskite-structure epitaxial KTO thin films were grown on STO.

References

1. J. H. Haeni et al., *Nature* (London), 2004, 430, 758.

2. H.-M. Christen et al., *Appl. Phys. Lett.*, 1996, 68, 1488.

PO-4

STRONGLY INHOMOGENEOUS DOMAIN CONFIGURATION IN EPITAXIAL LEAD ZIRCONATE TITANATE FILMS

M. Plekh, J. Levoska, J. Narkilahti, M. Tyunina

Microelectronics and Materials Physics Laboratories, University of Oulu, Finland

e-mail: marinat@ee.oulu.fi

In thin films of perovskite-structure ferroelectrics, the width of ferroelectric domains is theoretically predicted to decrease with decreasing films thickness. In polycrystalline films with nano-sized grains, domain width is also limited by grain size. In epitaxial films without grains, presence of misfit and thermal strain affects domain configuration and domain width. During film growth, misfit strain is known to relax with increasing thickness of epitaxial film, mainly through formation of misfit dislocations. This can be followed by a change of growth mode from 2D layer-by-layer mode to 3D island growth. The resulting microstructure of the film is not homogeneous. Respectively this can affect the width and configuration of ferroelectric domains in such films. Here we demonstrate strongly inhomogeneous domain configuration and switching behaviour in epitaxial films of rhombohedral $PbZr_{0.65}Ti_{0.35}O_3$ (PZT).

Epitaxial PZT films were grown by in situ pulsed laser deposition using an oxide bottom electrode layer of $La_{0.5}Sr_{0.5}CoO_3$ and single-crystal substrates (MgO, LaAlO3). Room-temperature x-ray diffraction analysis revealed that PZT films were pseudocubic perovskite, with (001) planes parallel to the substrate surface. Electrical characterization was performed macroscopically using vertical capacitor structures with Pt top electrodes, and locally by piezoresponse force microscopy (PFM). Ferroelectric domains were imaged with high resolution through the Pt top electrodes. Domain width was about 100 – 150 nm for PZT film thickness 500 nm. Domains were investigated under applied dc electric field of two different polarities. Local electromechanical response loops of differently performing domains were recorded. Studies of switching behavior of domains revealed different local coercive fields, suggesting strongly inhomogeneous internal electrical and mechanical conditions.

PO-5

ULTRATHIN STRONTIUM TITANATE FILMS BY PULSED LASER DEPOSITION

J. Narkilahti, M. Plekh, M. Tyunina

Microelectronics and Materials Physics Laboratories, University of Oulu, Finland

e-mail: marinat@ee.oulu.fi

Growth and properties of perovskite-structure $SrTiO_3$ (STO) films have attracted much attention due to great application potential of such films. Industrial technology for STO gate dielectric has been already demonstrated [1]. Of special practical interest is possible strain-induced onset of ferroelectricity in epitaxial films quantum paraelectric STO [2]. Understanding of growth mechanisms and better knowledge of microstructure-properties relationship in STO films would allow development of novel electronic and optical devices.

To study STO growth and obtain strained epitaxial STO films, ultrathin (12 – 15 nm) STO films were deposited by pulsed laser ablation on various single-crystal substrates. The room-temperature crystal structure of the films was studied by x-ray diffraction using Cu Kα radiation with a postmonochromator. The crystal orientation, epitaxy, strains, and crystal perfection were analyzed using θ-2θ, ω-2θ, and ϕ scans, and ω rocking curves.

Epitaxial STO films were grown on $LaAlO_3$, $DyScO_3$, and $KTaO_3$ single-crystal substrates. Polycrystalline STO films were obtained on MgO due to large lattice misfit strain. Despite a good match of the (111) STO planes with (0001)Al_2O_3, epitaxial growth of STO required an additional epitaxial Pt buffer-electrode layer.

References

1. N. Menou et al., *Proc. IEEE 2008 International Electron Devices Meeting*, December 15 – 17, 2008, San Francisco, CA, USA, 2008, 929.

2. J. H. Haeni et al., *Nature* (London), 2004, 430, 758.

PO-6

ELECTRIC PROPERTIES OF $Na_{0.5}K_{0.5}(Nb_{1-x}Sb_x)O_3+0.5MnO_2$ CERAMICS (X=0.04, 0.05 AND 0.06)

J. Suchanicz[1], A. Finder[2], K. Konieczny[1], I. Jankowska-Sumara[1], B. Garbarz-Glos[1], R. Bujakiewicz-Korońska[1], K. Pytel[3], M. Antonova[4], I. Smeltere[4], A. Sternberg[4]

[1]*Institute of Physics, Pedagogical University, ul. Podchorążych 2, 30-084 Kraków, Poland,*

[2]*High National School, ul.Mickiewicza 21, 38-500 Sanok, Poland,*

[3]*Institute of Technics, Pedagogical University, ul. Podchorążych 2, 30-084 Krakow, Poland,*

[4]*Institute of Solid State Physics, University of Latvia, Kengaraga 8, LV-1063 Riga, Latvia*

e-mail: ilze.smeltere@hotmail.com

Lead-based materials such as PZT and PZT-based multicomponent ceramics are widely used due to their superior piezoelectric properties. However the lead compounds are toxic and the high volatileness of PbO causes compositional inhomogeneities and formation of the unwanted pyrochlore phase. Therefore it is necessary and urgent to search for lead-free materials with properties comparable with those found in lead-based ceramics. Some lead-free materials, including potassium sodium niobate $(Na_{0.5}K_{0.5})NbO_3$ (KNN) and KNN-based solid solutions could be good candidates with promising electromechanical properties.

Lead-free ceramics $Na_{0.5}K_{0.5}(Nb_{1-x}Sb_x)O_3+0.5MnO_2$ (x=0.04, 0.05 and 0.06) were prepared by the solid phase hot pressing sintering process and their dielectric properties have been studied. The obtained results were compared with these for pure KNN. The obtained samples showed a pure perovskite structure. Low frequency (100Hz-100kHz) investigations revealed the diffuse phase transitions. The obtained materials are expected to be a new and promising candidate for lead-free electronic ceramics.

PO-7

SYNTHESIS AND CHARACTERIZATION OF LEAD-FREE $1\text{-}x(K_{0.5}Na_{0.5})Nb_{1-y}Sb_yO_3\text{-}xBaTiO_3$

I. Smeltere[1], M. Antonova[1], M. Livinsh[1], B. Garbarz-Glos[2]

[1]*Institute of Solid State Physics University of Latvia, 8 Kengaraga Str., Riga, LV-1063, Latvia,*

[2]*Institute of Physics, Pedagogical University, ul.Podchorażych 2, 30-084 Krakov, Poland*

e-mail: ilze.smeltere@hotmail.com

Lead-free ceramics based on potassium sodium niobate (KNN) are considered to be a possible replacement for the widely used lead containing ceramics such as PZT, PMN-PT.

In the present work synthesis and characterization of new lead free ceramics based on KNN have been studied. Compositions based on our previous results [1] with a formula $(1\text{-}x)(K_{0.5}Na_{0.5})Nb_{1-y}Sb_yO_3\text{-}xBaTiO_3$ (x=0.02, 0.04; y=0.04, 0.07) were produced by conventional ceramic technology. MnO_2 was added to compositions to investigate the role of this doping element on the sintering of ceramics. X-ray diffraction analysis confirmed that obtained samples had a pure perovskite structure. Microstructural investigation reveals that ceramic samples have homogenous structure with cubical grain shape; the smaller ones ~0.5μm were slightly rounded. The grain sizes (0.4-2 μm) are quite similar for different compositions however MnO_2 addition suppresses the grain growth. Electron probe micro-analyzer (EPMA) examination showed even distribution of elements on the polished surface of investigated polycrystalline material samples. Phase transition point T_c is shifted to lower temperatures (200°C) in comparison to Sb-substituted KNN ceramics. Phase transition peak at T_c is broad indicating the diffuse phase transition.

References

1. M. Dambekalne; M. Antonova; M. Livinsh; A. Kalvane; A. Mishnov; I. Smeltere; R. Krutohvostov; K. Bormanis; A. Sternberg, *Integrated Ferroelectrics*, 2008, 102, *1*, 52 – 61

PO-8

MICROWAVE DIELECTRIC INVESTIGATIONS OF THE $0.7BaTiO_3$–$0.3(Ni,Zn)Fe_2O_4$ MULTIFERROIC COMPOSITES

T.Ramoška[1], J.Banys[1], L.Mitoseriu[2], V.Buscaglia[3]

[1]*Faculty of Physics, Vilnius University, Saulėtekio al. 9, Vilnius, Lithuania,*

[2]*University "Al. I. Cuza", Faculty of Physics, Bv. CarolI nr 11, Iasi 700506, Romania,*

[3] *Inst. of Energetics & Interphases IENI-CNR, Via de Marini 6 Genova I-16149, Italy*

e-mail: tadas.ramoska@ff.stud.vu.lt

The multiferroics are materials combining several properties in the same structure, such as electrical polarisation and magnetisation. The study of multiferroics is one of the most active field of the material science in the last 3 years.

Dielectric measurements of the $0,7BaTiO_3$–$0,3(Ni,Zn)Fe_2O_4$ (0,7BT-0,3NZF) in the temperature range of 170 K to 420K show three phase transitions, which temperatures matches those of bulk barium titanate.

Dielectric measurements in the frequency range of 100 Hz to 40 GHz show pronounced volume conductivity at lower frequencies range (lower than 100 kHz.). At frequencies higher than 100 kHz, the conductivity is practically eliminated and the fundamental dielectric dispersion can be observed.

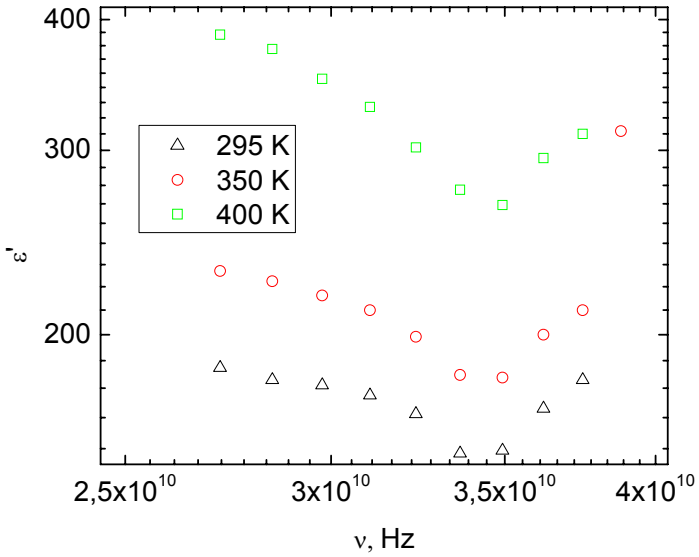

Fig.1 Frequency dependence of the real part of dielectric permittivity of $0,7BaTiO_3$–$0,3(Ni,Zn)Fe_2O_4$.

References

1. M. E. Lines and A. M. Glass, *Principles and Applications of Ferroelectrics and Related Materials*. Clarendon Press, Oxford, U.K., 1977.

2. B. Hallouet, B. Wetzel, and R. Pelster, *Journal of Nanomaterials*, 2007, 11.

3. B. Hallouet, P. Desclaux, B. Wetzel, A.K. Schlarb and R. Pelster, *Journal of Physics D: Applied Physics*, 2009, Volume 42, 064004.

PO-9

DIELECTRIC SPECTRA OF BARIUM TITANATE DOPED WITH LANTHANUM MAGNESIUM TITANATE

P. Keburis[1], J. Banys[1], A. Brilingas[1], A. N. Salak[2], V. M. Ferreira[2]

[1]*Physics Faculty of Vilnius University, Lithuania,*

[2]*Department of Ceramics and Glass Engineering/CICECO, University of Aveiro, Portugal*

e-mail: povilas.keburis@ff.vu.lt

Lead-free perovskite relaxors are known to be mainly solid solutions based on ferroelectrics like $BaTiO_3$, $(Na_{1/2}Bi_{1/2})TiO_3$ and $NaNbO_3$ with non-ferroelectric compositions. A number of relaxors have been derived from barium titanate (BT). Intentional cationic homovalent and heterovalent substitutions as well as both anionic and cationic heterovalent substitutions were done in the BT host matrix. Some of the resulting compositions are promising for environment-friendly application. It was shown that heterovalent substitutions suppress the ferroelectric phase transitions in BT and induce a relaxor behavior at much lower substitution rates than in the case of homovalent ones.

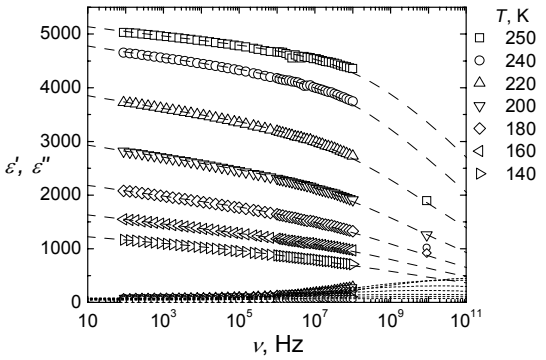

Fig.1 Frequency dependence of the real and imaginary parts of dielectric permittivity of 0.05LMT-BT ceramics for different temperatures.

Our earlier investigations have shown that even as low as 2.5 mol% doping with lanthanum magnesium titanate (LMT) were found to exhibit the features typical of both ferroelectrics and relaxors.

From the frequency dependences of the real and imaginary parts of the dielectric permittivity the parameters of dielectric dispersion and the real distribution function of the relaxation times $f(\tau)$ have been calculated. The dielectric spectra do not behave as it is typical for relaxors. The dielectric spectra show at least two different processes – one similar to relaxor, another one typical for the phase transition.

PO-10

RECONSTITUTION EFFECT OF LAYERED DOUBLE HYDROXIDE CONTAINING DIFFERENT CATIONS

K. Klemkaitė[1, 2], A. Khinsky[2], A. Kareiva[1]

[1]*Department of General and Inorganic Chemistry, Vilnius University, Lithuania,*

[2]*Norta Ltd, Kaunas, Lithuania*

e-mail: kristina.klemkaite@chf.stud.vu.lt

Layered Double Hydroxide (LDH) or hydrotalcite (HT) type materials are well known in catalysis, ion-exchange, adsorption and pharmaceutics applications [1]. The general formula is $[M^{II}_{1-x} M^{III}_{x} (OH)_2]^{x+} (A^{m-}_{x/m}]nH_2O$, where M is metal with different oxidation state usually +2 and +3, A is interlayer anion, mostly CO_3^{2-}. LDH with different cations composition were successfully synthesized by low supersaturation method, thermally decomposed and reconstituted in water and nitrate media. X-ray diffraction, X-ray fluorescence, thermal gravimetric analyses and scanning electron microscopy were used to investigate the difference of formed layered materials after synthesis and reconstitution process. There are only few studies where the influence of the third metal cation to the reconstitution process is analyzed. In this investigation transitional metal cations are already in the formed mixed oxide. Partial substitution of magnesium with cobalt and nickel cations do not lead to fundamental changes in the layered double hydroxide behaviour during the cycle (synthesis-thermal decomposition-reconstitution), investigated in this work. However some details, such as not full reconstitution of transitional metal containing samples at room temperature can be noted. Some features of the regeneration in liquid media, which are the influence of nature of media and its temperature are revealed. During regeneration in selected media no loss of essential transition metals were observed.

References

1. F. Li, X. Duan in: X. Duan, D.G. Evans, Editors, *Layered Double Hydroxides*, Springer-Verlag Berlin Heidelberg, 2006, 194-208.

2. J. Perez-Ramirez, S. Abello, N.M. van der Pers, *J. Phys. Chem.*, 2007, 111, 3642-3650.

3. T. Stanimirova, T. Stoilkova, G. Kirov, *Geochemistry, Mineralogy and Petrology*, 2007, 45, 119-127.

PO-11

DIELETRIC SPECTROSCOPY OF xNBT–(1-x)LMT CERAMICS

S. Rudys[1], M. Ivanov[1], J Banys[1], P. Vyshatko[2], A. N. Salak[2]

[1]*Vilnius University Faculty of Physics, Vilnius, Lithuania,*

[2]*Institute of Solid State and Semiconductor Physics, Belarus*

e-mail: rudys@elmika.com

Lead-free ceramics based on (Na0.5Bi0.5)TiO3 (NBT) are of an increasing interest due to high dielectric permittivity, making these materials promising in a wide spectrum of applications including those in a microwave range. Furthermore, there are evidences of good piezoelectric properties of the NBT-based ceramics. Pure NBT ceramics exhibit high dielectric losses, which are greatly reduced by doping with La(Mg0.5Ti0.5)O3 (LMT).

Dielectric properties of the xNBT–(1-x)LMT ceramics with x=0.95 were studied by means of dielectric spectroscopy over 150 – 800 K temperature and 100 Hz – 1000 MHz frequency ranges. These ceramics exhibit ferroelectric relaxor-like behavior in a vicinity of room temperature and high conductivity at high temperatures. Besides, there is a ferroelectric phase transition with dispersion region at microwave frequencies. In this work relaxation dynamics as well as conductivity parameters at high temperatures will be presented.

PO-12

PHASE TRANSITION DYNAMICS IN $Pb_5Ge_3O_{11}$ CRYSTALS

A. Dziaugys[1], J. Banys[1], M. P. Trubitsyn[2]

[1]*Departament of Radiophysics, Faculty of Physics, Vilnius University, Saulėtekio av. 9, Vilnius, Lithuania,*

[2]*Department of Solid State Physics, Dniepropetrovsk National University, vul. Naukova 13, Dniepropetrovsk, 49050 Ukraine*

e-mail: andrius.dziaugys@ff.vu.lt

Lead germanate is a well studied uniaxial ferroelectric crystal undergoing a second order ferroelectric phase transition at T_C = 441 K. Neutron and X-ray diffraction study[1, 2] have shown that PGO structure in paraelectric phase corresponds to hexagonal $P6(C^1_{3h})$ space symmetry group. On cooling below T_C lattice symmetry reduces to $P3(C^1_3)$ space group and spontaneous polarization appears along trigonal c axis. V. Vazhenin with co-authors reported the results of EPR investigations of PGO:Cu2+ crystals and concluded that magnetic ions occupy off-center positions in the structure [3]. Many papers are written about this crystal optical and dielectric properties but in narrow frequency range.

In this paper we present the dielectric permittivity measurements of PGO in wide frequency (20 Hz to 1 GHz) and temperature (120 K to 470 K) range. Dielectric dispersion was described with empirical Cole-Cole formula. On cooling mean Cole-Cole relaxation time τ_{CC} strongly increase and follows Vogel-Fulcher's law. Low frequency and temperature measurements indicate dipolar glass disorder which is presumably associated with domain walls motion. That proves dielectric measurements were done in applied external electric field.

References

1. Y. J. Iwata, *J. Phys. Soc. Jpn.*, 1977, 43, 961

2. M. I. Kay, R. E. Newnham, and R. W. Wolfe, *Ferroelectrics*, 1975, 9, 1

3. V. A. Vazhenin, A. D. Gorlov, and A. I. Krotkij, In: Radiospectroscopy of impurity centers in crystals with phase transitions (Kiev, IPM AN USSR, 1989), pp. 5–7 (in Russian).

PO-13

EFFECT OF ANNEALING ON POLARIZED STATE STABILITY IN SBN CRYSTALS

O.V. Malyshkina, V.S. Lisitsin, A.A. Movchikova, B.B.Pedko

[1]*Tver State University, Tver, Russia,*

[2]*State Marine Technical University of St. Petersburg, St.-Petersburg, Russia*

e-mail: Olga.Malyshkina@mail.ru

High electrooptical coefficients make it possible to use strontium-barium niobate (SBN) crystals for optical frequency conversion, development of optical memory and holography. For applications it is important to ensure the stability of polarization state with respect to temperature. So it is necessary to study the polarization state stability of this material.

The polarization profile of SBN crystals was studied by the TSW method [1, 2]. It was found that preliminary annealing of SBN crystals at 200 ^{o}C facilitates the uniform distribution of the polarization throughout the thickness of the sample poled ion an external electric field. Annealing also promotes the establishment of unipolarity of the sample as it is evidenced by the recovery of the polarized state after cooling from the paraelectric phase. The polarized state stabilization may be explained by the redistribution of Sr and Ba in the structure of these crystals [3].

This work was performed within the Federal Target Program "Research and Research-Pedagogical Personnel of Innovation Russia for 2009-2013" and supported by the Russian Foundation for Basic Research, project no. 08-02-97502-r_centre_a.

References

1. O.V. Malyshkina, A.A. Movchikova, G. Suchaneck, *Phys. of the Sol. St.*, 2007, 49, 2144 – 2147.

2. O.V. Malyshkina, A.A. Movchikova, *Phys. of the Sol. St.*, 2009, 51, 1381–1384.

3. M.P. Trubelja, E. Ryba, D.K. Smith, J. Mater. Sci., 1996, 31, 1435-1443.

PO-14

EFFECTS OF AXIAL PRESSURE ON THE ELECTRICAL PROPERTIES OF $Li_{0.06}Na_{0.94}NbO_3$ CERAMIC

W. Śmiga[1], A. Budziak[2], M. Antonova[3], M. Livinsh[3], B. Garbarz-Glos[1]

[1]*Institute of Physics, Pedagogical University, ul.Podchorążych 2, 30-084 Kraków, Poland,*

[2]*The H.Niewodniczanski Institute of Nuclear Physics Polish Academy of Sciences, ul.Radzikowskiego 152, 31-342 Kraków, Poland,*

[3]*Institute of Solid State Physics, University of Latvia, 8 Kengaraga Str., LV-1063 Riga, Latvia*

e-mail: mlivins@cfi.lu.lv

ABO_3-type compounds with perovskite structure are one of the most interesting group of materials. A great attention is focussed on crystalline- and ceramic $NaNbO_3$ as well as $NaNbO_3$-based solid solutions, which are the most useful materials for many applications. The solid solution with the formula $Li_{0.06}Na_{0.94}NbO_3$ was synthesized by the conventional solid-state reaction. The X-ray measurements showed, that the investigated compound at room temperature is characterised by the space group *Pm3m*. XRD results demonstrate that the values of lattice parameters *a, b, c,* and the volume of the unit cell *V* for $Li_{0.06}Na_{0.94}NbO_3$ are lower than for pure $NaNbO_3$. This is related to the fact that the ionic radius of Li^+ is much smaller than ionic radius of Na^+ which causes the decrease in the values of lattice parameters. The performed EDS investigations revealed that the $Li_{0.06}Na_{0.94}NbO_3$ sample was perfectly sintered. They contained a little glassy phase and their grains were well shaped. It was shown that dielectric behaviour of $Li_{0.06}Na_{0.94}NbO_3$ ceramics was sensitive to the applied compressive stress. The pressure shifts the temperature of phase transitions toward lower temperatures and decreases the values of electric permittivity, pyroelectric current and remanent polarization. This behaviour of the investigated material and the presence of remanent polarization above the temperature of phase transition (~575 K) indicate a diffused phase transition. The disappearance of the thermal hysteresis demonstrates the change in the nature of the phase transition from the first to second order. The obtained results of investigations of the lead-free ceramic $Li_{0.06}Na_{0.94}NbO_3$ suggest the possibility of practical application of this material. The solid solution $Li_{0.06}Na_{0.94}NbO_3$ is favourable in many applications as piezoelectric and pyroelectric elements taking into account the fact that it causes relatively low environmental pollution.

PO-15

MAGNETIC AND VIBRONIC THEORY OF THE INFLUENCE OF FERROELECTRICITY ON MAGNETIC PROPERTIES OF Bi-BASED MULTIFERROICS

P. Konsin, B. Sorkin

Institute of Physics, University of Tartu, Riia 142, 51014 Tartu, Estonia

e-mail: konsin@fi.tartu.ee

Multiferroics are multifunctional materials, in which two or more order parameters (ferroelectric, ferro(antiferro)magnetic and ferroelastic) coexist in a single compound [1-3]. In [4-6] it is shown that the electron-phonon (vibronic) covalent hybridization in the ABO_3 -type oxide-perovskites between empty d^0 states of the B ions and occupied oxygen 2p electronic states leads to the occurrence of the ferroelectric order. The theory of ferroelectric displacive phase transitions with an order-disorder component in the ABO_3 -type perovskites is developed in [6]. In [7] an approach is proposed for explaining of ferroelectric properties of the Bi-based multiferroic-perovskite-oxides ($BiFeO_3$, $BiMnO_3$, etc.). It is shown that the electron-lattice covalent hybridization between the Bi $6s^2$ lone electron pair and the empty oxygen 2p states causes instability of R_{25} and R_{15} polar vibrations in the reference cubic phase. The ferroelectric instability holds in the $R\bar{3}c$ phase and the observed ferroelectric transition $R\bar{3}c \rightarrow R3c$ is connected with the softening of the A_{2u} mode. In this report we take into account magnetic and vibronic couplings in the Bi-based multiferroics. Magnetism and ferroelectrcity are involved with local spins (Fe,Mn) and off-center structural distortions (Bi), respectively. We obtained the free energy of the Bi-based multiferroics in external electric and magnetic fields. On the basis of this free energy we investigated the magnetoelectric effects in the Bi-based multiferroics.

This work is supported by Estonian Science Foundation grant No. 7389.

References

1. G.A.Smolenskii and I.E.Chupis, *Sov. Phys. Usp*., 1982, 25, 475-493.

2. W.Eerenstein, N.D.Mathur, and J.F. Scott, *Nature,* 2006, 442, 759-765.

3. R.Ramesh and N.A.Spaldin, *Nature Mater*., 2007, 6, 21-29.

4. P.Konsin and N.Kristoffel, In: E.Bursian, Y.Girshberg, eds. *Interband Model of Ferroelectrics. Leningrad: Hertzen Pedagogical Institute*; 1987, 32-68; *Phys. Status Solidi* (b), 1988, 149, 11-40.

5. I.B.Bersuker, *The Jahn-Teller Effect. Cambridge: Cambridge University Press*; 2006, pp.616.

6. P.Konsin and B.Sorkin, *Ferroelectrics,* 2007, 353, 497-503; 2009, 379, 318-324.

7. P.Konsin and B.Sorkin, *Integrated Ferroelectrics*, 2009, 109, 81-94.

PO-16

DIELECTRIC AND MAGNETIC PROPERTIES OF CARBON-COATED NICKEL CAPSULES IN WIDE MICROWAVE FREQUENCY RANGE

M. Ivanov[1], S. Rudys[1], S. Lapinskas[1], J. Banys[1], J. Macutkevic[2], A. Ye. Yermakov[3], M. A. Uimin[3], A. A. Mysik[3], O. Shenderova[4]

[1]*Vilnius University Faculty of Physics, Lithuania,*

[2]*Semiconductor Physics Institute, Lithuania,*

[3]*UInstitute of Metal Physics, Ural Division, Russian Academy of Sciences, Russia,*

[4]*International Technology Center, Raleigh, North Carolina 27715, USA*

e-mail: maksim.ivanov@ff.stud.vu.lt

More and more different composites containing ferromagnetic and dielectric or ferroelectric materials are produced in the recent years, and one of the trends are composites exhibiting interesting both dielectric and magnetic properties, e. g. multiferroic ceramics. In case of complex magnetic permeability ($\mu^*=\mu'-j\mu'$) only frequencies below 1 MHz are available. However, to describe the new class of composites measurements must be performed in a wide frequency range, and preferably measurements of both magnetic and dielectric constant should be performed simultaneously.

There were previous works [1], where a toroidal sample of Ni@C was measured in a coaxial line in 2 – 18 GHz frequency range. In that study, the sample showed natural resonance at 5.5 GHz. There were relatively high dielectric losses and the sample showed diamagnetic properties above 6 GHz

In this work measurements of complex dielectric permittivity and complex dielectric permeability of carbon-coated capsules of Ni (Ni@C) embedded into polyurethane matrix were performed in 60 MHz – 36 GHz frequency range. Measurements showed, that Ni@C introduce both magnetic and dielectric losses, and at lower frequencies real part of magnetic permeability value is slightly bigger than 1.

References

1. X. F. Zhang et al., *Appl. Phys. Lett.*, 2006, 89.

PO-17

BROADBAND DIELECTRIC INVESTIGATION OF SODIUM POTASSIUM NIOBATE WITH 10% ANTIMONY SUBSTITUTION

S. Bagdzevicius[1], R. Grigalaitis [1], J. Banys [1], A. Sternberg [2], K. Bormanis [2]

[1]*Faculty of Physic, Vilnius University, Lithuania,*

[2]*Institute of Solid State Physic, University of Latvia, Latvia*

e-mail: sarunas.bagdzevicius@ff.stud.vu.lt

Lead containing ceramics like $Pb(Zr_xTi_{1-x})O_3$ (PZT) have excellent piezoelectric properties and are widely used in actuators, sensors, transducers and other electromechanical devices. However the use of lead-containing materials has caused serious environmental issues and should be replaced with lead-free materials [1]. One of such ceramic potentially could be sodium potassium niobate $K_xNa_{1-x}NbO_3$ (KNN) near morphotropic phase boundary (MPB) which is at about 50% K and 50% Na for KNN. The main problem with KNN is sintering: it is difficult to obtain well-sintered KNN ceramic using an ordinary sintering process because of the high volatility of alkaline elements at high temperatures [2].

In this work we present dielectric permittivity results of KNN ceramics doped antimony $(K_{0.5}Na_{0.5})(Nb_{0.9}Sb_{0.1})O_3$ with sintering aid MnO_2 (0.5 mol.%MnO_2). Its dielectric properties was investigated in broad frequency (from Hz to GHz) and temperature (from 25 K to 560 K) range.

Above room temperature obtained results shows two phase transitions at T= 498 K and T=389 K which could be attributed to phase transitions from paraelectric cubic into ferroelectric tetragonal state and from tetragonal into orthorhombic state because in undoped $K_{0.5}Na_{0.5}O_3$ ceramics it was observed the same sequence of transitions with T_c=677 K and T_{T-O}=464 K respectively [3]. Partial substitution of Nb^{+5} ions with Sb^{+5} lowers both of these phase transitions temperatures compared to undoped KNN ceramics. Below room temperature investigation revealed one more dielectric permittivity dispersion, which could be attributed to diffused phase transition corresponding to phase transition in pure KNN from orthorhombic into rhombohedral ferroelectric state at T_{O-R}=165 K [3]. Below 165 K there is a dielectric dispersion which is similar to the relaxor ferroelectric from the real part of dielectric permittivity frequency dependence, what is confirmed by linear dependence of dielectric losses.

References

1. Council Epat, Directive 2002/95/EC of the European parliament and of the council of January 2003 on the restriction of the use of hazardous substances in electrical and electronic equipment. *Eur. J.*, 2003, 37**,** 19.

2. M. Dambekalne et al, *Integrated Ferroelectrics*, 2008, 102, 1, 52-61.

3. E. Buixaderas, V. Bovtun, M. Kempa, M. Savinov, D. Nuzhnyy, F. Kadlec, P. Vanek, J. Petzelt, M. Eriksson and Z. Shen, *J. Appl. Phys*., 2010, 107, 014111.

PO-18

DIELECTRIC RESPONSE IN $(K_{0.5}Na_{0.5})(Nb_{1-x}Sb_x)O_3$+0.5mol%$MnO_2$ CERAMICS TO WEAK SINUSOIDAL FIELDS OF LOW AND INFRA-LOW FREQUENCIES

I. Smeltere[1], K. Bormanis[1], A.V. Sopit[2], A.I. Burkhanov[2]

[1]*Institute of Solid State Physics, University of Latvia, Riga, Latvia,*

[2]*Volgograd State Architectural and Engineering University, Volgograd, Russia*

e-mail*: bormanis@cfi.lu.lv*

Results of a study of dielectric response at low and infra-low frequencies in ferroelectric $(K_{0,5}Na_{0,5})(Nb_{1-x}Sb_x)O_3$+0,5mol%$MnO_2$ ceramics within the range of temperatures where the system undergoes a morphotropic transition between two orthorhombic phases are reported. Thermal behaviour of dielectric permittivity ε′(T) in samples of different antimony concentrations (*x*) is studied at frequencies from 1 to 1000 Hz under conditions of heating (1 °C/min) up to annealing of the sample at T = 300 °C.

The thermal anomaly as a shoulder on the ε′(T) curve corresponding to the structural phase transition caused by increasing *x* is found shifting to lower temperatures, for instance, in the case of 1 Hz (Fig. 1) – from T ≈ 185 °C to T ≈ 140 °C at changing concentration *x* from 0 mol % to 0.05 mol %. Another anomaly – a maximum on the ε′(T) curve is revealed at lower temperatures. Position (dotted arrows in Fig. 1) and size of the maximum depends on concentration *x*. Different from the shoulder the maximum shifts to higher temperatures and decreases with the growth of *x*. The anomaly at T ~ 80 °C is strongly dependent on the frequency of the measuring field (shrinking with increasing the frequency) and the sample history. In particular, it has been discovered not to show up at cooling from high temperatures being observed again at heating after having been left at room temperature for a few days. The grounds of the behaviour of dielectric response to low and infra-low frequencies in the range of structural phase transition and at lower temperatures are discussed.

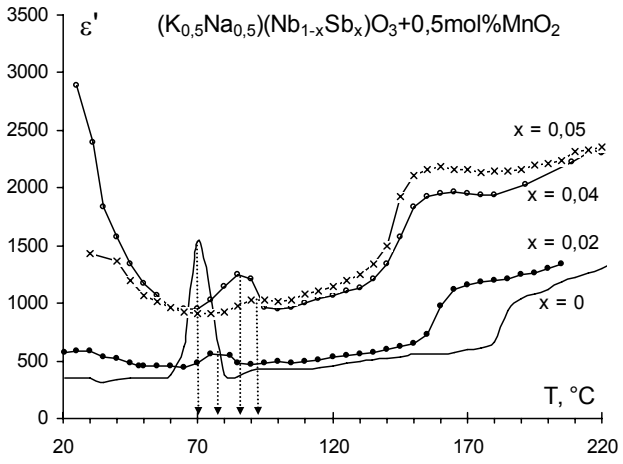

Fig. 1 Thermal behaviour of dielectric permittivity of $(K_{0,5}Na_{0,5})(Nb_{1-x}Sb_x)O_3$+0,5mol%$MnO_2$ ceramics (x=0; x=0.02; x=0.04; x=0.05 mol %.) at 1 Hz frequency of the measuring field.

PO-19

THE EFFECT OF BIAS FIELD ON DIELECTRIC RESPONSE IN LEAD FERROTANTALATE CERAMICS

K. Bormanis[1], A.I. Burkhanov[2], A.I. Vaingolts[2], A. Kalvane[1]

[1]*Institute of Solid State Physics, University of Latvia, Riga, Latvia,*

[2]*Volgograd State Architectural and Engineering University, Volgograd, Russia*

e-mail: bormanis@cfi.lu.lv

Lead ferrotantalate $PbFe_{1/2}Ta_{1/2}O_3$ is known as ferroelectric with a broad phase transition an anti-ferromagnetic ordering in which may occur at low temperatures [1].

The presently reported study of dielectric properties of the $PbFe_{1/2}Ta_{1/2}O_3$ ceramics at low and infra-low frequencies is made a wide range of temperatures under a bias field.

Behaviour of the effective depth of dielectric permittivity $\Delta\varepsilon(T)$ ($\Delta\varepsilon' = \varepsilon'_{1Hz} - \varepsilon'_{1kHz}$) over a range of temperatures is illustrated in Fig. 1. The inset shows behaviour of the parameter in the thermal range where anti-ferromagnetic ordering occurs (the Neel temperature T_N).

Applied field of $E_{=}$= 6 kV/cm enhances broadening of $\varepsilon'(T)$ maximums and shifts the maximums to higher temperatures.

Additional anomalies of the dielectric response are revealed at $T<T_m$. At bias field of 6 kV/cm applied to the sample the minimum of the $\Delta\varepsilon'(T)$ curve shifts considerably to a lower temperature (T_1 and T_2 respectively). Such anomalous behaviour of the dielectric response around T_N most likely is due to magneto-electric interaction rather than "freezing" of the domain structure as often observed in ordinary ferroelectrics at low temperatures in which case T_1 would shift to a higher temperature.

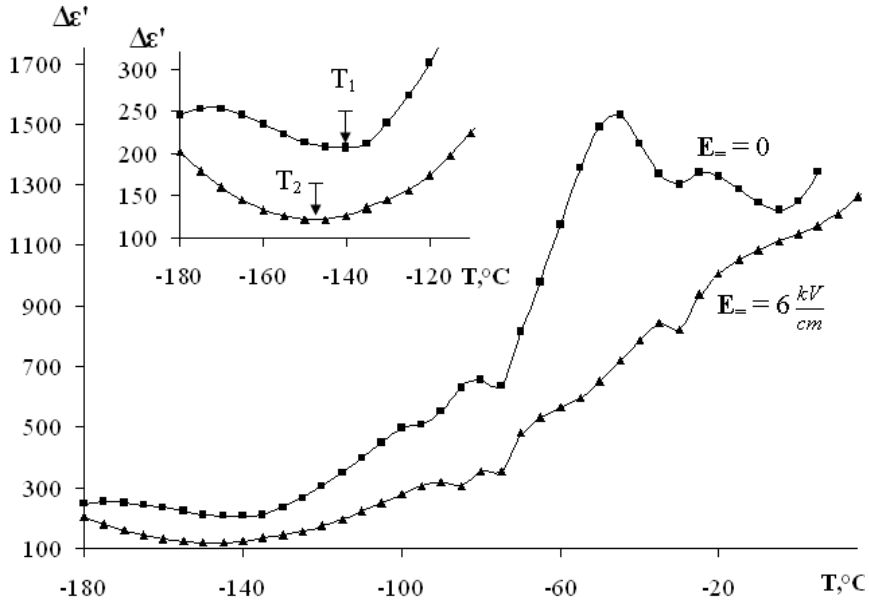

Fig.1

References

1.Yu.N. Venevtsev, V.V. Gagulin, and V.N. Ljubimov. *Ferromagnetics*. Moscow, Science, 1982.

PO-20

ELASTIC PROPERTIES OF BARIUM ZIRCONATE TITANATE CERAMICS

B. Garbarz-Glos[1], K. Bormanis[2], A. Kalvane[2], A. Budziak[3], W. Śmiga[1]

[1]*Institute of Physics, Pedagogical University, Podchorążych 2, 30-084 Krakow, Poland,*

[2]*Institute of Solid State Physics, University of Latvia, Kengeraga 8, LV-1063, Riga, Latvia,*

[3]*The H.Niewodniczanski Institute of Nuclear Physics Polish Academy of Sciences*

e-mail: bormanis@cfi.lu.lv

The barium zirconium titanate samples $BaZr_xTi_{1-x}O_3$ were prepared by conventional ceramic technology. Microstructure and material constants of polycrystalline ferroelectric materials $BaZr_xTi_{1-x}O_3$ for $0 \le x \le 0.35$ were investigated to determine their dependence on zirconium concentration. The performed measurements show that the material is chemically homogeneous. The examined samples are good quality, the grains are well shaped and there is a very small amount of a glassy phase. Material constants: the Young′s modulus E, the shear modulus G and the Poisson′s ratio ν were determined by ultrasonic method. The measurements were carried out with the INCO -VERITAS Ultrasonic Measuring Set UZP-1. Material constants were calculated from the longitudinal and transverse ultrasonic wave propagation velocity and the apparent density of the samples, using the following formulas:

$$E = V_L^2 \cdot \rho(1+\nu)(1-2\nu)/(1-\nu), \quad (1)$$

$$G = V_T^2 \rho, \quad (2)$$

$$\nu = (V_L^2 - 2V_T^2)/(2V_L^2 - 2V_T^2), \quad (3)$$

where E is Young′s modulus, G – shear modulus, ν - Poisson′s ratio, ρ - density, V_L – velocity of the longitudinal wave, V_T - velocity of the transverse wave.

The investigation of elastic properties was performed in order to determine the effect of the load of material on its properties, thus on the durability of the devices made of this material.

The ultrasonic wave velocity and the values of both Young′s modulus and the shear modulus are the highest for $BaZr_{0.30}Ti_{0.70}O_3$ sample (V_L = 5980.9 m/s, V_T = 3550.6 m/s, E = 163.88 GPa and G = 66.73 GPa). It has been shown that the Young′s modulus value increases with the increase of zirconium concentration in $BaTiO_3$. The dependence of shear modulus G on sample composition is similar to the respective dependences of Young's modulus E whereas the Poisson′s ratio ν decreases with the increase in zirconium concentration. The lowest value has been found for $BaZr_{0.275}Ti_{0.725}O_3$.

PO-21

DIELECTRIC PROPERTIES AND CONDUCTIVITY OF FERROELECTRIC $Li_xNa_{1-x}Ta_{0.1}Nb_{0.9}O_3$ SOLID SOLUTIONS

M.N. Palatnikov[1], V.A. Sandler[1], V.V. Efremov[1], N.V. Sidorov[1], K. Bormanis[2]

[1]*Institute of Chemistry, Kola Science Centre RAS, Russia,*

[2]*Institute of Solid State Physics, University of Latvia, Latvia*

e-mail: bormanis@cfi.lu.lv

Ferroelectric solid solutions (SS) of the perovskite sodium niobates possess properties of practical interest: in comparison with PLZT they have relatively low values of density and dielectric permeability, high values of sound velocity and piezoelectric parameters, and a wide range of mechanical Q-quality. Apart from that, the compounds do not contain lead for which reason industrial production of the group of materials comply with the up to date ecological requirements.

The presence of compositional and thermal phase transitions, including transitions related to change of the type of dipole ordering, and morphotropic regions of coexisting phases of different distortions of the perovskite structure is specific to phase diagrams of the $Li_xNa_{1-x}Ta_{0.1}Nb_{0.9}O_3$ SS.

Results of a study of dielectric properties and conductivity of the $Li_xNa_{1-x}Ta_{0.1}Nb_{0.9}O_3$ (x = 0.03 – 0.135) perovskite SS in a wide range of temperature and measuring field frequency are reported.

Ionic type of conductivity confirmed by the data obtained with the tested ceramic samples of $Li_xNa_{1-x}Ta_{0.1}Nb_{0.9}O_3$ (x = 0.03 – 0.135) SS is likely due to Li^+ ions of small radius since the perovskite crystal chemistry of the ABO_3 compounds providing a “conductivity window” between four BO_6 octahedrons mostly facilitates transport of the *A*-cations of a low activation enthalpy. The same is also suggested by the value of activation enthalpy H_a ~ (0.3 – 0.6) eV the bulk ion transport providing the major contribution to conductivity.

Results obtained within the studied range of temperatures indicate the presence of a first-order phase transition close to the second-order transition in the perovskite $Li_xNa_{1-x}Ta_{0.1}Nb_{0.9}O_3$ (x = 0.03 – 0.135) SS. The features of the second-order phase transition are enhanced by increasing the concentration of lithium.

PO-22

DIELECTRIC AND ELASTIC PARAMETERS OF $Li_xNa_{1-x}Ta_{0.1}Nb_{0.9}O_3$ FERROELECTRIC SOLID SOLUTION CERAMICS

M. Palatnikov[1], V. Efremov[1], O. Makarova[1], N. Sidorov[1], K. Bormanis[2]

[1]*Institute of Chemistry, Kola Science Centre RAS, Apatity, Murmansk Region, Russia,*

[2]*Institute of Solid State Physics, University of Latvia, Latvia*

e-mail: bormanis@cfi.lu.lv

The complex perovskite oxides are actively studied to reveal the nature of the observed properties and possible applications. The ferroelectric sodium niobate solid solutions (SS) of general formula $Li_xNa_{1-x}Ta_yNb_{1-y}O_3$ are distinguished among the well-known ferroelectric perovskite oxides for exceptional combinations of properties not encountered in other perovskite solid solution systems. As compared with PLZT ceramics, the sodium niobate SS have relatively low values of density and dielectric permittivity, higher sound velocity, excellent piezoelectric features, and a wide range of mechanical Q-quality. The $Li_xNa_{1-x}Ta_yNb_{1-y}O_3$ (x = 0 – 0.16) SS belong to the class of complex ferroelectric ABO_3 perovskites. The voids of cubic octahedrons (AO_{12} polyhedrons) in the structure of the solid solutions are occupied by two kinds of cations (A`, A``). The small size of cations (Li^+ and Na^+) compared with the size of the AO_{12} polyhedrons they occupy causes considerable distortion of the perfect perovskite sub-cell, which manifests itself in deformation and disorientation of the anion octahedrons, as in case of other sodium niobate SS. All that is the reason for a large amount of compositional structural transformations (morphotropic regions – MR) in the SS system of which the published data are rather contradictive. Similar structural transformations are going along with a series of electric and elastic anomalies with concentration.

Results of the studies of electric and elastic parameters as functions of concentration in the $Li_xNa_{1-x}Ta_{0.1}Nb_{0.9}O_3$ (x = 0 – 0.16) ferroelectric solid solutions are presented along with comparative data on elastic properties obtained by acoustic and contact techniques. Original experimental values of elastic modules, Poisson's coefficient, and Debye temperature determined from acoustic measurements are reported. The values of the elasticity modulus measured on a C3M "NanoScan" instrument well correlate with the acoustic data. Both the electric and elastic properties of the ferroelectric $Li_xNa_{1-x}Ta_{0.1}Nb_{0.9}O_3$ (x = 0 – 0.16) SS are shown to be sensitive to distortions of the structure at transformations triggered by changing the concentration. On the whole, the observed anomalous behaviour of the elastic properties at changing the concentration occurs together with the anomalies of different electrical factors.

The study is supported by RFBR grants 09-03-00141, 09-03-00189, 09-03-90401.

PO-23

GROWTH OF LITHIUM NIOBATE SINGLE CRYSTALS FROM GRANULATED CHARGE

M. Palatnikov[1], N. Sidorov[1], I. Biryukova[1], K. Bormanis[2]

[1]*Institute of Chemistry, Kola Science Centre RAS, Russia,*

[2]*Institute of Solid State Physics, University of Latvia, Latvia*

e-mail: bormanis@cfi.lu.lv

Finding the way of synthesis providing high purity single phase product of high degree of chemical homogeneity and perfect structure, predetermined proportion of the main components, a large discharge weight, and homogeneous grain composition is the main problem at preparing the mixture for lithium niobate.

The most popular procedure of preparing the mixture for lithium niobate comprises solid phase interaction between niobium pentoxide and lithium carbonate within the range of 600 – 1100 °C the difficulty of obtaining single phase final product with absolutely replicable proportion of alkali metal and niobium is a disadvantage of solid state synthesis. Completed reaction, single phase result, and composition of the final product depend on the size of grains, homogeneity of the mixture, and on deactivation of certain particles by the products of reactions. Unfinished solid state interaction is most possible when removing of gases from the reaction site is difficult in cases large quantities of the mixture are synthesised. Presence of unwanted phases causes formation of clustered heterogeneity of the density in single crystals deteriorating the physical quality of optical devices in which they are used.

A detailed study of circumstances under which granulated mixtures are obtained was made with the purpose to optimise technology of growing lithium niobate single crystals. The temperature of anomalous re-crystallisation of lithium niobate allowing to obtain mixtures of high discharge weights substantially improving economic measures of crystal technology is found to be within the pre-melting range (1240 – 1250 °C). The maximum discharge weight of granulated mixture is shown o be achieved with fired lithium niobate tablets, somewhat smaller with powdered mixture, and the smallest – in the synthesis-granulation cycle from Li_2CO_3-Nb_2O_5 mixture. Nevertheless, from time-consuming considerations of the process performing of synthesis and granulation is recommended in a single technological cycle from the Li_2CO_3-Nb_2O_5 mixture.

The study has been supported by RFBR grant 09-03-00141-a.

PO-24

PHYSICAL PROPERTIES AND STRUCTURE OF NIOBIUM PENTOXIDE CERAMICS TREATED BY CONCENTRATED LIGHT FLOW

M. Palatnikov[1], O. Shcherbina[1], A. Frolov[2], P. Chufyrev[1], N. Sidorov[1], K. Bormanis[3]

[1]*Institute of Chemistry, Kola Science Centre RAS,*

[2]*Frantsevich Institute for Problems of Materials Science of NASU,*

[3]*Institute of Solid State Physics, University of Latvia, Latvia*

e-mail: bormanis@cfi.lu.lv

A study of the effect of treatment by high-energy concentrated light flows (CLF) on formation micro- and nano-structures, thermal expansion, elastic properties, and Raman spectra (RS) of ceramic niobium pentoxide is reported. Regions of negative or near to zero thermal expansion in samples of Nb_2O_5 ceramics arise due to formation of fractal micro- and nano-structures under treatment by CLF. Elastic modules of Nb_2O_5 ceramics treated by CLF have been measured by contact techniques under a probe nano-indenter microhardness meter. The modulus of elasticity of ceramic Nb_2O_5 is found to increase with increasing intensity of the CFL.

Raman studies of ceramic Nb_2O_5 pre-treated by CLF show increase of relative intensity of the 118 cm^{-1} band corresponding to librations of tetrahedrons and of the 1002 cm^{-1} band corresponding to the stretch of the Nb–O bond. Intensity of the 55 cm^{-1} Raman band corresponding to librations of octahedrons is maintained constant. Thus, under CLF the bonding of Nb—O—Nb in the octahedron chains is destructed, more so of the tetrahedrons, creating marginal Nb–O bonds. The structure of Nb_2O_5 becomes partly separated. Proportion of the octahedrons and tetrahedrons with marginal Nb–O bonds significantly increases with the intensity of the CLF the reason of which is extremely fast melting of ceramic Nb_2O_5 under CLF partial dissociation in the liquid state and fast out of equilibrium crystallisation after removal of the sample from the CLF zone. As a result, the structure is likely comprised of partly separated islands emergence of which possibly contributes to decrease of thermal expansion along with formation of fractal micro- and nano-structures under CLF.

The study is supported by grant of RFBR 09-03-00141.

PO-25

KINETICS OF PHOTOREFRACTIVE LIGHT SCATTERING IN $LiNbO_3$:Cu[0.015 % mass] AND $LiNbO_3$:Zn[0.5 % mass] SINGLE CRYSTALS

N.V. Sidorov[1], E.A. Antonicheva[2], A.V. Syuy[2], M.N. Palatnikov[1], K. Bormanis[3]

[1]*Institute of Chemistry, Kola Science Centre RAS, Russia,*

[2]*Far Eastern State Transport University, Khabarovsc, Russia,*

[3]*Institute of Solid State Physics, University of Latvia, Latvia*

e-mail: bormanis@cfi.lu.lv

Lithium niobate ($LiNbO_3$) single crystal is a promising material for transformers of laser radiation, holography, and active nonlinear laser media comprising regularly polarised domains of sub-micron size. Photorefractive light scattering (PRLS) is one of most essential factors deteriorating parameters of optical elements. Because of PRLS laser beam in the single crystal is sturdily destructed. Published data on PRLS in lithium niobate concern studies either of ostensibly pure congruent single crystals or single crystals with admixture of Fe and Rh. Lithium niobate single crystals containing admixture of Cu present are prospective as material to be used in optical elements for holographic recording.

Reported is a study of the kinetics of PRLS in optically non-linear $LiNbO_3$ single crystals of congruent composition (Li/Nb = 0.946) containing admixture of polyvalent cations – photo-refractive Cu[0.015 % mass] and non-photo-refractive Zn[0.5 % mass]. The PRLS was excited by radiation of an MLL-100 Y:Al garnet laser of wavelength λ_o = 501 – 561 nm the power being varied from 35 to 160 mW. More powerful radiation of 640 mW was provided by a “Spectra Physics” 2018-RM Argon laser (λ_o = 514.5 nm).

Intensity of the effect of photo-refraction and the indicator diagram of the PRLS in single crystals containing admixture of Cu and in single crystals containing Zn were found to be different. In both cases the angle of the PRLS intensity indicator diagram reaches its stationary size faster at higher laser radiation intensities. Distribution of the bivalent and trivalent Cu cations in the structure of the lithium niobate single crystals, even at small concentrations, is strongly non-uniform for which reason the samples for studies of PRLS being of interest for developing technologies of growing large-size commercial homogeneous single crystals were cut from different parts of the single crystal ingot (the raw single crystal block as grown).

The effect is most pronounced in samples cut from the cone site of the ingot suggesting of higher concentrations of defects in this part of the grown crystal. The relatively weak photo-refraction in the $LiNbO_3$:Cu[0.015 % mass] single crystal compared with that observed in the $LiNbO_3$:Zn[0.5 % mass] single crystal is due to the Cu cations being mostly in the bivalent state within the structure of $LiNbO_3$ while the fraction of Cu^{3+} cations is insignificant. Recharging of Cu cations and intensification of photo-refraction do not occur at laser irradiation of such crystals.

PO-26

MODELLING OF CLUSTER FORMATION IN OPTICALLY NONLINEAR LITHIUM NIOBATE CRYSTAL

V.M. Voskresenskiy[1], O.R. Starodub[1], N.V. Sidorov[1], M.N. Palatnikov[1], K. Bormanis[2]

[1]*Institute of Chemistry, Kola Science Centre RAS, Russia,*

[2]*Institute of Solid State Physics, University of Latvia, Latvia*

e-mail: bormanis@cfi.lu.lv

Computer-aided modelling of ordering structural units and formation of clusters determining the optical and optically nonlinear characteristics if lithium niobate ($LiNbO_3$) crystals is of practical importance. On the basis of such calculations the properties of the crystal at changing the composition may become predictable.

In the present paper the clusters in the structure of lithium niobate with different Li/Nb ratio studied by using of original software are reported. Obtained results are compared with data of vacancy models describing disordering of structure of the lithium niobate crystal containing 30 ions in the elementary cell of the R3c symmetry. The cluster for modelling is obtained by translating the elementary cell along X, Y, and Z axes. The coordinates of ions considered as point charges are set according to X-ray analysis. The “critical” ions “perturbing” equilibrium of the system are revealed by calculating the total energy in the cluster brought to a stable state removing ions of a positive energy of interaction. However a non-zero dipole moment is found along the crystallographic axes X and Y it gradually decreases with growth of the cluster along those axes. The maximum value of dipole moment is obtained along the polar axis Z. The possibility of forced displacement of atoms in the cluster is provided in the software complex to examine the process of defect formation. The calculations show increase of energy and the dipole moment in case parameters of the cell increase. The change of energy is fastest with changes along the Y axis, then along X axis and slowest with changes along Z axis.

The studies suggest conclusions related to formation and dynamics of structural defects of the crystal lattice and being valuable for interpretations of photo-refractive and non-linear optical properties, as well as for agreement between the obtained data and theoretical models.

PO-27

POLARISATION DEPENDENT RAMAN STUDY OF SINGLE-CRYSTAL NICKEL OXIDE

N. Mironova-Ulmane[1], A. Kuzmin[1], I. Sildos[2], M. Pärs[2]

[1]*Institute of Solid State Physics, University of Latvia, Latvia,*

[2]*Institute of Physics, University of Tartu, Tartu, Estonia*

e-mail: ulman@latnet.lv

In this work we have studied the domain structure and Raman scattering in single-crystal NiO with three different (100), (110) and (111) orientations. Due to the antiferromagnetic ordering present in NiO at room temperature, the two-magnon Raman band at 1500 cm^{-1} is clearly observed for all three orientations. However, its intensity varies significantly relative to that of one-phonon and two-phonon bands, located below 1300 cm^{-1}.

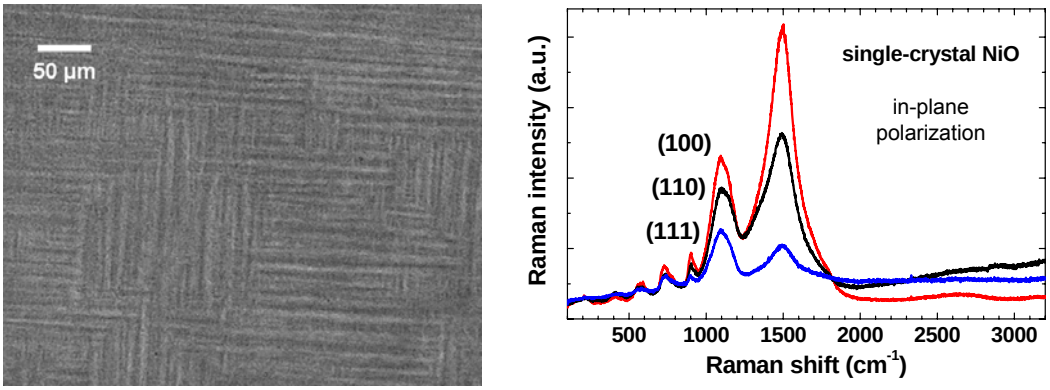

Left panel:domain structure of NiO(100) observed in crossed-polarizers geometry. Right panel: micro-Raman spectra of (100), (110) and (111) NiO single-crystals, measured with in-plane orientation of laser polarization.

The domain structure with different patterns has been observed for three different NiO orientations: chess-like for NiO(100), stripe-like for NiO(110) and mono-domain for NiO(111). We will show that it can be distinguished using the ratio of the phonon (at 1100 cm^{-1}) to magnon (at 1500 cm^{-1}) bands intensity, measured for two specific in-plane orientations of the single crystals. The method can be applied for determination of microcrystals orientation.

PO-28

INVESTIGATION OF THE TEMPERATURE-STIMULATED STRUCTURE CHANGES IN THIN GARNET FILMS BY USING OF THE ELECTROMAGNETO-OPTICAL METHOD

V. Koronovskyy

Department of Radiophysics, Taras Shevchenko Kiev National University, 2, Prospekt Glushkova Street, 03127 Kiev, Ukraine

e-mail: koron@univ.kiev.ua

Magneto-electric properties of temperature-influensed bismuth-substituted ferrite-garnet films have been investigated by using optical polarimetry method (the electromagneto-optical (EMO) effect). This method deals with the registration of the changes of light polarization plane Faraday rotation under action of an external electric field applied to the film [1-4]. The appearance of such changes (α_{EMO}) has been termed as the EMO effect [1]. Experiments were carried out at room temperature in geometry **H**□**E**□**k**, where **H** – static magnetic field, **E** – low-frequency variable electric field, **k** –light wave vector. Thermal influence on the film was spent at temperature $T = 973K$ throughout 120 minutes with the subsequent slow cooling.

We experimentally reveal changes in magnetic-field and electric-field dependences of EMO effect in investigated film after thermal influence - the α_{EMO} parameter is grown. To interpret such change of EMO effect we present the following explanation. Ferrite-garnet films grown on mismatched substrates and can be strained. Further, on film volume there can be thin layers or local sites where the centro-symmetric cubic crystal structure that is characteristic for single crystals samples of ferrite-garnet is broken. Thermal influence on the sample (initially directed to the purposeful change of density of dot defects in film) can remove local pressure in films and our experiments show the results of such an influence.

Thus, thermal influense leads to increase in the electromagneto-optical effect value, because of temperature-stimulated relaxations of non-uniform mechanical pressure in the studied sample and relaxation of the film deformations by substrate.

References

1. B. B. Krichevtsov, R. V. Pisarev, A. G. Selitskij, *JETP Lett.,* 1985, 41, 317.

2. V.E. Koronovskyy, S.M. Ryabchenko, V.F. Kovalenko, *Phys Rev B*, 2005, 71, 172402-172406.

3. V.E. Koronovskyy, *J Apl Phys*, 2009, 106, 6, 063914-063916.

4. V.E. Koronovskyy, *Integrated Ferroelectrics*, 2009, 109, 76-80.

PO-29

APPLICATION OF METAL COATINGS FOR FUNCTIONALIZATION OF LEACHED GLASS FABRICS

A. Lusis, E. Pentjuss, L. Petersone, J. Balodis

Institute of Solid State Physics of University of Latvia, Kengaraga Street 8, Riga, LV-1063

e-mail: lusis@latnet.lv

The functionalization of technical glass fibers and fabrics will be discussed. The plasma treatment and thin film coatings in combination with sonochemical processes are used for nanostructuring and functionalization of fibers and fabrics. The leached K-glass fabric had been coated with Ni by DC magnetron sputtering in 100% Ar and studied as electrode in electrochemical cell with NaOH electrolyte. The sheet resistances of such electrodes are 38 kOhm cm^2.

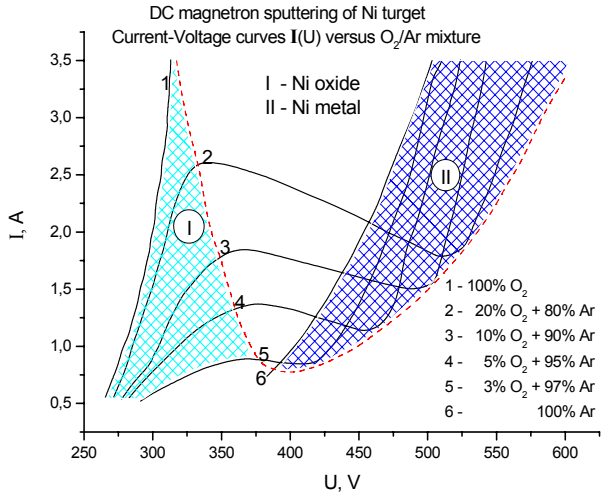

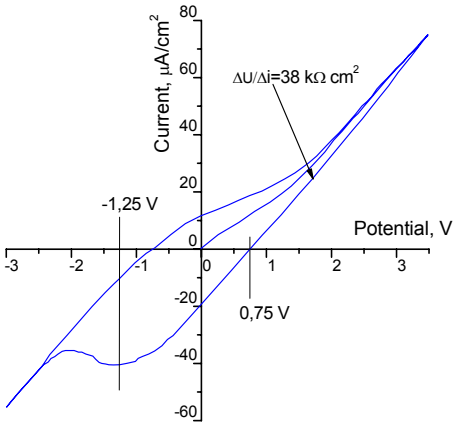

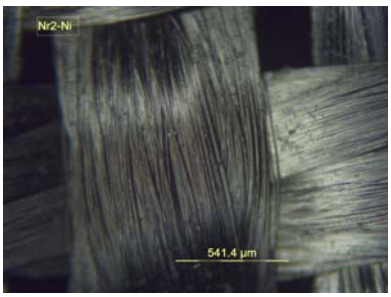

The cyclic valtamperogram of such Ni electrode:

PO-30

NOVEL Pd SUPPORTED CATALYSTS FOR GLYCERIC ACID SELECTIVE PRODUCTION

S. Cornaja[1], L. Kuļikova[2], V. Serga[2], V. Kampars[1], K. Dubencovs[1], S. Žižkuna[1], O. Muravjova[1]

[1]*Faculty of Material Science And Applied Chemistry, Riga Technical University, Latvia,*

[2]*Institute of Inorganic Chemistry, Riga Technical University, Latvia*

e-mail: svetlana@ktf.rtu.lv

Catalytic oxidation of glycerol by molecular oxygen in presence of novel Pd supported catalysts in alkaline water solutions in various types of reactors is researched. Glyceric acid is obtained with high yield and selectivity. New method of supported Pd catalysts synthesis, i.e. extraction-pyrolysis method, is developed. Nanopowders of Al_2O_3, Si_3N_4 and Y_2O_3 (the specific surface area 20-46.7 m^2/g), prepared by plasma method were used as supports.

It is found that glycerol conversion and selectivity of glyceric acid yield depends from both catalyst composition and conditions of oxidation (table).

Table

Glycerol catalytic oxidation with molecular oxygen in presence of novel supported Pd catalysts

№	Catalyst	c_0(NaOH), M	n(glic)/n(Pd) mol/mol	t, h	Glycerol conversion, %	Glyceric acid	
						Yield, %	Selectivity, %
1[a]	1,25% Pd/Al_2O_3	0.7	400	7.5	100	76	76
2[a]	1,25% Pd/Al_2O_3	1.5	400	7.5	92	68	74
3[b]	1,25% Pd/Al_2O_3	1.5	300	7.0	95	70	74
6[a]	2,5% Pd/Al_2O_3	0.7	300	10.0	100	78	78
7[a]	2,5% Pd/Al_2O_3	0.7	400	10.0	93	72	77

T=333K, $P_{O_2} = 1$ bar, c_0(glic) = 0,3 M, a - barbotage type reactor, b – closed thermostated gasometrical equipment

PO-31

NANOSIZED DEFECTS ON THE SURFACE OF IRRADIATED LiF CRYSTALS

A. Dauletbekova[1], M.Zdorovets[2], A. Akilbekov[1], A. Abdrahmetova[1], F. Abuova[1]

[1]*L.N. Gumilyov Eurasian National University, 5 Munaitpassov str., 010008, Astana, the Republic of Kazakhstan,*

[2]*Institute of Nuclear Physics, the cyclotron ion accelerator DC-60, 2/1 Abylaikhan av., 010008, Astana, the Republic of Kazakhstan*

e-mail: alma_dauletbek@mail.ru

Pyramidal depressions of each track can be noticed on SEM images of the irradiated surface after etching process. AFM image of the same surface gives information about the depth of etching pit that equals to 90 nm. From our optical measurements radius of the track for N is 4 nm and path length is 11 microns that is the pyramidal etching pit is the ion excited region. After the irradiation with various ions all crystals reveal appearance of nanostructures named hillock on the surface of the crystals. The number of hillocks is in compliance with ion fluence to a precision of 10 %. Heights have been received from topographical micrograph. Considering values of electronic energy loss 1.65 keV/nm for nitrogen, 12.11 keV/nm for krypton and 18.85 keV/nm for xenon, one can observe height increase of the hillocks from 13 nm, 24 nm and 39 nm, accordingly, average roughness of unirradiated surface is 5 nm. We offer dipole creation mechanism of hillocks.

PO-32

PALLADIUM NANOCRYSTALLINE FILMS PRODUCED BY EPM. PHASE COMPOSITION AND MAGNETIC PROPERTIES

V. Serga[1], L. Kulikova[1], M. Maiorov[2], A.Krumina[1]

[1]*Institute of Inorganic Chemistry, Riga Technical University, Latvia,*

[2]*Institute of Physics, University of Latvia*

e-mail: vera_serga@inbox.lv

The extractive pyrolytic method (EPM) is a modern method, which allows producing volume samples and film materials on substrates [1]. Earlier [2], the EPM was also applied to produce high disperse palladium particles on nanoporous microgranules α- Al_2O_3. The investigation of produced nanocomposites is complicated by the presence of a large amount of the carrier (>90%). In this investigation, palladium films were produced on a water-soluble carrier (crystalline NaCI), and after its removal the phase composition and magnetic properties of the films were studied.

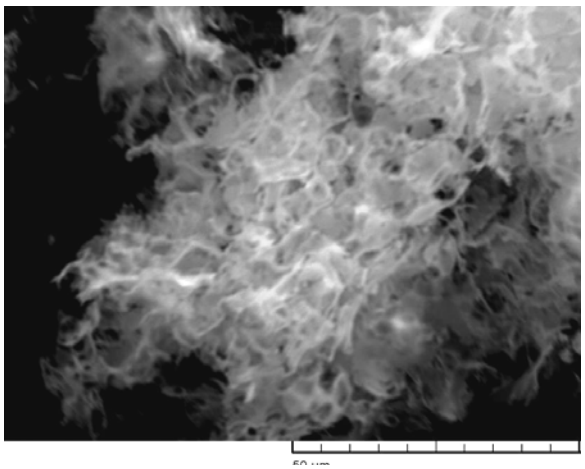

Fig.1 SEM image of the palladium films.

The micrograph of the palladium films prepared by pyrolysis at 300 ^{0}C during 5 minutes is presented in Fig. 1. X-ray diffraction data demonstrated that under the above-described conditions two crystalline phases of palladium existed, moreover, the peaks of the fist (basic) phase corresponded to the standard maxima of X-ray diffraction and those of the second phase were shifted towards the crystal lattice parameter increase. It has been found that the increase of the thermal treatment period to 20 minutes results in increase of final product crystallinity. The phase composition also changes: the basic palladium phase is present only, and PdO phase appears.

The results of magnetic measurements showed that all samples had weak ferromagnetic properties at room temperature regardless of the phase composition and crystal size.

References

1. A.I.Kholkin, T.N.Patrusheva. Extractive-pyrolytic method. M., “Com Book”, 2006.

2. V.Serga, L.Kulikova, E.Palcevskis, M.Maiorov, A.Krumina. Proc. Int. Baltic Sea Reg. Conf. FM&NT, Riga, 2009, 158.

PO-33

SULPHIDE NANOSTRUCTURE FABRICATION USING PULSED LASER DEPOSITION

A. Petruhins[1], B. Polyakov[1], E. Tamanis[2], I. Tale[1], P. Kulis[1]

[1]*Institute of Solid State Physics, University of Latvia, Latvia,*

[2]*G.Liberta Microscopy Center, University of Daugavpils, Latvia*

e-mail: andrejs.petruhins@cfi.lu.lv

Lead sulphide (PbS) is a direct band gap (E_g=0.4eV), well-known p-type semiconductor material, widely used for manufacturing of near infrared and radiation detectors. Recently PbS nanocrystals have gained much interest, most notably for ability of bandgap to be tailored in range 0.4-2.5 eV by decreasing nanocrystal size due to quantum confinement [1]. ZnS may be easily doped to be p- or n-type semiconductor (E_g=3.6-3.9 eV). ZnS is often used for passivation of sulphide nanoparticles [2]. Nanocrystalline PbS may be combined with ZnS for ETA-type (Extremely Thin Absorber) solar cells. ZnS and PbS don't form solid solutions. Introducing ZnS in deposition process gives several advantages such as stabilization of PbS nanocrystals, and opens a gateway for thermal annealing.

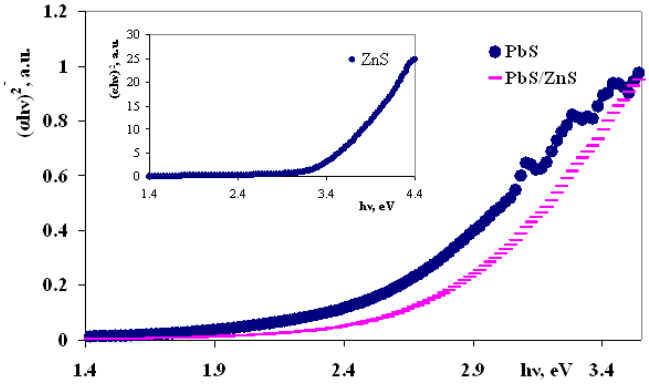

Fig.1 Absorption spectra of pure PbS and PbS/ZnS thin film. Insert: absorption spectrum of ZnS thin film.

Pure PbS and ZnS thin films were deposited using pulsed laser deposition (PLD) on various substrates. Optical band gap of ZnS is about 3.5 eV (Fig.1, insert). Optical absorption spectrum of PbS thin film is blue shifted in comparison with bulk material. Band gap of PLD deposited PbS thin film was found to be around 2.4 eV, however some absorption is present at smaller photon energies. AFM measurements reveal that PbS nanocrystals over broad size range are present in the film, therefore both bulk and nanocrystal component is visible in absorption spectrum. Simultaneous deposition of PbS and ZnS material results in small additional blue shift of absorption edge respective to pure PbS film (Fig. 1).

References

1. M.Hines, G.Sholes, *Adv. Mater.*, 2003, 15, 21, 1844.

2. M.Santos, J.Ferreira, E.Radovanovic, R.Romano ,O.Alves , Egirotto, *Thin Solid Films,* 2009, 517, 5523.

PO-34

LASER INDUCED ABLATION ANALYSIS OF POST-MORTEM TILES OF ASDEX UPGRADE TOKAMAK

A. Voitkans, J. Butikova, I. Tale

Institute of Solid State Physics, University of Latvia

e-mail: sf11029@lanet.lv

The control of accumulation of the impurities is the crucial issue for the fusion devices [1]. The evaluation of the concentration and depth profiling of the impurities in the post-mortem tiles from the chamber of the ASDEX (Axially Symmetric Divertor EXperiment) Upgrade tokamak was performed using ablation by the sequence of single laser pulses.

In the graphite tiles, the concentration of deuterium decreases during the first few laser pulses and corresponds to the layer depth of 0.8 to 1.2 μm. The reference sample containing implanted deuterium, exhibits the maximum concentration of deuterium in about 200 μm.

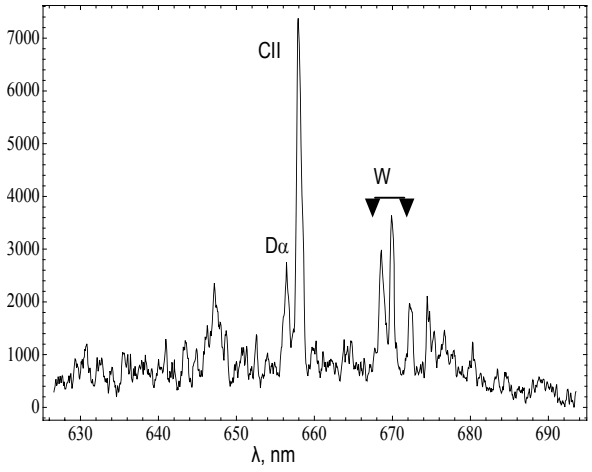

Fig.1 Spectrum of the tungsten coated graphite tile demonstrates growth of carbon line intensity after the 6th laser pulse.

In the tungsten coated graphite sample, deuterium is accumulated mainly above the tungsten layer. The growth of carbon content in the region of tungsten layer indicates that a single ablation event can built destroyed islands in the tungsten layer leading to appearance of the carbon line in the spectrum.

References

1. E.Gauthier, *J.Nucl.Mater.*, 2009, 390-391, 1059-1065.

PO-35

POSITRONICS AND NANOTECHNOLOGIES: POSSIBILITIES OF STUDYING NANOOBJECTS IN TECHNICALLY IMPORTANT MATERIALS AND NANOMATERIALS

E.P. Prokopev[1, 2], V.I. Grafutin[2], S.P. Timoshenkov[1]

[1]*Moscow state institute of electronic technology (MIET), Zelenograd, pas. 4806, bld. 5, 124498, Moscow, Russia,*

[2]*A.I.Alikhanov Institute for theoretical and experimental physics (ITEP), B.Cheremushkinskaya steet, 25, 117259, Moscow, Russia*

e-mail: epprokopiev@mail.ru

The article proves that one of the effective methods to define sizes of nanodefects (vacancies, clusters of vacancies), free pore volumes, cavities and holes, and their concentration and chemical composition in annihilation place in nanomaterials and other technically important materials, is positron annihilation spectroscopy (PAS) method. There is given a brief review of experimental researches of nanodefects in porous silicon, silicon and monocrystals of quartz irradiated by protons as well as in powders of quartz. By PAS method there are defined chemical composition of environment in a annihilation place: on external valent electrons of silicon atoms pore"wall", the sizes and the concentration of nanodefects in a number of nanomaterials: in monocrystal silicon plates and in monocrystals of quartz irradiated by protons, in porous silicon, and also in powders of quartz.

References

1. Y.A.Chaplygin, S.A.Gavrilov, V.I.Grafutin, E.P.Svetlov-Prokopiev, and S.P.Timoshenkov. Positronics and nanotechnologies: possibilities of studying nano-objects in technically important materials and nanomaterials. *Proc. IMechE. Part N: J. Nanoengineering and Nanosystems*. 2007. Vol. 221. №4. P.125-132.

PO-36

NANOSIZED PEROVSKITES FOR PHOTOCATALYTICAL WATER DECOMPOSITION

L. Grinberga

Institute of Solid State Physics, University of Latvia

e-mail: Liga.Grinberga@cfi.lu.lv

Hydrogen is considered to be one of the most prospective candidates to meet the rising demand for renewable sources of energy across the world. Hydrogen powered fuel cells and solar energy is the best hope for a more environmentally friendly and resource-sparing energy supply in the future [1]. However, at the present only about 5% of the commercial hydrogen is produced by water electrolysis, while other 95% of the hydrogen is directly or indirectly obtained from fossil fuels [2]. Photocatalysis of water molecules induced by the sunlight is considered to be particularly "green" method for hydrogen production.

Nanosized perovskites among huge variety of the materials possess excellent photocatalytical properties, for example, quantum efficiency of the hydrogen production under UV illumination in La-doped $NaTaO_3$ reaches 56% [3].

In this work an overview of the most prospective nanosized perovskite type materials will be given and different synthesis techniques will be analyzed.

The financial support of ESF project 2009/0202/1DP/1.1.1.2.0/09/APIA/VIAA/141 is greatly acknowledged.

References:

1. T. Nann, S. K. Ibrahim, P. M. Woi, S. Xu, J. Ziegler, C. J. Pickett, *Angewandte Chemie*, 2010, **49**, 9, 1574 – 1577.

2. Y. Li, J. Wu, Y. Huang, M. Huang, J. Lin, *International Journal of Hydrogen Energy*, 2009, **34**, 19, 7927 – 7933.

3. D. G. Porob, P. A. Maggard, *Journal of Solid State Chemistry*, 2006, **179**, 1727 – 1732.

PO-37

SPEEK AND PANI BASED MEMBRANES FOR FUEL CELLS

J. Hodakovska, J. Kleperis

Institute of Solid State Physics of University of Latvia

e-mail: julia_h_lv@yahoo.co.uk

Polymer membrane fuel cells are working at comparably low temperatures – from room temperatures till around 200 °C, but typically around 60 – 100 °C. One of the problem of these devices is to provide good contact between membrane, catalyst, gas diffusion layer and electrode. Now carbon cloth – material very different from polymer membrane – is used as carrier for catalyst and gas diffusion layer. One from the possible improvements would be to use instead carbon cloth the same polymer material as for membrane one, but with additive of electron conductive material.

In our work the composition based on well-known proton conductive polymer – sulfonated poly(ether-ether-ketone) (SPEEK) and electron conductive polyaniline (PANI) is elaborated and studied.

PO-38

ANION EXCHANGE MEMBRANE BASED ON ALKALI DOPED POLY(2,5-BENZIMIDAZOLE) FOR ALKALINE MEMBRANE FUEL CELL

H. Luo[1], G. Vaivars[2], S. Nonjola[1], M. Rohwer[1], M. Mathe[1]

[1]*The Council for Scientific and Industrial Research, South Africa,*

[2]*Institute of Solid State Physics, University of Latvia*

e-mail: Guntars.Vaivars@cfi.lu.lv

Alkaline membrane fuel cell (AMFC) has been received increased attention among the different types of fuel cells. Ammonium quaternized polymers such as poly(arylene ether sulfones) are being developed and studied as candidates of ionomeric materials for AMFCs, due to their low cost and promising electrochemical properties. However, the performance of AMFC based on this type of membrane is still low due to the easy degradation in alkaline medium at temperatures above 60 °C [1-3]. Nevertheless, the development of anion exchange membranes for AMFC with improved performance is still required [4].

In this work, an anion exchange membrane based on alkali doped ABPBI is reported for the first time. The alkali doped poly(2,5-benzimidazole) membrane is a promising candidate as anion exchange membrane for fuel cell application. The alkali doped poly(2,5-benzimidazole) membrane reached an anion conductivity of 2.3×10-2 S cm-1 at room temperature. The alkali doped poly(2,5-benzimidazole) membrane showed excellent anion conductive stability in the alkali media up to 100 °C and high thermal stability comparing with membranes based on quaternized polymers.

References

1. A.A.Zagorodni, D.L.Kotova, V.F.Selemenev, *React.Funct.Polym.*, 2002, 53, 157-171.

2. V.Neagu, I.Bunia, I.Plesca, *Polym.Degrad.Stabil.*, 2000, 70, 463-468.

3. T.Sata, M.Tsujimoto, T.Yamaguchi, K.Matsusaki, *J.Membrane Sci.*, 1996, 112, 161-170.

4. H.Hou, G.Sun, R.He, B.Sun, W.Jin, H.Liu, Q.Xin, *Int.J.Hydrogen Energ.*, 2008, 33, 7172-7176.

PO-39

SHORT DURATION VOLTAGE AND CURRENT TRANSIENTS ON WATER ELECTROLYSES CELL

M. Vanags, J. Kleperis, G. Bajars

Institute of Solid State Physics, University of Latvia

e-mail: sf11053@gmail.com

Special power supply based on inductive spikes (kick-back voltage impulses) is made for water electrolysis cell. Different electrodes (stainles steel SUS304 and 316L, W, Ni and Pt) and electrolyte solutions (0,1, 1 and 2 M KOH) were tested. The voltage and current characteristics are measured as oscillogramms, from which the double layer charge time is calculated and efficiency of electrolysis estimated. Separate current and voltage pulses on oscillogramms were integrated to calculate power in one pulse and to estimate efficiency. It is determinate, that charging time of double layer between electrode and electrolyte solution isn't dependent from an area and material of the electrode. Nevertheless, using direct, not kick-back voltage pulses, the dependence from an area and material of the electrode is clearly observed. This mean that the length of kick-back voltage pulses is so small (1 microsecond), that no additional double layer is formed between electrode and solution. It is proved that efficiency of electrolysis is higher for kick-back voltage powered cell, as for traditional direct current (DC) electrolysis. Efficiency isn't dependent from supplied power when electrolysis is made with kick-back voltage pulses, because DC constituent is quit small, and is independent from material of the electrode.

PO-40

PREPARATION AND CHARACTERIZATION OF SUBSTITUTED BY NIOBIUM $Li_{1.4}Ti_{1.9}P_3O_{12}$ CERAMICS

A. Dindune[1], Z. Kanepe[1], J. Ronis[1], V.Venckutė[2], J. Banytė [2], V. Kazlauskienė[3], J. Miškinis[3], T. Šalkus[2], A. Kežionis[2], E. Kazakevičius[2], A.F. Orliukas[2]

[1]*Institute of Inorganic Chemistry, Riga Technical University, Miera iela 34, LV-2169 Salaspils, Latvia,*

[2]*Faculty of Physics, Vilnius University, Saulėtekio alėja 9/3, LT-10222, Vilnius, Lithuania,*

[3]*Institute of Applied Research, Vilnius University, Saulėtekio al. 9/3, LT-10222 Vilnius, Lithuania*

e-mail: tonija@nki.lv

The development of fast lithium conductors is attracting much attention because of their applications in high-energy Li-ion batteries and electrochemical sensors. It is known that $LiTi_2P_3O_{12}$ with the NASICON structure has been used as a host compound for lithium ion transport and a series of new Li-ion conductors have been found by different ion substitution. High values of the ionic conductivity, low their activation energy stimulate the search and investigations of new materials with fast Li-ion transport. In the present work we report the technological conditions for the synthesis of $Li_{1.4}Ti_{1.9}P_3O_{12}$ substituted by $Nb_{0.1,\ 0.2,\ 0.3}$ instead of P, sintering of the ceramics, the results of the investigations of X-ray diffraction (XRD) from the powder, X-ray photoelectron spectroscopy (XPS) and electrical properties of the ceramics in the frequency range from 1 to $3\cdot10^9$ Hz in the temperature range from 300 to 600 K. The structure parameters of powder were obtained at room temperature from X-ray powder diffraction patterns using Cu $K_{\alpha1}$ radiation. From the results of the X-ray diffraction study we conclude that $Li_{1.4}Ti_{1.9}P_3O_{12}$ and compounds substituted by Nb in the system $Li_{1+4x}Ti_{2-x}Nb_yP_{3-y}O_{12}$ (where x = 0.2, 0.3; y =0.1, 0.2, 0.3) exhibit hexagonal symmetry (space group $R\bar{3}c$) with six formula units in the lattice. The results of the investigation of Ti 2p, P 2p, Nb 3d, O 1s core level XPS have shown that substitution by $Nb_{0.1,\ 0.2,\ 0.3}$ influence the values of binding and splitting energies of Ti 2p, Nb 3d, and P 2p spin-orbit doublets. The external permanent electric field changed the amount of Li on the surface of the ceramics. The Li 1s core level XP spectra were deconvoluted into two peaks. It shows that Li ions occupy two different positions in the lattice. Two probe ac measurements of electrical impedance in the frequency range (10-10^7) Hz in temperature range (300-600) K were performed. In the frequency range ($3\cdot10^5$-$3\cdot10^9$) Hz the measurements were carried out by Agilent Network Analyser E5062A connected to coaxial line. Transmission coefficient of the coaxial line loaded with the sample was measured at different temperatures to calculate impedance. It is discussed about peculiarities of Li-ion transport in the solid electrolyte ceramics.

PO-41

ACCUMULATION OF RADIOLYSIS PRODUCTS AND DEFECTS IN NANOPOWDERS OF LITHIUM ORTHOSILICATE

A. Zarins, A. Supe, G. Kizane, J. Tiliks Jun., L. Baumane, J. Grabis, I. Steins

Institute of Chemical Physics, University of Latvia, Riga, Latvia

e-mail: gunta.kizane@lu.lv

Lithium-containing ceramic materials are an important element of a fusion reactor. The main requirements for these materials are a high radiation and thermal stability, low tritium retention under the operating conditions of the blanket. Lithium containing materials will take place in a blanket zone of the fusion reactors (ITER, DEMO). The Helium Cooled Pebble Bed (HCPB) is one of the models of the blanket zone. The HCPB consist of layers of lithium ceramics and beryllium pebbles in consecutive order. Lithium orthosilicate or lithium meta titanate will be used as tritium breeding materials and beryllium pebbles will be used as a neutron multiplier in the future fusion reactors.

Ultra disperse Li_4SiO_4 powders were obtained by a method of plasma synthesis by means of a high-frequency plasmatron in the Institute of Inorganic Chemistry of the Riga Technical University. The average particle size of the powders are about 70-50 nm (the surface area 25-30 $m^2 \cdot g^{-1}$).

EPR spectra of investigated samples after irradiation with doses up to 70 kGy showed presence at least 3 different lines with g-factors 2.001, 2.016 and 2.018. Those spectra were similar to previously reported for irradiated "pure" Li_4SiO_4 [1] and can be interpreted as superposition of signals from so called E' and HC2 centres (ion radicals SiO_3^{3-} and SiO_4^{3-}, respectively).

Accumulation of the radiation defects and of the products of radiolysis was investigated by method of chemical scavengers. The method is based on different redox properties of electrone and hole centres and was realized by dissolution the samples in acid-ethyl alcohol and acid-nitrate a.o. solutions. Electron radiation defects are transformed into atomic hydrogen, but radiolysis products into molecular hydrogen. Dose curves of the accumulation the radiation defects and products of radiolysis have two stages of powders of lithium orthosilicate, the amount of simple electron defects are 10^{17} def./g, the amount of products of radiolysis 10^{18} def./g.

References

1. Y. Poitevin, L.V. Boccaccini, A. Cardella, L. Giancarli, R. Meyder, E. Diegele, R. Laesser, G. Benamati, The European breeding blankets development and the test strategy in ITER, Fusion Eng. Des. 75-79 (2005) 741-749.

2. Abramenkovs A., Tiliks J., Kizane G., Tanaka S., Supe A., Grishmanov V. The Influence of Magnetic Field on the Radiolysis of the Lithium Orthosilicate// Fus. Technol., Lisbon 2 (1996) p. 1507.

PO-42

TRITIUM RELEASE PROPERTIES OF BERYLLIUM PRODUCTS FOR FUSION DEVICES

A. Vitins, V. Zubkovs, G. Kizane, E. Pajuste, G. Ivanov

Institute of Chemical Physics, University of Latvia, Riga, Latvia

e-mail: aigars.vitins@lu.lv

Beryllium pebble beds are considered as a neutron multiplier of the European Helium Cooled Pebble Bed (HCPB) tritium breeding blanket for future fusion power reactors. The tritium accumulated in the beryllium pebbles may cause operational and environmental problems, and therefore tritium release properties of the beryllium pebbles are an important factor for safe operation of the fusion reactor. Under the operating conditions of the HCPB, the beryllium pebbles will be under action of high neutron flux (10^{18} n m^{-2} s^{-1}), high temperature (up to 920 K) and intense magnetic field (up to 7-10 T) [1].

In this study, we present results on tritium release from the beryllium pebbles irradiated for 294 full power days from 17 April 2003 to November 2004 in the pebble-bed assemblies (PBA) experiment in the high flux reactor (HFR) at Petten, the Netherlands [2]. Two distinct stages of tritium release – a stage of gradual increase and a stage of abrupt release peaks are evident in the tritium release of the PBA Be pebbles at a temperature ramp of 2.4-4.8 K/min. The transition temperature from the first to second stage normally is 1173-1221 K. These two stages may be related to the tritium release by atomic diffusion and bubble venting respectively. The main maximum of the tritium release rate of the PBA Be pebbles was found to be in the temperature ranges of 1178-1309 K and 1178-1350 K at the temperature ramps of 2.4 and 4.8 K/min respectively.

Tritium release properties of the beryllium pebbles irradiated in the PBA, EXOTIC 8-3/13 and BERYLLIUM experiments are compared in this study. Total tritium activity in 1 g of sample increases in the sequence of pebbles: EXOTIC 8-3/13 (2.5-20 MBq/g) < BERYLLIUM (0.6-1.5 GBq/g) < PBA (4-10 GBq/g). Abundance ratios of chemical forms of tritium localized in the pebbles were determined with the method of chemical scavengers. A general trend can be concluded that tritium release from the EXOTIC 8-3/13 pebbles takes place at lower temperatures than that of the PBA and BERYLLIUM pebbles.

References

1. L.V. Boccaccini, L. Giancarli, G. Janeschitz, S. Hermsmeyer, Y. Poitevin, A. Cardella, E. Diegele, *J. Nucl. Mater.*, 2004, Vols. 329-333, 148-155.

2. J.G. van der Laan, L.V. Boccaccini, R. Conrad, J.H. Fokkens, M. Jong, A.J. Magielsen, B.J. Pijlgroms, J. Reimann, M.P. Stijkel, S. Malang, *Fusion Eng. Des.*, 2002, Vols. 61-62, 383-390.

PO-43

INCREASED RADIATION HARDNESS OF CdZnTe BY LASER RADIATION

A. Medvid'[1, 2], A. Mychko[1], E. Dauksta[1], E. Dieguez[3], Y. Naseka[2]

[1]*Institute of Technical Physics, Riga Technical University,*

[2]*Institute of Semiconductor Physics, Kyiv, Ukraine,*

[3]*University of Madrid, Spain*

e-mail: mychko@latnet.lv

Radiation damage occurred in semiconductors detectors of ionizing radiation during their operation and it impairs the ability of device.

The work deals with study of possibility to increase the radiation hardness of CdZnTe crystal using laser radiation. Nd:YAG laser with following parameters: wavelength λ=0.532 μm, pulse duration τ=10 ns, intensity range I=0.5-2.0 MW/cm^2 was used as source of light. The method of photoluminescence (PL) was used in the experiments for estimation of crystalline lattice damage after irradiation by gamma ray. $Cd_{0.9}Zn_{0.1}Te$ crystal was used as object of investigation. It is known that γ-radiation causes intrinsic defect generation in a semiconductor. The effect consists in increasing of A^0X band in PL spectrum of CdZnTe by ten times after γ-irradiation by ^{60}Co source (E_γ = 1.2 MeV) at room temperature with dose of 5x10^5 Rad = 5 kGy. Experimental results showed this effect is suppressed by five times in CdZnTe crystal after preliminary irradiation by the laser at intensity more than 2MW/cm^2. The decrease of A^0X band intensity in PL spectrum indicates the decrease of vacancies of Cd generation in CdZnTe after preliminary irradiation by the laser. The mechanism of this effect is explained in the following way: γ radiation leads to generation of additional Cd vacancies near the surface layer, which causes an increase of A^0X line in PL spectrum. Laser radiation has an opposite effect on $Cd_{0.9}Zn_{0.1}Te$ crystal interstitial Cd atoms are concentrated near the irradiated surface layer, but vacancies in the bulk of semiconductor [1]. This leads to A^0X line decrease and increase of D^0X band in PL spectrum [2]. Increase of Cd atoms concentration near the surface layer leads to increase of materials radiation hardness due to Cd atomic weight larger comparing to other atoms - Zn and Te.

References

1. A.Medvid' *Defects and Diffusion Forum*, 2002, 89, 210-212.

2. A. Medvid', L. Fedorenko, A. Mychko, *Radiation Measurements*, 2007, 42, 701 – 703.

PO-44

Si, CdTe NANOCRYSTALS AND SURFACE STRUCTURING FOR SOLAR CELL APPLICATIONS

T. Puritis[1], J. Kaupuzs[2], A. Medvid'[1], P. Onufrijevs[1], E. Dauksta[2]

[1]*Institute of Technical Physics, Riga Technical University, Azenes 14, LV-1048, Riga, Latvia,*

[2]*Institute of Mathematics and Computer Science, University of Latvia, Raina bulvaris 29, LV-1459, Riga, Latvia*

e-mail**:** puritis@latnet.lv

Photons with energy smaller than the band gap are not absorbed. Photons with energy approximately equal to the band gap are absorbed and whole photon energy is converted into the electric one. Photons with energy remarkably larger than the band gap are absorbed and a fraction of energy is converted into heat, i.e., lost. The voltage increases proportionally to the band gap, whereas the number of absorbed photons decreases with broadening the band gap. The resulting power has a maximum at 1.3 eV. Si with 1.1 eV and CdTe with 1.5 eV band gap are close to this optimal value and therefore these elements are perspective for solar cell applications. – The e-e-h Auger recombination can take place in Si monocrystals [1, 2]. In this case the reverse phenomenon – the impact ionization must exist, too. The second conduction sub-band electron collides with the valence band electron and lifts it to the first conduction sub-bad, therefore one hot electron generates two lower energy electrons, and thus the solar cell efficiency is enlarged. - To decrease reflection losses, we have developed method, which consists of semiconductor surface microstructuring by laser radiation.

References.

1. T.Puritis, J.Kaupuzs, *Physica E*, 2006, 35, 16.

2. T.Puritis, J.Kaupuzs, *Optical Materials* (in press).

PO-45

Si^+ ION BEAM MIXING IN SiO_2/Si STRUCTURES

H.-J. Fitting[1], D. A. Zatsepin[2]

[1]*University of Rostock, Physics Dept., D-18051 Rostock, Germany,*

[2]*Institute of Metal Physics – Russian Academy of Science, Ekaterinburg 620219, Russia*

e-mail: hans-joachim.fitting@uni-rostock.de

Scanning transmission electron microscopy (STEM) and energy filtered transmission electron microscopy (EFTEM), see [1], in combination with electron energy loss spectroscopy (EELS), soft X-ray emission spectroscopy (SXES), and cathodoluminescence (CL) have been used to investigate Si nanocluster formation in amorphous silicon dioxide layers implanted with Si^+ ions. As samples we have used amorphous, thermally grown SiO_2 layers, 20 and 500 nm thick, wet oxidized at 1100 °C on Si substrate. The layers are of microelectronic quality and doped by Si^+ ions with an energy of 12 and 150 keV and a dose of 10^{16} and 5×10^{16} ions/cm^2 , respectively, leading to an atomic dopant fraction of about 7 and 4 at.% at a mean depth of 20 and 200 nm, respectively.

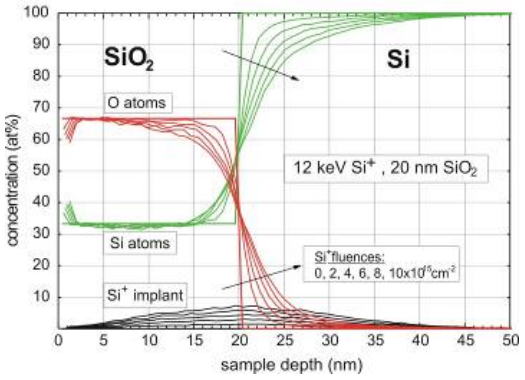

After high fluence Si^+ ion implantation into and around the interface of the thin 20 nm *a*-SiO_2 layer the formation of an ion-beam mixed buffer layer SiO_x in this region was detected by means of soft X-ray emission spectroscopy (SXES) and compared with a TRIDYN computer simulation, [3]. This structure modulation is due to atomic knock-on and knock-off effects and respective ion beam mixing processes during the high-fluence Si^+ ion implantation into the interface region. Thus the buffer layer is extended over about 20 nm, even 10 nm into the previous Si substrate and consists mainly of an understoichiometric SiO_x matrix $2 < x < 0$ with gradually decreasing of *x* into the Si substrate, see the figure inserted.

Thus additional luminescence bands are observed in the green-yellow region as described in [2]. The CL spectra in the near infrared (NIR) region indicate such structural changes by appearance of an additional side-band shifting with thermal annealing and respected Si nanocluster growth towards lower energies, probably, due to quantum confinement effects as we had seen previously in [2].

References

1. H.-J. Fitting, L. Fitting Kourkoutis, Roushdey Salh, M. V. Zamoryanskaya, B. Schmidt, *Phys. Stat. Sol. A*, 2010, 207, 117 – 123.

2. Roushdey Salh, A. von Czarnowski, M.V. Zamoryanskaya, E.V. Kolesnikova, H.-J. Fitting, *Phys. Stat. Sol.* A, 2006, 203, 2049.

3. D. A. Zatsepin, S. Kaschieva, M. Zier, B. Schmidt, H.-J. Fitting, *Phys. Stat. Sol.* A 2010, submitted.

PO-46

ELECTRON BEAM REFINING OF SOLAR SILICON

V. Zauls[1], G. Chikvaidze[1], M. Gadzyra[2], A. Viksna[3], V. Osokin[4], V. Panibratskiy[4], V. Solonenko[5]

[1]*Institute of Solid State Physics, University of Latvia,*

[2]*Institute of Problems for Material Sciences of the National Academy of Sciences of Ukraine,*

[3]*Faculty of Chemistry, University of Latvia,*

[4]*The State Scientific Research Institute "Helium", Vinnitsa, Ukraine,*

[5]*State Pedagogical University of Vinnitsa, Ukraine*

e-mail: vism@latnet.lv

We report on experimental studies to develop an electron beam refining (EBR) process to obtain purified solar grade polycrystalline silicon (SG-Si) from metallurgical grade (MG-Si) raw material.

The main advantage of proposed remelting method is to combine subsequent refining steps (namely – vacuum smelting, oxidative refinement and crystallization) into single processing cycle within vacuum chamber. The initial raw material was fed into the central part of water cooled copper cruicible and smelted by moving electron beam slice by slice. Afterwards oxygen treatment was applied to remove impurities from the melt surface, thus combining vacuum and oxidative refinement processing cycles. EBR method provides high precision energy distribution control over the heated surface of the melt and the ability to arbitrarily configure the heating zone. The potential for automation of the electronbeam remelting process is also obvious.

After a series of silicon vacuum remelting experiments with variable melt-refining parameters the impurity content of final silicon ingots was determined using Perkin Elmer ELAN DRC-e (ICP-MS) mass spectrometer as highly sensitive quantitative analysis tool, while dopant type and concentration was monitored by carrier life-time and four-probe specific electric resistance measurements.

In conclusion, our experiments demonstrate feasibility of EBR method as energy efficient approach towards the production of solar grade silicon of high quality as required by growing demand for photovoltaic applications.

PO-47

MODELLING THE PROCESSES OF ELECTRO-RAY REFINING OF SILICON

N. Grimalovsky[1], V. Panibratskiy[1], V. Sveshnikov[2]

[1]*The State Scientific Research Institute "Helium", Ukraine, Vinnytsia*

[2] *Institute of Computational Mathematics and Mathematical Geophysics SB RAS, Russia, Novosibirsk*

e-mail: panvaleriy@ukr.net

The work aims at creation of software for effective and overall modelling the processes of electro-ray refining of silicon for solar power engineering. The problem under consideration is an interdisciplinary task of high-end technology production and requires a broad spectrum of work to be done. This also includes such difficult algorithmic and software operations as modelling of charged-particle beam in electron guns with plasma emitter, that are moving under low vacuum conditions, estimation of thermal, diffusion and oxidation processes, as well as the effect of oriented crystallization and mechanical stress in the refined silicon. Thus we take into consideration not only the tasks of the analysis, but also the synthesis of refining process installations. Much attention is paid in the work to designing effective and reliable numerical algorithms that are necessary for carrying out such large-scale calculations. It is basically impossible to model a number of installations in two-dimensional approximation, therefore the work provides algorithm and programme design for calculations not only in two-dimensional, but also in three-dimensional statement. Besides, to better understand the phenomena in refined silicon and, as consequence, to effectively and qualitatively design the corresponding installations it is necessary to trace the process of silicon refining, that is to solve not only stationary, but also non-stationary problems, that involves creation of stable algorithms possessing adequate accuracy.

It becomes impossible to carry out the calculations that include all the above-mentioned problems using personal computers due to both lack of RAM needed and the slow speed of computations. Therefore the work considers the problem of designing software not only for personal computers but for multiprocessor supercomputer as well. This involves a large amount of work connected with paralleling the algorithms and creation of essentially new software to be done.

PO-48

IMPACT OF LASER RADIATION ON MICROHARDNESS OF A SEMICONDUCTOR

A. Medvid'[1], P. Onufrijevs[1], G. Chiradze[2], F. Muktupavela[3]

[1]*Riga Technical University, Latvia,*

[2]*Akaki Tsereteli State University, Georgia,*

[3]*Institute of Solid State Physics, University of Latvia, Latvia*

e-mail: onufrijevs@latnet.lv

It was found that strong absorbed Nd:YAG laser radiation induces non monotonous change of the microhardness (MH) in p and n type of Si crystal depending on laser intensity (MH-I) at different load on indenter. Two maxima are observed on MH-I dependence in p-Si(B) and one in n-Si(P) samples.

The maximum of MH-I dependence at low intensity of the laser radiation (LR) I=5MW/cm^2 in p-Si(B) samples is explained by inversion of the conductivity type from p to n due to drift of the boron atoms in the bulk of the semiconductor and interstitials toward the irradiated surface. The drift of the atoms arises in semiconductor due to presence of temperature gradient at strongly absorbed LR, so called Thermogradient effect. The second maximum observed at 6 MW/cm^2 is explained by formation of mechanical compressed stress of the top layer by interstitials and following its plastic relaxation by formation of nanno-hills.

The MH-I dependence on n-Si(P) is more simple in comparison with p-Si samples and characterized by presence only one maximum. The MH-I dependence shows non monotonous dependence and can be explained by the same mechanism as in p-Si sample at the second stage of the MH-I dependence by the plastic relaxation of the compression stress of the top layer.

An evidences of the proposed mechanism of the MH-I dependence are the following: formation of p-n junction on the irradiated surface of p-Si by laser radiation at low intensity of LR and formation of nano-hills on the irradiated surface both p-Si and n-Si as observed on the irradiated surface at I> 5MW/cm^2 using atomic force microscopy.

PO-49

MICROSCOPIC STUDY OF GRAPHENE AND SILICON/OXIDE/GRAPHENE/OXIDE STRUCTURES

J. Kozlova[1, 2], H. Alles[1], A. Niilisk[1], J. Aarik[1], V. Sammelselg[1, 2]

[1]*Institute of Physics, University of Tartu, Tartu, 51014, Estonia,*

[2]*Institute of Chemistry, University of Tartu, Tartu, 50011, Estonia*

e-mail: jekaterina.kozlova@ut.ee

Graphene sheets and ultrathin HfO_2 layers deposited by atomic layer deposition on unmodified graphene from $HfCl_4$ and H_2O were investigated with HR-SEM, AFM, OM, and μ-Raman spectromicroscopy. Graphene flakes were prepared by the micromechanical cleaving method, and fixed on oxidized silicon substrates [1]. The structure was investigated firstly with optical microscopy following μ-Raman and AFM studies. After hafnia film deposition graphene areas were characterized in the second run. Some structures were investigated before and after hafnia deposition with HR-SEM.

Surface RMS roughness down to 0.5 nm was obtained for amorphous, 30 nm thick hafnia film grown at 180ºC. The HfO_2 layers grown at low temperature were amorphous. The HfO_2 layers grown at higher temperature of 300ºC had monoclinic structure, but the growth was nonuniform and the surface of these layers was rough, with RMS value of about 5 nm. HfO_2 was deposited also in a two-step temperature process where the initial growth of about 1 nm at 170 ºC was continued up to 15–40 nm at 300ºC. This process yielded uniform, monoclinic HfO_2 films with RMS roughness of 2.5 nm for 30 nm thick films. Raman spectroscopy studies revealed that the deposition process caused compressive biaxial strain in graphene whereas no extra defects were generated.

Our studies proved that using the low-temperature ALD method allow modifying graphene surface without its preceding functionalization.

The possibilities and advantages of HR-SEM imaging of graphene and structures based on it will be discussed in presentation.

References

1. H. Alles, J. Aarik, A. Aidla, A. Fay, J. Kozlova, A. Niilisk, M. Pärs, M. Rähn, M. Wiesner, P. Hakonen, V. Sammelselg. *Central European Journal of Physics* 2010 Submitted.

PO-50

DIAMOND SYNTHESIS AT ROOM TEMPERATURE BY ELECTRODEPOSITION TECHNIQUE

A. C. Peterlevitz, J. Tsukada, H. J. Ceragioli, H. G. Zanin, V. Baranauskas

Departamento de Semicondutores, Instrumentos e Fotônica, Faculdade de Engenharia Elétrica e Computação, Universidade Estadual de Campinas, UNICAMP, Avenida Albert Einstein N 400, CEP 13083-852, Campinas, Brazil

e-mail: apeterlevitz@gmail.com

The purpose of this work is to investigate the growth of nano diamond grains on polished silicon substrates at room temperature using mid electrical fields (up to 1.2 x 10^4 Vm^{-1}) between the electrodes. The substrate surface was treated by sonification in acetone. Pure ethanol diluted in deionized water was the carbon source. Micro-sized and nano-sized diamond and diamond-like structures were observed to be grown in a carbonaceous film matrix. The morphological and structural analyses of the samples were performed by Optical Microscopy, Scanning Electron Microscopy and Surface Mapping Raman Spectroscopy, respectively.

The electron microscopy work was performed with the JSM-5900 LV microscope of the LME/LNLS - Campinas. We wish to thanks the Brazilian agencies FAPESP, CAPES and CNPq for financial support.

PO-51

INDENTATION INDUCED DEFORMATION BEHAVIOR OF ZnO

R. Zabels[1], F. Muktepavela[1], V. Sursajeva[2] , E. Tamanis[3]

[1]*Institute of Solid State Physics, University of Latvia,*

[2]*Institute of Solid State Physics, Russian Academy of Sciences, Chernogolovka,*

[3]*University of Daugavpils, Latvia*

e-mail: rzabels@gmail.com

The production and practical use of functional materials in devices is often connected with contact-induced processes that influence mechanical stability of the device. Nanoindentation is a well suited method for testing the deformation behavior and mechanical properties of materials because it is associated with the contact-induced deformation.

In this work the nanoindentation was used for characterization including estimate of the adhesion and contact stability of small-sized ZnO single crystals, nanocrystalline thin films on glass, silicon and quartz,. Thin films were obtained by very simple mechanoactivated oxidation method (MAOM) developed in LU CFI [1]. Results showed that the ZnO single crystal is relatively soft material with hardness of 2.0 GPa on the prismatic plane and Young's modulus of 160 GPa. Detailed analysis of the load–displacement curves showed plasticity 89%. Plastic deformation in this crystal is connected with the mechanism of dislocation sliding.

Nanostructured ZnO films on glass when compared to single crystal are characterized by increased hardness – up to 9 GPa and decreased modulus – up to 120 GPa. This is due the phase-structure factor. No evidence of dislocation activities during indentation induced deformation in ZnO films or formation of micro-cracks were observed. ZnO/glass contact interface was stabile and exhibited high adhesion: at load P_{max}>2N no signs of delamination were detected. In the system ZnO/Si weak adhesion with Si (cracks and delamination at P_{max}<1N) was observed. On the ZnO/SiO_2 contact interface adhesion depends on the development of mechanoactivated topochemical reactions. The obtained results demonstrate the dependence of ZnO deformation behavior on structure factor and adhesion processes on contact interfaces.

PO-52

OBTAINING $CuInSe_2$ HETEROSTRUCTURES ON NANOSTRUCTURED ZnO FILMS

I. Mihailova[1], V. Gerbreders[1], E. Sledevskis[1, 2], E. Tamanis[1]

[1]*Innovation Centre of Microscopy, Daugavpils University, 1 Parades St., Daugavpils, LV-5401, Latvia,*

[2]*Institute of Solid State Physics, University of Latvia, 8 Kengaraga St., Riga, LV-1063, Latvia*

e-mail: irena.mihailova@du.lv

$CuInSe_2$ (CIS) chalcopyrite has been successfully used as an absorber layer in highly efficient thin film solar cells. The ZnO/$CuInSe_2$-interface also is of vital interest because it determines the performance within $CuInSe_2$ based thin film solar cells. ZnO/$CuInSe_2$ heterostructures were obtained during the experiment. Needle-shaped nanostructures of ZnO have initially been grown by thermal annealing in air of evaporated layer of Zn on glass substrate. Onto these structures Se and In layer were successive evaporated by thermal evaporation method and Cu layer – by ion evaporation method in vacuum. Obtained structures were annealed in air. The morphology, composition and phase identification are obtained using scanning electron microscopy, energy-dispersive X-ray spectroscopy and X-ray diffraction analysis methods. Photovoltaic properties of these structures also were studied.

PO-53

INFLUENCE OF THERMAL ANNEALING ON PHOTOSENSITIVITY OF GaOHPc:PCBM/P3HT:PCBM BULK HETEROJUNCTION SYSTEM

I.Kaulachs[1], I.Muzikante[2], L.Gerca[2], G.Shlihta[1], M.Roze[3], J.Kalnachs[1], A.Murashov[1], G.Rozite[1]

[1]Institute of Physical Energetics, Aizkraukles 21, Riga, Latvia, [2]Institute of Solid State Physics, University of Latvia, Kengaraga str.8, Riga, Latvia [3]Riga Technical University, Azenes 14, Riga, Latvia

e-mail: kaulacs@edi.lv

To increase spectral range of widely used organic bulk heterojunction blend P3HT:PCBM a new bi-layer system GaOHPc:PCBM/P3HT:PCBM has been built by spin coating technique. ITO glass was covered by 30 nm thick PEDOT:PSS (Clevios 1000) layer followed by hydroxygallium phthalocianine (GaOHPc) and soluble C_{60} derivative (PCBM) according to method described in Latvian patent P-08-14 [1]. This bulk heterojunction layer was covered by P3HT:PCBM blend by well known method described in [2]. Top Al electrode was evaporated in vacuum 10^{-8} - 10^{-7} Torr. All measurements were performed in vacuum ~10^{-6} Torr. The samples were irradiated with constant incident photon flux. As shown in Fig.1, the value of short circuit photocurrent efficiency (EQE) of our samples is increased more than two times after thermal annealing at 100ºC in vacuum 10^{-6} Torr.

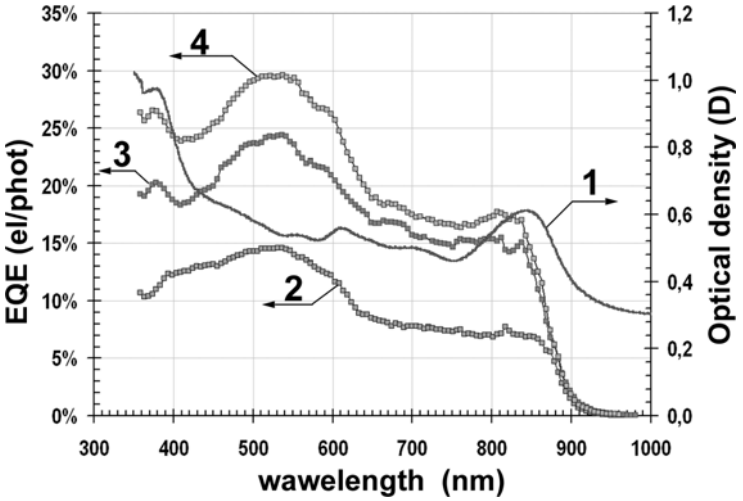

*Fig.1. Spectral dependences of external quantum efficiency (EQE) of short circuit photocurrent at light intensity 10^{11} phot/(cm^2*s) and optical density for ITO/PEDOT:PSS/GaOHPc:PCBM/P3HT:PCBM/Al cell.*
1 – Optical density of bilayer system GaOHPc:PCBM/P3HT:PCBM;
2 – EQE at room temperature (RT) for unheated sample;
3 – EQE at T = 100ºC;
4 – EQE at RT after sample thermal annealing in vacuum at T = 100ºC;

References.

1. I.Kaulachs et al, *Latvian patent P-08-14*, 2009

2. J.Y.Kim, S.H.Kim, H.Lee, K.Lee, W.Ma, X.Gong, A.J.Heeger, *Advanced Materials*, 2006, 18, 572-576.

PO-54

MANIPULATION OF GOLD NANOPARTICLES INSIDE SCANNING ELECTRON MICROSCOPE

B. Polyakov[1, 2], S. Vlassov[1], L. Dorogin[1], R. Lohmus[1]

[1]*Institute of Physics, University of Tartu, Estonia,*

[2]*Institute of Solid State Physics, University of Latvia*

e-mail: boris.polyakov@cfi.lu.lv

Rapidly developing nanotechnology and nanodevice engineering demands of precise and deep understanding of nanoobject interaction with different surfaces. AFM (Atomic Force Microscope) usually used to move nanoparticles [1, 2]. Main problem of conventional AFM manipulation is a "blindness" of the process. Usually, actual shape of small metal nanoparticle is unknown (tip convolution effect, tip contamination).

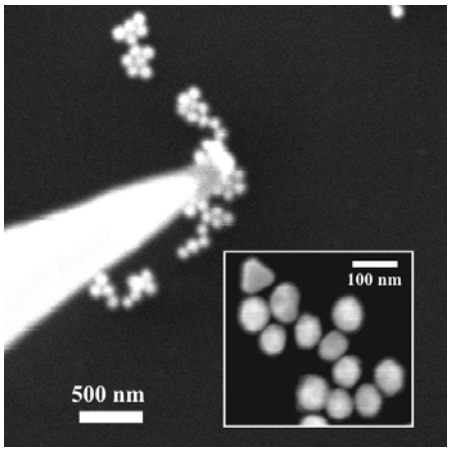

Fig.1 Manipulation of gold nanoparticles on a silicon substrate inside SEM. Insert: high-resolution image of gold particles.

We use AFM tip glued on quartz tuning fork (QTF), which is mounted on a nanomanipulator placed inside SEM. QTF works as a force sensor during manipulation. SEM allows visualizing actual shape of metal particles (Au) on a substrate, and shape of the tip (Fig.1). QTF can be positioned to oscillate perpendicular or parallel to a sample plane. In the first case, oscillation geometry is similar to AFM normal operation mode. In the second case, the tip will interact with surface in shear mode. It allows excluding normal force component, and push nanoparticles parallel to sample surface only.

References

1. K. Mougin, E. Gnecco, A. Rao, M. Cuberes, S. Jayaraman, E. McFarland, H. Haidara, E. Meyer, *Langmuir*, 2008, 24, 1577

2. D. Dietzel, M.Feldmann, H. Fuchs, U. Schwarz, A.Schirmeisen, *Appl. Phys. Lett.*, 2009, 95, 053104.

PO-55

INVESTIGATION OF NANOSIZED COLLOIDAL PARTICLES TRANSFER THROUGH A POROUS LAYER

V. Shints, G. Kronkalns, E. Blums, A. Mezulis
Institute of Physics, University of Latvia
e-mail: viesturs.shints@gmail.com

The magnetic fluid (MF) is a suspension of ferromagnetic nanoparticles with diameter 8... 15 nm in a carrier liquid. In the present investigation MF is identified as a binary solution, and the particle transfer through a porous layer is studied in uniform external magnetic field.

The experimental set-up consists of two equal cylindrical thermostated volumes containing MF, that are separated by a porous layer, characterized by thickness of 0.75 mm and average diameter of a pore 1 μm. Experiment demands measuring temperature, concentration of magnetic particles and pressure in the volumes. The concentration of magnetic particles is obtained by measuring the inductance of coils inside the volumes [1]. The mean MF temperature in the volumes is measured by ohmic resistance of coils. The pressure levels in both volumes are measured by a simple manometer, which consists of glass tubes joined to the volumes.

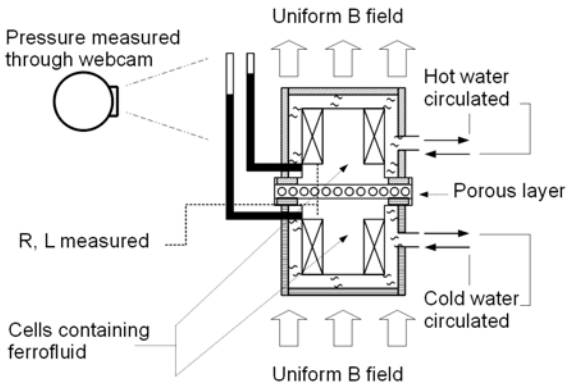

Performed experiment series indicate a major effect related to the colloidal particle transfer through a porous layer that behaves over well known thermal diffusion (Soret effect). It is proved by different methods that MF thermal diffusion, respectively, development of the concentration difference ∇c between the volumes decreases with increasing external magnetic field inductance B ($\nabla T \| B$). The porous layer between the volumes changes the nanoparticle transfer process so that the development of ∇c is roughly independent on B in examined range 0…80 mT. Theoretical model of this phenomenon, related to osmotic effects, as well as further experiments are in progress.

References:

1. E.Blums, S.Odenbach, A.Mezulis, M.Maiorov, *J. Magn. and Magn. Mat.*, 1999, 201, 268-270.

2. E.Blums, G.Kronkalns, M.Maiorov, *Thermoosmosis in Magnetic Fluids in the Presence of a Magnetic Field, 7-th Int. Pamir conf. on Fundamental and Applied MHD*, Presqu' Ile de Giens, France, 2008, 2.

PO-56

CREATING CONCENTRATION PROFILES OF NANOSIZED MAGNETIC PARTICLES IN NON-UNIFORM MAGNETIC FIELD

A. Mezulis, D. Zablockis

Institute of Physics, University of Latvia

e-mail: ansis@sal.lv

In the present work different concentration profiles of nanosized particles are created with the aim to compare them with theoretically calculated ones. This comparision allows to conclude about usability of the chosen theoretical model.

To create different concentration profiles, the nanosized particles are that of a magnetic fluid, subjected to non-uniform magnetic field. A non-linear concentration profile grows in 2D Hele-Shaw cell of the height 10 mm and thickness 0.2...0.5 mm. The magnetic field gradient is created along the height of the Hele-Shaw cell by two adjacent permanent magnets of 0.5 T on the outside surface with opposite orientation of polarities (see picture). The main variable parameter of the experiment is the lift of the cell over the magnet surface. With used magnetic fluid sample of nanoparticle volume concentration 4% the theoretical model predicts increase of concentration of nanoparticles more than 5 times at the bottom of the cell even at lift of 10 mm. With properly chosen cell thickness it is enough to delay a coherent transmitting light for some periods. Therefore an optical interferometry method to read the concentration profile is applicable. It is put into practice by concept of Mach-Zehnder interferometer, adjusted initially to image some fringes at 45 degree angle over the height of the cell. Due to small diffusion coefficient of the nanoparticles ($\sim 2 \cdot 10^{-11}$ m^2/s) the building of stationary concentration profile takes hours. During this time the fringes become strongly distorted, which is the effect to determine the creation of concentration profile from.

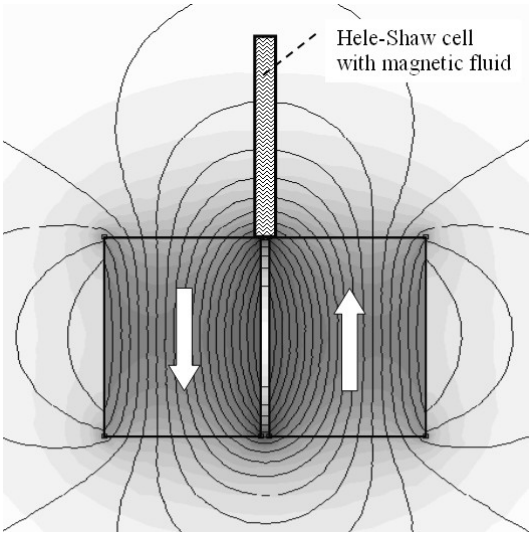

References:

1. A.Mialdun, V.M.Shevtsova, *Int. J. Heat and Mass Transfer*, 2008, 51, 3164-3178.

2. E.Blums, A.Cebers, M.M.Maiorov, *book: Magnetic Fluids*, Walter de Gryuter, Berlin, 1997.

PO-57

FUNCTIONAL NANOCOMPOSITE MATERIAL FOR VISUALIZATION OF IRREVERSABLE IMPACT OF STATIC MAGNETIC FIELD

V. Vorohobovs

University of Latvia

e-mail: riga2006@googlemail.com

This material is a mixture of oil and solid magnetized particles. It behaves like Plasticine and different shapes can be sculptured from it. But it has additional peculiarity: it can be easily destroyed by magnetic field. In certain condition it can also change its color after impact of the magnetic field.

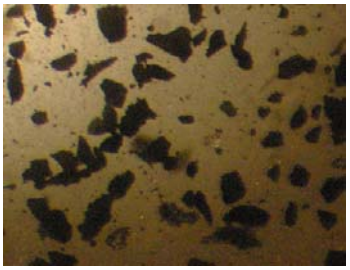

Fig 1 particles before magnetization

This material has an interesting application – it can be used in seals to register illegal attempt to stop water meter by application of a strong magnet. In such seals the material is distributed in circular pattern (see Fig. 2 top image) which is obtained during the construction of the seal by application of electric current in axial direction. According to Maxwell equations once destroyed, such ring can not be restored by any external force if there is no electric current through its centre. However such current is impossible if after manufacturing the ring was placed in closed camera of the seal.

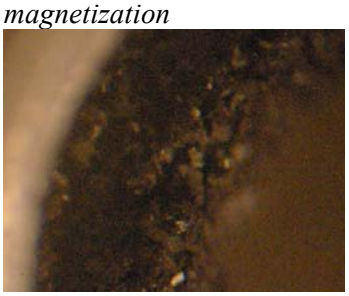

Fig 2 particles after magnetization

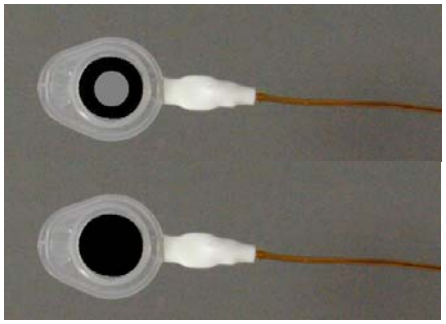

Fig.3 Magnet sensitive seal before and after application of magnetic field.

Necessity to improve the sensitivity of such seals leads to study of lubrication processes between solid particles immersed in different liquids. Zone of contacts between particles is always very small – about one nano meter, and behaviour of the lubricating liquid in these zones determines the sensitivity and other properties of the material.

In my presentation micro-magnetism and micro-fluidics inside this material will be discussed.

PO-58

CHARACTERIZATION OF NANODEVICES INSIDE NANOWIRE ARRAYS USING CONDUCTIVE AFM AND *IN-SITU* NANOMANIPULATION TECHNIQUES

P. Birjukovs[1], G. Kunakova[1], J. Prikulis[1], J. D. Holmes[2], D. Erts[1]

[1]*Institute of Chemical Physics, University of Latvia,*

[2]*Department of Chemistry, National University of Ireland, Cork, Ireland*

e-mail: Pavels.Birjukovs@lu.lv

Using templates such as anodised aluminium oxide as a host for semiconductor nanowires allows development of nanodevices with high density. Good filling of the membrane pores is critically important in design of electronic devices. We report on characterization of conductive properties of individual nanowires inside large arrays.

A recently developed method [1] to access to the full length of nanowires inside a membrane was used to fabricate and characterise multiple individual field effect transistors (FET) built on Bi_2S_3 nanowires. Source electrode of the nanowire was produced by deposition of 50 nm Au on membrane in contact with one end of the nanowires. Gate electrode was fabricated using electronic beam lithography on the open surface of the nanowires. Conductive boron doped diamond tips (NT-MDT DCP10) were used as a drain electrode in the experiments. An AFM (MFP-3D, Asylum Research) in contact mode was used for topography and current mapping and also to determine FET parameters.

Adapted SmarAct GmbH 13D-manipulation system inside a Field Emission Scanning Electron Microscope Hitachi S-4800 was used to design FET on nanowires inside membrane. Drain and gate electrodes were formed by spatial manipulation of conductive tip electrodes. This configuration allows in-situ examination of FET electrical parameters such as I-V and gate dependency characteristics with different source and drain geometries.

References

1. P. Birjukovs, N. Petkov, J. Xu, J. Švirksts, J.J. Boland, J.D. Holmes, D. Erts, *J. Phys. Chem. C*, 2009, 112, 19680-190685.

PO-59

DEVELOPMENT AND CHARACTERIZATION OF NANOELECTROMECHANICAL SWITCHES

R. Meija[1], J. Andzane[1], J. Prikulis[1], J.D. Holmes[2], S. Kubatkin[3], D. Erts[1]

[1]*Institute of Chemical Physics, University of Latvia,*

[2]*Department of Chemistry, National University of Ireland, Cork, Ireland,*

[3]*Microtechnology and Nanoscience - MC2, Chalmers University of Technology, Sweden*

e-mail: Raimonds.Meija@lu.lv

Nanoelectromechanical systems (NEMS) have great potential in electronic applications, especially switches due to their high speed (on/off ratio 0.2 ns), small size and large integration level (10^{12} 1/cm^{-2}), low energy consumption and heat capacity. Because of NEMS small mass and relatively large number of surface atoms, Van der Waals forces and adhesion become very important for the physical model of these systems. Two and three terminal NEMS based switches have been demonstrated in several works [1-3]. Potential applications for such devices are diverse high density logic units. As a particular example we consider a nanowire based multiplexer, which could switch between arbitrary numbers of data sources and therefore would require multipositional switch.

Here we present investigation of multipositional NEMS switches based on individual nanobeams, which connect to one of eight terminals arranged in a circular array. The beam was positioned using attocube manipulator and switching achieved through application of electrostatic field. Gold terminals with apex radii of 700 nm were produced using EBL and connected to larger electrodes for conductivity measurements. We also discuss potential reduction mechanisms of contact adhesion. All measurments were made using *in-situ* techiques in SEM Hitachi S-4800, thus allowing simultaneous acquisition of visual and electric data.

References

1. S. Lee, D. Lee, R. Morjan, S. Jhang, M. Sveningsson, O. Nerushev, Y. Park, E. Campbell, *Nano Lett.*, 2004, 4, 2027.

2. J. Andzane, N. Petkov, A. Livshics, J.J. Boland, J.D. Holmes, D. Erts, *Nano Lett.*, 2009, 9, 1824.

PO-60

A NANOINJECTOR BASED ON NANOPOROUS ANODIZED ALUMINIUM OXIDE PROBES

R. Poplausks[1], U. Malinovskis[1, 2], I. Pastore[1], I. Muiznieks[2], D. Erts[1]

[1]*Institute of Chemical Physics, University of Latvia, Latvia,*

[2]*Faculty of Biology, University of Latvia, Latvia*

e-mail: Raimonds.Poplausks@lu.lv

Technologies for introducing biological macromolecules into living cells or for collecting molecules from precisely determined cell's regions are vital for experimental cell biology.

Our created nanoporous anodized aluminium oxide (AAO) coated probes with pore diameters of 40-60 nm and tip radius of 50-2000 nm could be utilized in such applications [1, 2, 3]. Here, we report the development of a cell injection system that uses porous AAO probes as nanoneedles for nanovolume fluids transfer. The system consist from three parts - an AAO needle attached to a quartz tuning force, homemade AFM system for movement control and targeting, and inverted optical microscope. The AAO nanoneedle was filled or emptied with fluorescent labelled DNA (fluorophore - YOYO and ethidium bromide) using applied electrical field and DNA deposition or elimination in or out AAO pores was monitored by epifluorescent microscope. Such fluid transport system cans spatially precise transfer small quantities of DNA molecules or minute volume ($10^2 – 10^7$ nm^3) of fluids.

We tested systems capability to deliver DNA into individual cells of multicellular organisms, using the epidermis of *Allium cepa*.

References

1. Latvian patent Nr 13872

2. Latvian patent Nr 13873

3. Latvian patent Nr 13875

PO-61

THE PREPARATION AND APPLICATION OF ULTRA THIN ANODIZED ALUMINIUM OXIDE MEMBRANES

I. Pastore, D. Erts

Institute of Chemical Physics, University of Latvia

e-mail: ilona.pastore@gmail.com

In recent years anodized aluminium oxide (AAO) has been widely used in nanotechnology due to its highly ordered nanoporous structure with pore diameter range 2 – 400 nm and with density 10^{11} pores/cm^2. AAO preparation is also known as one of the most controllable self organizing process. Isolated element arrays can be obtained using material deposition in pores, which can be further used as building blocks of electronic circuits. Nanopores also allow separation, protection and transport of macromolecule such as DNA for incorporation in technological processes e.g. controlled diffusion. In addition the AAO membranes exhibit a high temperature resistance, which is useful for material deposition and annealing. Typically AAO membranes are produced with thickness in 5 – 200 μm range. However, some applications, e.g., separation, masking in electron lithography, and production of quantum dots, require ultra thin AAO membranes [1, 2].

Here we present a two step anodization process of aluminium surface in a sulphuric or oxalic acid for production of AAO membranes with thickness less than 1 μm. A DC voltage of 6 – 25 V and 10 – 40 V were used for sulphuric and oxalic acid respectively. To make process more environment friendly copper(II) chloride and Paraloid B72 solution in acetone were used for membrane transfer on the surface instead of earlier recipe which utilises mercury(II) chloride and polystyrene solution in chloroform.

Scanning Electron Microscope analysis of the surface and thickness of the obtained AAO membranes showed pore diameters 30 and 50 nm and thickness 30 – 210 nm, which several times smaller than previously reported [1, 2].

As an application of the ultrathin AAO membranes we evaporated chromium through the pores onto a silicon surface using Etching Coating System. The resulting nanoparticles or quantum dots had diameters of 10 - 20 nm and ordered periodic arrangement.

References:

1. Ding G. Q., Zheng M. J, Xu W. L. Shen W. Z., *Nanotechnology,* 2005, Vol. 16 , 1285–1289

2. Woo L., Hee H., Lotnyki A., Schubert M., Hesse D., Baik S., Gosele U., *Nature Nanotechnology,* 2008, Vol. 3 402-407.

PO-62

STIMULATED CHANGES IN BILAYER Sb/Se FILM

O. Shiman, V. Gerbreders, V. Kolbjonoks, E. Sledevsky, A. Bulanov

Innovation Centre of Microscopy, Daugavpils University, Latvia

e-mail: osimane@gmail.lv

The process in Sb/Se bilayered thin film has been studied. Bilayer Sb/Se films are irradiated from a focused He-Ne laser (micron-sized areas). It was shown that essential changes of optical parameters (transmission and reflection) and of the electrical conductivity occur due to the interdiffusion stimulated by direct heating or by the influence of the laser beam unlike the chalcogenide–chalcogenide nanostructures, where the photo-induced effects may dominate. Observed photo- and thermoeffects critically change with time. The origin of these phenomena is discussed.

PO-63

MULTIBEAM HOLOGRAPHIC RECORDING

U. Gertners, J. Teteris

Institute of Solid State Physics, 8 Kengaraga Str., Riga, LV-1063, Latvia
e-mail: gertners@gmail.com

This work is devoted to the topical issue - photoinduced formation of relief in thin layers of chalcogenide vitreous semiconductors (ChVS) without following complicated chemical processing. Direct holographic recording technique is on of the advanced methods for surface relief structuring in light sensitive materials. Because of the high light gradient it is possible to obtain surface structures like no one else method can. In this report the study of direct holographic recording of the surface-relief gratings on ChVS like As-S, As-S-Se and organic films has been presented. Holographic recording was performed by 532nm wavelength and by using multibeam recording setup. Also the mechanism of the direct recording of surface-relief on amorphous chalcogenide films based on the photoinduced plasticity has been discussed.

PO-64

INVESTIGATIONS OF As-S-Se THIN FILMS FOR USE AS INORGANIC PHOTORESIST FOR DIGITAL IMAGE-MATRIX HOLOGRAPHY

A. Bulanovs[1], G. Kirilovs[1], V. Gerbreders[1], J. Teteris[2]

[1]*Innovative Microscopy Center, Daugavpils University, Daugavpils, Latvia,*

[2]*Institute of Solid State Physics, University of Latvia, Riga, Latvia*

e-mail: bulanov@inbox.lv

For applied research of optical properties of As-S-Se chalcogenide thin films experimental installation of digital image-matrix holographic recording on the basis of 100 mW 405 nm semi-conductor lasers and Spatial Light Modulator (SLM) has been created. By means of this device recording of diffraction grating and security holograms on As-S-Se thin films was performed. In work experimental results of dependences DE (diffraction efficiency) of received relief-phase holographic grating versus the exposition and the period are present. Samples with DE=60 % has been received that allows to use chalcogenide film as alternative to organic photoresist in applied dot-matrix and image-matrix holography.

PO-65

THE DIFFERNCE OF SURFACE RELIEF FORMATION IN As_2S_3-POLYMER AND As_2S_3-DR1-POLYMER COMPOSITES

A. Gerbreders, J. Teteris

Institute of Solid State Physics, University of Latvia

e-mail: andrejmah@gmail.com

The method for preparation of thin polymer-photochrome-chalcohenide composite films is described, and some features of photoinduced changes of optical properties and holographic recording of these materials are studied.

Films of composite were obtained from solution of arsenic sulphide, Disperse Red 1 and polymer «Disperbyk-161» (produced by BYK-Chemie GmbH) in organic solvents. The solution was spread on glass substrates and dried at 150^o temperature. The dry film thickness was 4-9 μm, correlation of arsenic sulphide, Disperse Red 1 and polymer in films was according to (in weight. %) 35 ÷ 5 ÷ 60.

The photoinduced changes of optical reflection and transmission of the films was observed and compared with other composites (As_2S_3-Disperbyk 161 and spiropyran-As_2S_3-polymers). The surface relief formation under direct influence of light (532 nm) through cylindric lens was studied. The graph of relief height dependence on exposure was made.

The holographic recording of diffraction gratings was performed by laser lines of 532 and 442 nm. During recording the diffraction efficiency of holographic recording was measured simultaneously in transmission and reflection mode. The influence of laser beam intensity on recording process was studied. The profile of the gratings was analyzed by AFM microscope.

PO-66

PHOTOINDUCED SURFACE RELIEF GRATINGS FORMATION AND PROPERTIES OF PMMA FILMS WITH AZOBENZENE DERIVATIVE CONTAINING N, N-DICYCLOHEXYL SULFONAMIDE MOIETY

I. Muzikante[1], J. Teteris[1], J. Aleksejeva[1], U. Gertners[1], A. Tokmakov[1], B. Stiller[2], D. Gustina[3]

[1]*Institute of Solid State Physics, University of Latvia, Riga, Latvia,*

[2]*Institute of Physics and Astronomy, Potsdam University, Golm, Germany,*

[3]*Latvian Institute of Organic Synthesis, Riga Latvia,*

e-mail: inta.muzikante@cfi.lu.lv

There has been observed a growing interest to use organic materials in optical and optoelectronic devices. Among them the formation of surface relief gratings (SRG) by irradiation of thin films with azobenzene derivatives has attracted a great deal of attention. Several models for the mechanism of SRG formation have been proposed [1]; however, phenomenon of photoinduced mass transport is still unclear. Also the relationship between molecular structures and SRG forming properties is indeterminated. In the case of azobenzene molecules, the photoinduced SRG formation may be caused by the *trans*–to-*cis* and *cis*–to-*trans* isomerizations of azobenzene chromophores.

In this work we will present studies of SRG formation in host-guest thin film of novel azobenzene derivative containing N, N-dicyclohexyl sulfonamide moiety. It is shown that absorption bands of cis- and trans-isomers of this molecule are overlapping and is situated at 450nm.

In our samples PMMA polymer was used as host and 15wt% of azobenzene derivative was used as guest molecules. The SRG writings of samples were done by holographic method with polarized light -45/45 at 3 different wavelengths – 325 nm, 441 nm and 553 nm. The depths of surface relief gratings were dependent of irradiation wavelength and at wavelength 441 nm maximum was observed.

In order to investigate process of transport of azobenzene molecules under irradiation, the writing was done by circular polarized light at 473 nm and SNOM. The topography of SGRs shows remove of molecules from illuminated region and study of the surface potential shows ordering of these molecules.

References

1. O.N. Oliveira, Jr., J.Kumar, L.Li, S.K.Tripathy, Surface-Relief Gratings on Azobenzene-Containing Films, in *Photoreactive Organic Thin Films,* 2002, Elsevier Science.

PO-67

NEW COMPATIBILISERS FOR IMPROVEMENT OF MAGNETO-PHYSICAL AND DEFORMATION PROPERTIES OF POLYMER NANOCOMPOSITES

I. Reinholds[1], V. Kaļķis[1], Z. Roja[1], J. Zicans[2], R. Merijs-Meri[2]

[1]*Faculty of Chemistry, University of Latvia,*

[2]*Institute of Polymer Materials, Riga Technical University*

e-mail: ingars.reinholds@inbox.lv

Six new design magnetic compatibilisers (MC) with different structure were synthesized with high yields (95%). Structure of the synthesized structures was affirmed with ESI-MS spectra. Thermal stability was evaluated with TGA/DSC. EPR spectra of pure MC and solutions in water analysed in room temperature (Fig. 1.) showed high paramagnetic properties.

The results showed great abilities to use these compounds as compatibilisers in polymer multiphase composites to improve their physical properties (viscosity, thermal stability, phase interaction of different polymers (thermoplastics and elastomers), as well as in polymer nanocomposites containing nano-clay.

Good radiation (gamma-rays, accelerated electrons) stability of the synthesised compatibilisers as well as increased outcome of radiation induced free radicals allow to predict possible use of these compounds as radiation promotors for obtaining of effectively cross-linked polyolefines (polyethylene etc.) or their blends with other polymers when a good phase interaction is needed.

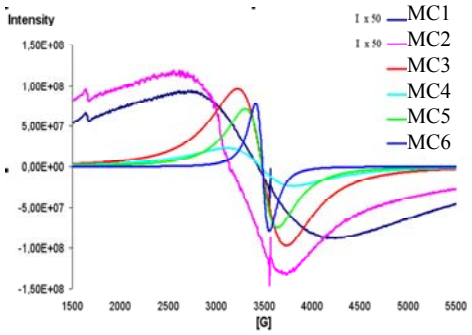

Fig.1 EPR spectra (293 K) of solid synthetized compatibilizers

PO-68

STRUCTURE AND PROPERTIES OF PLASMA SYNTHESIZED FERRITES AS MODIFIERS OF POLYMER COMPOSITIONS

S. Strode[1], R. Merijs-Meri[1], I. Bockovs[1], I. Zalite[2], V. Kaļķis[3]

[1]*Institute of Polymer Materials, Riga Technical University,*

[2]*Institure of Inorganic Chemistry, Riga Technical University,*

[3]*Department of Chemistry, University of Latvia*

e-mail: zicans@ktf.rtu.lv

Ferrites have proven themselves as perspective modifiers for broad range of thermoplastic and thermosetting polymers. Such materials already now are widely used in information technologies, medicine, environmental treatment, auto-motive industry and other branches of national economy. Especially promising is use of nanostructured ferrite particulates for modification of conventional thermoplastic resins.

The current research is devoted to the investigation of ferrite modified thermoplastic polyester (TPE) composites. Zn containing ferrite (ZnF) nanofillers has been synthesized by plasma route. The ferrite nanofiller have been introduced in the polycarbonate matrix by means of melt processing. Different TPE/ZnF compositions with nanofiller concentration from 0,5 to 10 wt. % have been obtained. Most important melt processing parameters have been defined. Structure of the nanofillers and polymer nanocomposites have been characterized by means of microscopy, differential scanning calorimetry and thermogravimetric analysis. Magnetic properties of the nanofillers and polymer nanocomposites have been characterized by means of electron paramagnetic resonance apparatus. Tensile and cyclic loading properties of the nanocomposites have been characterized by means of universal testing machine.

Results of the investigation demonstrate satisfactory dispersion of the nanostructured filler in the TPE matrix. Elastic modulus and tensile strength of the TPE/ZnF nanocomposite is remarkably increased by raising the ferrite content up to certain limit. Besides it results of the investigation discover that addition of the magnetic filler even at minor amounts allow to change magnetic properties of the composites. Some interesting structure-property relationships have been also revealed.

PO-69

DEVELOPMENT OF LIQUID CRYSTAL POLYMER MODIFIED POLYETHYLENE COMPOSITES AND INVESTIGATION OF ITS ELASTIC PROPERTIES

I. Elksnite[1], T. Ivanova[1], M. Kalnins[1], J. Zicans[1], R. Maksimovs[2]

[1]*Institute of Polymer Materials, Riga Technical University,*

[2]*Institute of Polymer Mechanics, University of Latvia*

e-mail: zicans@ktf.rtu.lv

Since very beginning of their systematic investigations, liquid crystal polymers (LCP) have attracted considerable attention from scientists. Due to the unique properties of LCPs (low melt viscosity, high thermal and mechanical resistance, good dimensional stability, optical anisotropy, ease of forming of oriented structures under the magnetic and electrical fields, etc) these materials also have attracted great interest from commercial manufacturers for production of high strength technical fibers, fabrics and *in situ* reinforced composites in textile, building, automotive a.o. branches of industries. At present moment, mainly due to the rapid development of information technologies, annual global growth of thermotropic LCPs has reached 25 %.

Up to now, most of the researches have been concentrated on the thermoplastic compositions containing considerable amounts of thermotropic LCPs (up to 30 %). It should be however mentioned that increased concentrations adversely affect superelasticity of polymer materials. Therefore in this investigation the effects of small additions of some thermotropic LCPs (up to 5 wt. %) on the elastic and structural properties of polyethylene are discussed.

Main results of the investigation reveal some technological peculiarities of the manufacturing of polyethylene composites modified with small amounts of thermotropic LCPs. Besides it, results of the investigation show that even minor amounts of the liquid crystalline modifier, allow achieving substantial reinforcing effect. It has been theoretically confirmed that the reinforcing effect is achieved due to orientation of the liquid crystalline inclusions in the thermoplastic matrix.

PO-70

MOLECULAR HYPERPOLARIZABILITIES OF INDANE DERIVATIVES MEASURED BY HYPER RAYLEIGH SCATTERING

A. Tokmakov[1], M. Rutkis[1], A. Ernstsons[1], V. Kampars[2]

[1]*Institute of Solid State Physics, University of Latvia 8 Kengaraga St.,LV-1063, Riga, Latvia,*

[2]*Riga Technical University, 14 Azenes St., LV 1048, Riga, Latvia*

e-mail: andrey.tokmakov@gmail.com

Large and fast nonlinear optical (NLO) response, low dielectric constant and simplicity of processing make organic materials of great current scientific and technological interest for photonic device applications such as superfast electro-optic modulators and switches.

NLO efficiency of chromophores are characterized by molecular hiperpolarizabillity (β), what can be calculated using quantum chemistry (QC) methods or experimentally determined in solutions by Hyper Rayleigh light scattering (HRS). In this presentation we will analyze relationships between the measured by HRS and QC calculated β values for more than 10 indane derivatives.

Mostly experimentally obtained β values are in good correlation with QC calculated. Although for some compounds significant deviations takes place. For instance, measured β values for compounds DDMABI and DDDMABI are significantly lower, while for the tBu-DMABI-dPh higher than predicted by QC calculations.

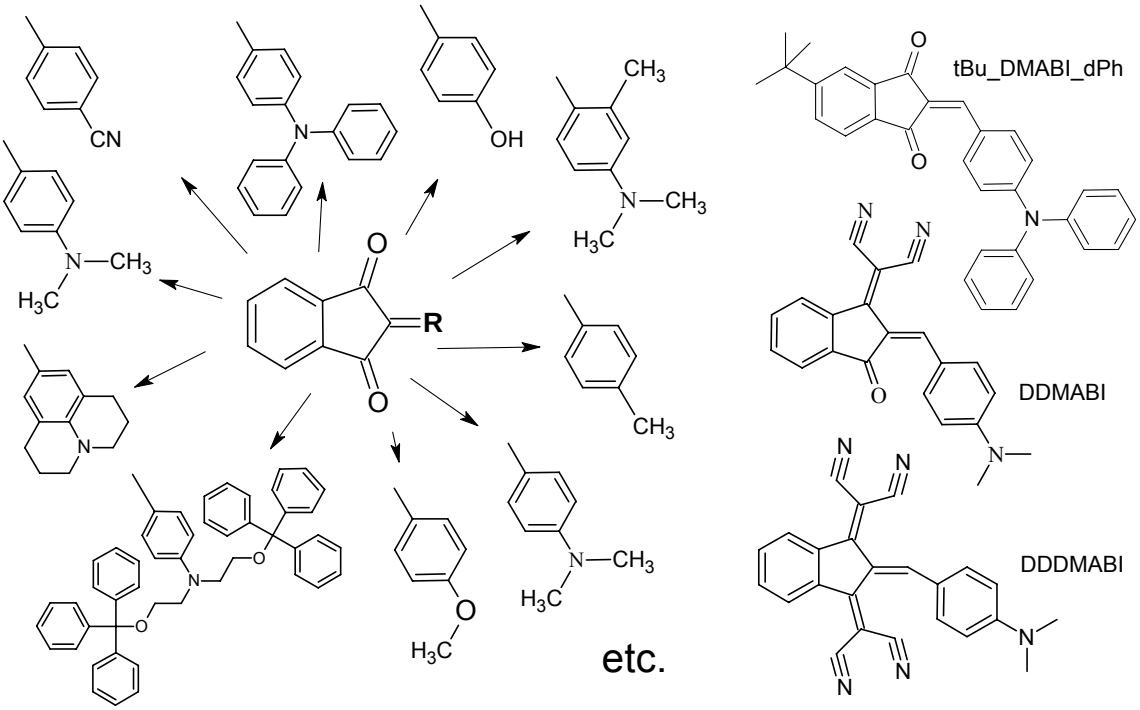

PO-71

SILICON DIOXIDE NANOPARTICLES AS A CARRIER OF ASCORBIC ACID

O. Strekalova, Yu. Dekhtyar

Riga Technical University, Biomedical engineering and nanotechnologies institute, Riga, Latvia

e-mail: olga.s.olga@inbox.lv

Silicon dioxide nanoparticles SDN were demonstrated as the carriers for the organic complexes [1]. The main idea to exploit the SDN as the complexes connector used electrical communication.

The present research is targeted to explore SDN as the "container" for the organic polarized molecules. The ascorbic acid (AA) was selected as the probe.

Solution of SDN was mixed with AA powder. Interaction of SDN and AA was indicated owing to detection of the optical attenuation in the range 200-1090 nm.

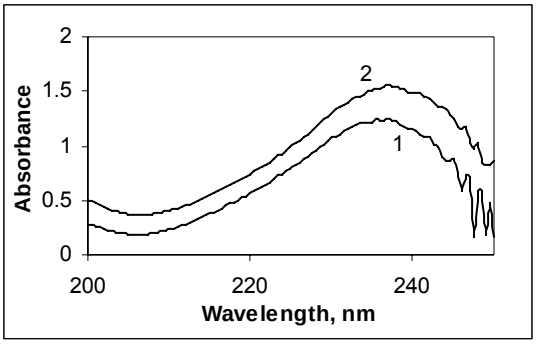

Fig.1 Differed spectra (concentrations 0.00005g/1ml and 0.001g/1ml for SDN and AA, coreespondly):
1 - non radiated SDN, 2- radiated SDN

The spectra were detected separately for SDN, AA and their solutions (SDN+AA). To indicate interaction the spectra of SDN+AA were differed from the superposition of the SDN and AA spectra.

The differed spectra (Fig.1) are characterised with the maximum (at 237 nm). This is in favour of interaction and indicates influenced/involved couples. To insure the electrical communication reason of interaction the SDN nanoparticles were radiated by the ultraviolet radiation that induces electrical charge of the particles. As the result the differed spectra demonstrated higher maximums at same wave length as above (Fig.1).

Reference

1. Dekhtyar Yu., Kachanovska A., Patmalnieks A., Pumpens P., Renhofa R., Romanova M., Sudnikovich A., *Biomedical engineering,* Kaunas, 2009, 183.-186.

PO-72

FABRICATION OF A CONDUCTIVE CERAMIC AND ITS USE IN WATER TREATMENT TECHNOLOGY

A. Pavlova[1], M. Reimanis[1], L. Berzina-Cimdina[1], J. Ozolins[1], T.Barloti[2], V. Teteris[2]

[1]*Riga Technical University, Riga Biomaterials Innovation and Development Centre, Latvia,*

[2]*Riga Technical University, Division of Electronic Equipment, Latvia*

e-mail: agnese.pavlova@rtu.lv

Ceramics containing titanium oxide have many unique properties, for example, good chemical durability, mechanical strength and good electrical properties.

Non-stoichiometric titanium dioxide ceramics with formula TiO_{2-x} (where $x < 2$) are thought to be a perspective material. By changing titanium and oxygen ratio and conditions of fabrication it is possible to considerably alter the properties of material and subsequently the probable uses of the material. Titanium oxide ceramics sintered in oxygen containing atmosphere are practically non-conductive. By sintering titanium oxide ceramics in vacuum ($6.6 * 10^{-3}$ Pa) conductive ceramic materials with semiconductor properties were obtained [1]. The obtained materials were researched: it was ascertained that the materials are n-type semiconductors; the activation energy (ΔE) was calculated using conductivity-temperature diagrams. ΔE for obtained materials is 0,049 – 0,061 eV.

Electrical properties of the obtained material enable to use it as an electrode for water electrolysis. It was established that the use of TiO_{2-x} electrodes in water electrolysis considerably lessens the amount of microorganisms present in water and the chances of their propagation [2].

References

1. A.Pavlova. L.Berzina-Cimdina, J.Locs, D.Loca, J.Bossert. Preparation and characterisation of dense TiO_2 ceramics. *Advances in Science and Technology*, 2008, No. 54, 261-264.

2. M.Reimanis, J.Ozoliņš, J.Mālers. Ūdens bioloģiskā piesārņojuma samazināšana pielietojot elektrolīzes procesā TiO_x saturošu keramikas elektrodus. *RTU zinātniskie raksti, Materiālzinātne un lietišķā ķīmija*, 2008, 18, 90.-96.

PO-73

IONIZATION OF CARBOXYLIC CATION-EXCHANGER AND SORPTION OF PROTEINS

V. Krilova

Institute of Biomaterials and Biomechanics, Riga Technical University, Latvia

e-mail: v.krilova@inbox.lv

Usage of sorption processes is the contemporary solution of many challenges in analytical, preparative and industrial chemistry dealing with purification, concentration or separation of target substances. Functional cross-linked polymers possess sorption activity which depends on polymer functional groups nature, their condition, polymer network structure, solution composition and many other factors. Sorbate nature and sorbent permeability are also decisive for the process, especially for sorption of proteins.

Porous cation-exchanger having two types of carboxylic groups has been synthesized by developed one-stage synthesis – suspension polymerization of methacrylic and acrylic acids (molar ratio 3:1) and triethyleneglycol dimethacrylate (15%) in the presence of a diluent [1]. Ionization parameters (at different ionic strength) were defined from potentiometric curves as $pK_\alpha - lg[(1- \alpha)/ \alpha]$ (α –ionization degree) dependence using Henderson-Hasselbach equation. The morphology of sorbent beads has been observed using SEM. Bovine serum albumin and lysozyme were model proteins for investigation of ionic strength influence at different pH on protein binding. Sorption regularities might be partially explained by carboxylic groups ionization increase with the increase of ionic strength, while the change affected sorption differently at different pH values.

References:

1.V.Krilova, J.Ģībietis, E.Ārens. *Latvijas Ķīmijas žurnāls*, 1994, 2, 226-233.

PO-74

WATER SOLUBLE BIOACTIVE ORGANIC-INORGANIC Si- AND Fe-CONTAINING HYBRID MATERIALS BASED ON LIGNOSULPHONATE

T. Dizhbite[1], G. Telysheva[1], G. Lebedeva[1], N. Mironova-Ulmane[2], A. Andersone[1], L. Belkova[1]

[1]*Latvian State Institute of Wood Chemistry,*

[2]*Institute of Solid State Physics, University of Latvia*

e-mail: ligno@edi.lv

The present work continues our researches aimed at synthesis of functionalized lignocellulose-silica hybrid products with incorporated bioactive metals [1]. A novel series of organic-inorganic hybrid materials were prepared *via* blending of solutions of lignosulphonate (LS - a water soluble lignin by-product from the pulp industry), silica and Fe^{3+}. The work was aimed at the design of novel efficient agrochemicals combining the positive effects of siliceous lignins [1] and already known Fe-containing LS [2] on plant development. The solid LS-silica-Fe hybrids (4-8 wt% of silica and 4-5 wt % of Fe) were characterized by FT-IR, SEM/EDS, EPR, Raman microscopy, DSC and TGA. The films obtained from hybrid materials were optically transparent, which revealed that inorganic components were well dispersed on scale smaller than the wavelength of visible light. It was shown that simultaneous presence of silica network and free Si-OH groups as well as hydrogen bond interactions between silica and lignin resulted in formation of physical micro cross-linking network structure in the hybrid system. The evidences of formation of two types of Fe^{3+} complexes differed by the cation micro- environment were obtained. Difference in the micro-environment of Fe^{3+} could be due to the involvement of Si-OH groups, besides various LS groups (-SO_3, -OH_{phen} and -C=O), in complexing interaction within the hybrid materials. The formation of nanoclusters of inorganic components of the hybrids with diameter of 50-300 nm located within the LS polymer matrix was demonstarted. The results of germination tests confirmed the auxine-like bio-activity of the water-soluble LS-silica-Fe hybrid products synthesized. The results obtained can serve as a convenient approach to prepare water-soluble hybrids and broaden the application field of silica-containing polymers.

References

1. G.Telysheva, T.Dizhbite, D.Evtuguin, N.Mironova-Ulmane, G.Lebedeva, A.Andersone, O.Bikovens, L.Belkova, *Scripta Materialia* 2009, 60, 687-690.

2. P.Rodriges-Lucena , N.Tomasi, R.Pinton, L.Hernandez-Apaolaza, J.J.Lucena, S.Ceseo, *Plant Soil*, 2009, 325, 53-63

PO-75

EPR AND MÖSSBAUER SPECTRA OF IRON IONS IN THE HEMOGLOBIN

M.Polakovs[1], N. Mironova-Ulmane[1], A. Pavlenko[1], S. Lebedev[2]

[1]*Institute of Solid State Physics, University of Latvia, Latvia,*

[2]*Institute of solid-state physics and semi-conductors NAS of Belarus*

e-mail: mpolakovs@latnet.lv

In this work we have studied the Fe^{2+} and Fe^{3+} ions in hemoglobin by EPR and Mössbauer spectroscopies**.** Hemoglobin for EPR spectroscopy was obtained from normal human adult venous blood, from Chernobyl clean-up workers, from adult patients with erythraemia and Hb from SIGMA. Mössbauer spectroscopy was performed Hb(SIGMA) only. The EPR spectra were recorded using an EMX-6/1 spectrometer (BRUKER) working at X-band frequency with 100 kHz modulation. Magnetic field varied between 100 and 7000 Gauss. The g-factors of EPR signals were determined by reference to the external magnetic field. The EPR signal intensities of samples were measured against fixed standard signals of crystal MgO-Cr^{3+} placed in resonant cavity.

It is shown that in Hb(SIGMA) the ion Fe of methemaglobin is in low-spin state with g = 2.3 and in the high spin state with g=6. The EPR signal g = 4.3 is assigned to transferrin Fe^{3+} ions. Ours results show that the blood of the Chernobyl` clean–up workers who have erythrocytosis contain methemoglobin higher normal. Perhaps the ion Fe^{2+} in the heme of hemoglobin is oxidized to the ion Fe^{3+} in the heme by radiation. While estimating the health status of clean-up workers part of the revealed pathology could be explained by the higher levels of strontium and other radionucleids in the body. It was found that the main radionuclide presented in teeth is Sr-90 and it contributed from 20% to 50% to the total absorbed dose [1]. EPR can detect the concentration of methemoglobin more accurately than any other technique.

References:

1. Mironova-Ulmane N, Pavlenko A, Eglite M et al. (2005) Chernobyl clean-up workers: 17 years of follow-up in Latvia. *Recent Advances in Multidisciplinary Applied Physics, pp.9-19, Elsevier 2005 (ISBN 0 08 0444 696-5)*

PO-76

UV-VUV SPECTROSCOPY OF SiO_2 PHOTONIC CRYSTAL DOPED WITH HEuEDTA PHOSPHOR

M. Kirm[1], M.I. Danilikin[2], K. Tarkpea[1], S.O. Klimonsky[3], A.S. Sinitskii[3], Yu.D. Tretyakov[3]

[1]*Institute of Physics, University of Tartu, Estonia,*

[2]*Institute of Chemistry, University of Tartu, Estonia,*

[3]*Department of Materials Science M.V. Lomonosov Moscow State University, Russia*

e-mail: marco@fi.tartu.ee

Photonic crystals (PCs) are attractive for various optical applications in the visible region due formation of photonic band-gap. SiO_2-based opal-like PCs were prepared at MSU with the average size of the microspheres ~ 270 nm, which results in a photonic band-gap < 600 nm. In the same wavelength range 4f transitions from the $^5D_0$ and $^5D_1$ states of Eu^{3+} ion occur. Thus the PCs structure can influence luminescence properties of Eu^{3+} ion. Europium (III) salt of ethylenediamine-tetraacetic acid (HEuEDTA) was embedded in silica PCs by infilling them with HEuEDTA water solution and further drying in air [1]. Thereafter, PCs doped with HEuEDTA were washed in water removing the excess of dopant from the inner surface of PCs. The resulting distribution of luminescent ions in the volume of PCs is mostly determined by the contact points between SiO_2 nano-particles. The aim of the present study was to investigate luminescence properties of such Eu^{3+} doped material using time-resolved spectroscopy under synchrotron radiation at DESY.

The dominating luminescence observed in studied samples is due to the $^5D_0 - {}^7F_J$ transitions covering range above 580 nm at 300 and 10 K. The emission lines are inhomogeneously broadened, typical consequence of nano-effects, indicating that an ensemble of Eu^{3+} ions at non-equivalent positions in PCs is involved. At low temperatures broad band UV emissions were revealed peaked at 330 and 470 nm. Both UV emissions as well as the Eu^{3+} $^5D_0 - {}^7F_2$ 4f luminescence are most efficiently excited in the transparency range of 4-8 eV of SiO_2 with optical gap > 8.5 eV for its various modifications. The stronger UV band at 330 nm has a decay time near 3 ns, having similar characteristics to UV emissions assigned to oxygen deficient centres in various SiO_2 modifications [2]. The excitations peaks observed are assigned to the defect centres. The origin of luminescence centres and energy transfer processes in Eu^{3+} doped SiO_2 based PCs will be discussed in this report.

References

1. A.S. Sinitskii, S.O. Klimonsky, Yu.D. Tretyakov *et al, Proc. of SPIE,* 2006, Vol. 6182, 61822N.

2. A.N. Trukhin, *J. of Non-Crystalline Solids*, 2009, vol. 355, 1013.

PO-77

NEAR-BAND LUMINESCENCE OF ZnO CRYSTALS IN SUBNANOSECOND RANGE

L. Grigorjeva, J. Grube, A. Sarakovskis, D. Millers

Institute of Solid State Physics, University of Latvia

e-mail: lgrig@latnet.lv

It is known that the decay time of excitonic luminescence is in subnanocecond time range [1]. The luminescence spectrum at low temperature consists of several bands attributed to exciton (Ex) bound at neutral donor (D^0Ex), two –electron satellite (TES), LO phonon replicas of D^0Ex (1LO_ D^0Ex and 2LO_ D^0Ex). At RT the Ex_1LO luminescence (at 3.26 eV) is dominant. The lifetimes of luminescence caused by excitons are in 50-900 ps time range.

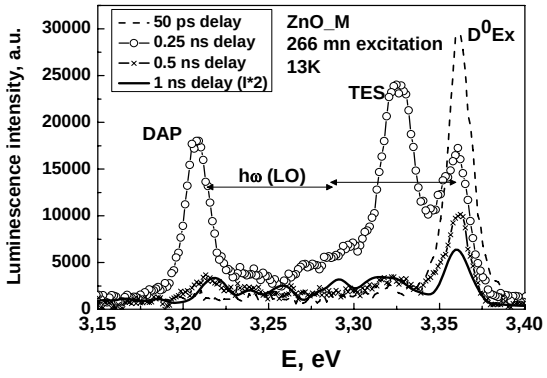

Fig.1 The luminescence spectra evolution in subnanosecond range

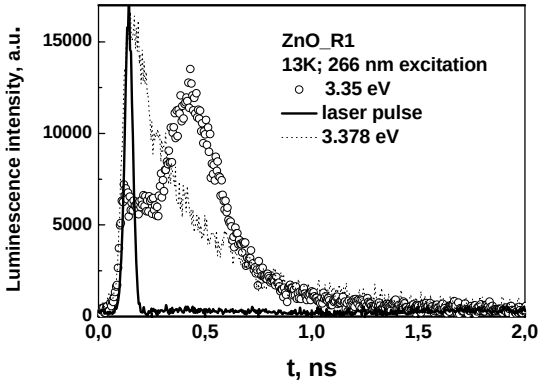

Fig.2 The luminescence decay of different spectral points of D^0Ex band

Therefore, for the excitonic process studies the tunable picoseconds solid state laser was used. The Streak scope C4334 was used for luminescence spectra and decay kinetic registration. The luminescence of ZnO crystals were studied in temperature range 13-300K.

The luminescence studies within subnanosecond range allowed to analyze the spectrum time evolution (Fig.1) and the exciton trapping mechanisms (Fig.2) in different ZnO crystals.

References

1. J.Wilkinson, K.B.Ucer, R.T.Williams. Picosecond excitonic luminescence in ZnO and other wide-gap semiconductors. *Radiation Measurements,* 2004, 38, 501-505.

PO-78

PHOTOLUMINESCENT AND PHOTOCATALYTIC ACTIVITY OF NANOSIZED ZINC TUNGSTATE PREPARED BY COMBUSTION SYNTHESIS

J. Grabis[1], D. Jankovica[1, 2], L. Grigorjeva[2], D. Millers[2]

[1]*Institute of Inorganic Chemistry, Riga Technical University,*

[2]*Institute of Solid State Physics, University of Latvia*

e-mail: lgrig@latnet.lv

Zinc tungstate nanoparticles have numerous potential applications in microwave amplification, X-ray scintillators, photoluminescent materials, photocatalysts and flame retardants. Nanosized $ZnWO_4$ powders have been synthesized by wet chemical methods such as co-precipitation, hydrothermal, mechanochemical synthesis and evaporation of polymerbased metal-complex precursor solution. It is well known that luminescent and photocatalytic activity of $ZnWO_4$ depend on preparation method, particle size and calcination temperature.

In the present work the photocatalysis rate and its correlation with luminescence was studied for $ZnWO_4$ nanopowders. Powders were prepared by simple combustion route. Solution of dissolved tungsten in hydrogen peroxide was mixed with zinc acetate solution. Then ethylene glycol and nitric acid were added. The reactants were stirred and heated for 3–4 h up to 250 ^oC until the burning of the formed viscous gel was started. The pure $ZnWO_4$ nanoparticles with different crystallite size (S_{BET} 21÷6.1 m^2/g) were obtained after calcinations at 600-1000 ^oC for 2 h. Photocatalytic activity of $ZnWO_4$ particles were evaluated by degradation of methilene blue (MB) solution under UV Hg lamp irradiation. Luminescence spectra and decay kinetics were studied under YAG:Nd laser excitation. The strong dependence of photocatalytic activity and luminescence decay time on $ZnWO_4$ crystallite size was determined (Fig.). The model for photo catalyti process was suggested.

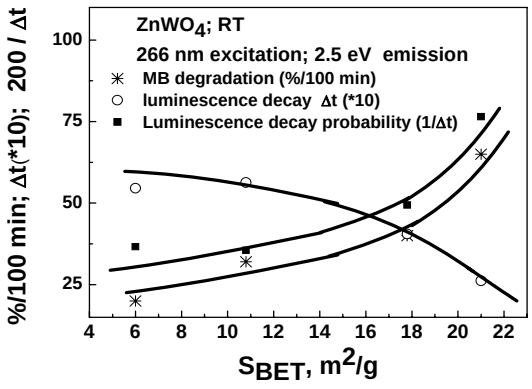

Fig. The correlation of photocatalytic efficiency an luminescence decay time for $ZnWO_4$ nanocrystals

PO-79

UP-CONVERSION LUMINESCENCE IN ZrO_2 NANOCRYSTALS

K. Smits[1], L. Grigorjeva[1], D. Millers[1], A. Sarakovskis[1], D. Jankovica[2], J. Grabis[2]

[1]*Institute of Solid State Physics, University of Latvia, Latvia,*

[2]*Institute of Inorganic Chemistry, Riga Technical University, Latvia*

e-mail: smits@cfi.lu.lv

There is a large interest to dope the zirconia with rare earth ions to obtain upconversion luminescence material for biological labelling [1] as well as for other applications, because ZrO_2 is very good candidate for doping due to low phonon energy (about 470cm^{-1}). The study of time-resolved luminescence of undoped and Er_2O_3 and Yb_2O_3 doped zirconia free standing nanocrystals, produced by sol - gel method was carried out. A set of samples with different Er and Yb concentration was prepared. The dopant concentration effect on luminescence was studied. The three polymorphs of zirconia are known–monoclinic, tetragonal and cubic. Only the monoclinic phase of pure ZrO_2 crystals is stable at room temperature; however the incorporation of Er and Yb ions led to the tetragonal phase stabilization. The correlation between Er and Yb related to tetragonal or even cubic structure stabilization and intrinsic defect concentration change was studied. The explanation about luminescence band change is provided. The mechanisms of excited state creation and the possible models of luminescence centres in the nanocrystals will be discussed.

The financial support of ESF project 2009/0202/1DP/1.1.1.2.0/09/APIA/VIAA/141 is greatly acknowledged.

References

1. G. Chen, G. Somesfalean, Y. Liu, Z. Zhang, Q. Sun, and F. Wang, *Physical Review B*, 2007, 75, 195204

PO-80

THE LUMINESCENCE PROPERTIES OF LANTHANIDES IONS IN $LiLn_{1-x}Ce_xP_4O_{12}$ POLYPHOPHATES

T. Shalapska[1, 2], G. Stryganyuk[3], P. Demchenko[2], A. Voloshinovskii[2]

[1]*Institute of Physics University of Tartu Estonia,*

[2]*Ivan Franko National University of Lviv, Ukraine,*

[3]*Institute for Scintillation Materials NAS of Ukraine, Ukraine*

e-mail: t_shalapska@ukr.net

Stoichiometric polyphosphates compounds based on the lanthanides are considered as the promising luminescent materials for different applications. For such a type of compounds a relatively long distance between the lanthanides ions is typical. This fact facilitates the decreasing of concentration quenching and helps in achieving high emission intensity. In particular, the Ce^{3+} luminescence in $CsGdP_4O_{12}$:10.0 at% Ce^{3+} powder sample delivers a high light yield (24 400 photon/MeV) [1] and $NaGdP_4O_{12}:Tb^{3+}$ is more preferable phosphor for PDP than $Zn_2SiO_4:Mn^{2+}$ [2].

We report on the investigation of the luminescent characteristics of $ALnP_4O_{12}:Ce^{3+}$ (A=Li, Na, Ln=Y, Pr, Gd) powder samples upon the excitation with high-energy quanta of synchrotron radiation in the VUV-UV range [3] and X-ray quanta. The mechanism of the excitation energy transfer processes involving the contribution of Ln -sublattice, the formations of electron-hole pairs and excitons are studied in these polyphosphates doped with cerium ions.

Basing on the VUV emission and excitation spectra data, the relationships between 5d energy level position of Ce^{3+} ion and crystalline environment were analyzed. The enhancing of the Ce^{3+} luminescence intensity upon high energy quanta excitation for $LiPrP_4O_{12}:Ce^{3+}$ and $LiGdP_4O_{12}:Ce^{3+}$ were revealed owing the effective energy transfer processes in Pr - Ce and Gd - Ce pairs. The peculiarities of the *5d-4f* luminescence of Pr^{3+} and Ce^{3+} and the *4f-4f* luminescence of Gd^{3+} and their decay time constants are used for evaluation of energy transfer efficiency. Besides the direct energy transfer from Gd^{3+} to Ce^{3+} the inverse process is observed [4].

References

1. J Zhong, H Liang, Q Su et al. *Optical Materials*, 2009, 32, 378-381.

2. J Zhong, H Liang, B Han, Q Su, Y Tao *Chemical Physics Letters*, 2008, 453, 192–196

3. G Zimmerer. *Radiations Measurements* 2007, 42, 859-864.

4. T Shalapska, G Stryganyuk, P Demchenko, A Voloshinovskii and P Dorenbos, *J Phys: Conds. Matter,* 2009, 21, 445901

PO-81

CHARACTERIZATION OF PURE AND RARE EARTH DOPED ZnO NANOPARTICLES FOR OPTICAL APPLICATIONS

D. Venkatesan[1], D. Deepan[1], R. Guru Hariharan[1], M. Velavan[1], R. Sankar[2], R. Jayavel[3], R. Dhanasekaran[4]

[1]*Department of Mechanical Engineering, Anna University Chennai, Chennai 600025, India,*

[2]*Centre for Condensed Matter Science, National Taiwan University, Taiwan,*

[3]*Centre for Nanoscience and Technology Anna University Chennai, Chennai 600 025, India,*

[4]*Crystal Growth Centre, Anna University Chennai, Chennai 600 025, India*

e-mail: venkatesan08@gmail.com

Pr and Nd doped ZnO nanoparticles are prepared by simple chemical route and precursors used are $ZnCl_2$ and NaOH. From XRD patterns, the particles size are found to be 15, 16, 17 nm for 1 wt%, 2 wt% and 3 wt% of Pr doped ZnO nanoparticles respectively and 17,18, 19 nm for 1 wt%, 2 wt% and 3 wt% of Nd doped ZnO nanoparticles respectively. Absorption studies are carried out from 200 to 800 nm. The ZnO cut off wavelength of both the Pr and Nd doped are found near 346 nm. Pr^{3+} absorption peaks are found at 446, 463 and 589 nm and these correspond to transitions from the ground state of $^3H_4$ to $^3P_2$, $^3P_1$ and $^1D_2$ and Nd^{3+} absorption peaks are found at 520, 578, 738 and 799 nm and these correspond to transitions from the ground state of $^4I_{9/2}$ to $^4G_{7/2}$, $^4G_{5/2}$ + $^2G_{7/2}$, $^4S_{3/2}$ + $^4F_{7/2}$, $^4F_{5/2}$ + $^2H_{9/2}$. Photoluminescence studies of the sample are also made and excitation wavelength was 325 nm. Emission bands characteristic of Pr^{3+} are observed at 450, 469, 482 and 493 nm for samples, which corresponds to $^3H_4$->$^3P_2$, $^1I_6$->$^3H_4$, $^3P_1$->$^3H_4$ and $^3P_0$->$^3H_4$ transitions, respectively. Emission bands characteristic of Nd^{3+} are observed at 450, 473, 480 and 530 nm for samples, which corresponds to $^2P_{3/2}$ -> $^4I_{13/2}$, $^2P_{3/2}$->$^4I_{15/2}$, $^2P_{1/2}$->$^4I_{11/2}$ and $^4G_{7/2}$->$^4I_{9/2}$ transitions, respectively. FTIR spectra show the Zn-O stretching at 535 cm^{-1} for the Pr doped and at 544 cm^{-1} for Nd doped ZnO nanoparticles. High resolution SEM images are taken and morphology of the particles was reported.

PO-82

SENSITIZING OF Sm^{3+} FLUORESCENCE BY SILVER DOPANT IN THE TiO_2 FILMS

L. Dolgov, V. Kiisk, V. Reedo, S. Pikker, I. Sildos, J. Kikas

Institute of Physics, University of Tartu, Estonia

e-mail: dolgov@fi.tartu.ee

Rare earth ion-doped materials are perspective for fluorescent and laser applications [1, 2]. Their emitting properties may be improved by using sensitizers, particularly silver. Sensitizing of rare earth emission can be achieved due to plasmonic effects caused by silver nanoparticles or energy transfer from silver ions. Thus plasmonically gained local electric field near silver nanoparticles can enhance fluorescence as found for Er^{3+} in the infra-red region of spectrum [3]. While fluorescence in the visible region caused by energy transfer from silver ions to rare earths is not so effective still [4].

Here we propose a TiO_2 based composite material with Sm^{3+} ions sensitized by silver nanoparticles. The co-doped samples of TiO_2 films were prepared using sol-gel method with subsequent annealing. Analysis of Raman scattering from films reveals that TiO_2-Sm^{3+} compound was obtained in anatase phase. At the same time samples doped with silver consist not only on anatase but also on rutile and amorphous phases. Fluorescence of Sm^{3+} centers was analyzed at direct (λ=488 nm) and indirect (λ=355 nm) excitations. It turned out that fluorescence of directly excited Sm^{3+} ions near the aggregates of silver particles is up to 20 times higher than in the TiO_2-Sm^{3+} system without silver. The possible reasons of revealed enhancement in Sm^{3+} fluorescence are discussed.

References

1. V. Kiisk et al., *Appl. Surf. Sci.*, 2005, 247, 412-417.

2. H.-S. Hsu et al., *Opt. Express*, 2009, 17, 25, 23265-23271.

3. A. C. Marques, R. M. Almeida *J. Non-Cryst. Solids*, 2007, 353, 2613-2618.

4. G. E. Malashkevich et al. *Phys. of Solid State*, 2008, 50, 8, 1464-1472.

PO-83

LUMINESCENCE OF HEXAGONAL BORON NITRIDE POWDER AND NANOTUBES AT DIFFERENT TEMPERATURES

V. Korsaks, B. Berzina, L. Trinkler

Institute of Solid State Physics, University of Latvia, 8 Kengaraga Str., LV-1063 Riga

e-mail: valdis.korsaks@inbox.lv

Hexagonal boron nitride (h-BN) and appropriate nanostructured materials are widely investigated in both theoretiacally and experimentally. A special interest is paid to the excitonic processes and exciton luminescence observed in the spectral region around 215 nm. Our attention is concentrated to the spectral region from 300 up to 600 nm.

The photoluminescence spectra (PL) and its excitation spectra (PLE) of the macrosize h-BN powder and nanomaterial consisting of the multiwalled h-BN nanotubes (BNNT) observed within the broad temperature range from 8 K up to 300 K are studied and reported. The material was excited with the 266 nm light from a pulse laser or under continuous irradiation with light of a deuterium lamp. The luminescence spectral groups at 300 nm, 400 nm and around 500 nm forming the total complex luminescence spectrum previously known are observed within the wide temperature range. The broad 400 nm band with its well resolved phonon structure is predominant in both materials the h-BN powder and BNNT. At present its origin is related to the excitonic processes influenced by the nitrogen vacancies. It was found that the ratio of the phonon related sub-bands intensities is sensitive to the temperature within the studied range. In the same time the intensity of the whole 400 nm band is sensitive to the material pretreatment (preheating, irradiation with UV light). In the case of the broad 500 nm luminescence band it was observed that its characteristic parameters (maximum position, band's half-width, intensity) are strongly dependent on the pretreatment of the material (preheating, irradiation with UV light) and external conditions (the sample is located in vacuum or in air). Especially it is observable in the case of irradiation with laser light. It allows conclusion that this complex luminescence band could be related to different surface defects caused by oxidation processes.

PO-84

PHOTOLUMINESCENCE OF Al_2O_3 BULK AND NANOSIZE POWDERS AT LOW TEMPERATURE

D. Jakimovica[1], L. Trinkler[1], B. Berzina[1], J. Grabis[2], I. Steins[2]

[1]*Institute of Solid State Physics, University of Latvia,*

[2]*Institute of Inorganic Chemistry, Riga Technical University*

e-mail: darjakasjane@inbox.lv

Photoluminescence (PL) has been studied in Al_20_3 bulk and nanosize powders in the temperature range 7-300 K. Bulk powder is characterized with 20-60 μm large particles and α phase of crystal structure, while nanosize powder contains grains of 20-50 nm, whose structure is ascribed to mixture of transition phases: θ and δ. UV-light induced PL spectra of both bulk and nanosize powders consist of two broad complex emission bands (300-600 nm and 650-900 nm), containing overlapping bands of different origin. It was observed that in Al_2O_3 nanosize powder ratio of the luminescence bands changes under exposure to air: the short wavelength band increases several times in intensity, while the long wavelength band decreases. The study of thermal evolution of PL has shown that in bulk and nanosize samples with the decrease of temperature 1) PL intensity of both luminescence bands increases by factor of 2 to 4, 2) shape of the short wavelength band changes due to the growth of the 470 nm subband, 3) the long wavelength band becomes resolved into fine structure.

Analysis of these features helps to ascribe emission subbands to definite defects taking part in the luminescence process. The luminescence properties of the studied alumina powders are determined mainly by presence of uncontrolled impurity defects, among them titanium ions playing the decisive role. Intrinsic and surface defects also contribute to the luminescence processes. Distinctions revealed in PL emission and excitation spectra of both sample types as well as behavior in air are explained by differences in grain structure and scaling effects.

PO-85

LUMINESCENCE AND OPTICAL PROPERTIES OF SEMICONDUCTOR QUANTUM DOTS IN VUV SPECTRAL RANGE

V. Pankratov[1], V. Osinniy[2], A. Kotlov[3], A. N. Larsen[1, 2], B. B. Nielsen[1, 2]

[1]*Institute of Solid State Physics, University of Latvia,*

[2]*Department of Physics and Astronomy, University of Aarhus, Denmark,*

[3]*HASYLAB at DESY, Hamburg, Germany,*

e-mail: vladimirpankratov@inano.dk

Semiconductor nanocrystals (NC) may have superior optical properties compared to bulk materials owing to quantum confinement effects. As examples, novel properties of devices containing nanocrystals have been demonstrated in photovoltaic solar cells, light-emitting diodes, electrochromic devices etc. However, the luminescent properties of semiconductor nanocrystals still remain poorly understood, especially in vacuum ultra violet (VUV) spectral range.

Multilayer and randomly distributed Si NC embedded into SiO_2 amorphous matrix were grown by means of radio frequency magnetron sputtering technique with subsequent thermal annealing in N_2 atmosphere at 1100 0C during 1 h. In the current study optical and photoluminescence (PL) properties of Si NC in UV-VUV spectral range have been studied under pulsed synchrotron radiation from DORIS III storage ring of (Hamburg, Germany). The Superlumi experimental station of HASYLAB was employed for investigation of emission, excitation as well as transmission spectra.

PL excitations and transmission spectra in the VUV (3.6 – 25 eV) spectral range were obtained for the first time for Si NCs embedded into SiO_2 matrix. It was clearly demonstrated that the PL excitation and transmission spectra are Si NCs size depended. It is suggested that the Si NCs size influences the energetical positions of the optical transitions and their oscillator strengths. The results obtained are compared with known theoretical calculations. Least but not last, it is suggested that Multiple Exciton Generation (MEG) processes, when absorbed photon causes the formation of two or more excitons, take place in Si NC with diameter smaler than 3 nm. It was obtained that the threshold excitation energy of MEG is about $2.7E_g$ for smallest (2.5 nm) Si NC.

PO-86

SILICON CARBIDE NANOWIRES: SYNTHESIS AND LUMINESCENCE PROPERTIES

A. Huczko[1], A. Dabrowska[1], V. Savchyn[2], I. Karbovnyk[2], V.Pankratov[3], A.I. Popov[3]

[1]*Department of Chemistry, Warsaw University, 1 Pasteur str., 02-093 Warsaw, Poland*

[2]*Department of Electronics, Ivan Franko National University of Lviv, 107 Tarnavskogo str, 79017 Lviv, Ukraine*

[3]*Institute of Solid State Physics, University of Latvia, Kengaraga 8, 1063 Riga, Latvia*

e-mail: popov@ill.fr

The β-SiC (or 3C-SiC) nanowires were efficiently produced using the thermal-explosion mode of self-propagating high temperature combustion synthesis.

We present the study of one-dimensional β-SiC structures [1,2] by means of cathodoluminescence (CL) technique. CL spectra of several nano 1D-SiC samples and of a reference commercially available 3C-SiC, measured at 77 K, are compared. It was demonstrated that the emission band at 1.97 eV related to irradiative transitions between the deep defect level (silicon vacancy) and the conduction band (weakly detected in the spectrum of the commercial SiC) becomes, under 10 keV electron beam irradiation, the prevailing band in CL of the purified silicon carbide nanowires. After the final stage of purification process the intensity of 1.97 eV band is almost 10 times stronger with respect to the 2.38 eV peak which, in turn, corresponds to band-to-band transition in 3C-polytype of silicon carbide. Observed behavior confirms that produced nanowires are defects-enriched. We have also compared CL spectra with those obtained under synchrotron excitation at SUPERLUMI station of HASYLAB at DESY.

Summarizing, a morphological characterization of the fabricated 3C-SiC 1D nanostructures has been performed by combining electron microscopy with CL measurements. Using those techniques as complementary tools can be helpful in the analysis of various nanomaterials having pronounced defect

References

1. A. Huczko, A. Dabrowska, V. Savchyn, A.I. Popov, and I. Karbovnyk, *Phys. Status Solidi B*, 2009, 246, 2806-2808.

2. V. Savchyn, I. Karbovnyk, A.I. Popov, and A. Huczko, *Acta Phys. Polon. A*, 2009, 116, S142-S145.

PO-87

SURFACTANT-ASSISTED SYNTHESIS OF $Cd_{1-X}Co_XS$ NANOCLUSTER ALLOYS AND THEIR STRUCTURAL, OPTICAL AND MAGNETIC PROPERTIES

R. Sathyamoorthy[1], P. Sudhagar[1], A. Balerna[2], C. Balasubramanian[3], S. Bellucci[2], A.I. Popov[4.5], K. Asokan[6]

[1]*R & D Department of Physics, Kongunadu Arts & Science College, Coimbatore, Tamilnadu 641 029, India*

[2]*INFN-Laboratori Nazionali di Frascati, Via E. Fermi 40000044, Frascati, Italy*

[3]*Facilitation Centre for Industrial Plasma Technologies, Institute for Plasma Research, Bhat, Gandhinagar 382428, India*

[4]*Institute of Solid State Physics, University of Latvia, 8 Kengaraga Str, LV-1063 Riga, Latvia*

[5]*Institite Laue-Langevin BP 1566, ru Jules Horowitz, 38042 Grenoble Cedex 9, France*

[6]*Inter University Accelerator Centre, Aruna Asaf Ali Marg, New Delhi 110 067, India*

e-mail: popov@ill.fr

We report the synthesis of Co-doped CdS nanoclusters ($Cd_{1-x}Co_xS$) for different doping concentrations ($x = 0.10$, 0.20 and 0.30) and characterization of their structural, optical, and magnetic properties [1]. The structural properties studied by X-ray diffraction revealed hexagonal-greenockite structure and a decrease of the lattice parameters (*a* and *c*) with doping, showing incorporation of Co in the lattice. The morphology of the nanoclusters was studied by scanning electron microscopy. The optical absorption studies, using diffused reflectance spectroscopy, revealed that Co doping modifies the absorption band edge. Ferromagnetic phase was observed in the magnetization measurements at room-temperature due to high carrier concentration. X-ray absorption near edge fine structure measurements at the sulfur (S) K-edge of the Co-doped samples revealed that the valence remains divalent and that there are some changes with Co doping in the spectral intensity.

References

1. R. Sathyamoorthy, P. Sudhagar, A. Balerna, C. Balasubramanian, S. Bellucci**,** A.I. Popov and K. Asokan, *Journal of Alloys and Compounds* 2010 (in press) corrected proof: http://dx.doi.org/10.1016/j.jallcom.2009.12.063

PO-88

$CsPbCl_3$ NANOCRYSTALS DISPERSED IN THE $Rb_{0,8}Cs_{0,2}Cl$ MATRIX STUDIED BY FAR-INFRARED SPECTROSCOPY

A. Voloshynovskii[1], P. Savchyn[1], I. Karbovnyk[2], S. Myagkota[3], M. Cestelli Guidi[4]
M. Piccinini[4], A.I. Popov[5]

[1]*Ivan Franko National University of Lviv, Department of Physics, 8 Kyrylo and Mefodii street, 79005, Lviv, Ukraine*

[2]*Ivan Franko National University of Lviv, Department of Electronics, 107 Tarnavskogo street, 79017, Lviv, Ukraine*

[3]*Lviv State Agrarian University, Dubljany, Lviv, Ukraine*

[4]*INFN–Laboratori Nazionali di Frascati, Via E. Fermi 40, 00044 Frascati, Italy*

[5]*Institute for Solid State Physics, University of Latvia, Kengaraga 8, LV-1063 Riga, Latvia*

e-mail: popov@ill.fr

The comparative far-infrared spectroscopy studies of $Rb_{0.8}Cs_{0.2}Cl$ and $Rb_{0.8}Cs_{0.2}Cl$ containing $CsPbCl_3$ nanocrystals between 170 and 320 K are performed [1]. Far infrared reflectivity of $Rb_{0.8}Cs_{0.2}Cl$ crystals was measured at the Daphne Light IR station, Laboratori Nazionali di Frascati in Italy. Obtained reflectivity spectra have been analyzed using FOCUS software. Detailed analysis of FIR spectra allows to determine and analyze, in particular, the temperature dependences of phonon frequencies (in cm^{-1}), damping constants and optical dielectric constants of $Rb_{0.8}Cs_{0.2}Cl$ and $Rb_{0.8}Cs_{0.2}Cl$:Pb. The effect of cesium lead chloride nanocrystals on the phonon modes of the host matrix, particularly manifested in different temperature behavior of LO–TO splitting and the temperature dependence of high frequency dielectric constant, was demonstrated as well.

References

1. A. Voloshynovskii, P. Savchyn, I. Karbovnik, S. Myagkota, M. Gestelli Guidi, M. Piccinini, and A.I. Popov, $CsPbCl_3$ nanocrystals dispersed in the $Rb_{0.8}Cs_{0.2}Cl$ matrix studied by far infrared spectroscopy. - *Solid State Commun.*, 2009, 149, 593-597.

PO-89

LUMINESCENCE OF $SrTiO_3$ SINGLE CRYSTALS EXCITED UNDER SYNCHROTRON RADIATION

A.I. Popov[1], V. Pankratov[1], A. Kotlov[2], I. Aulika[1,3], A.G. Dejneka[4], D. Engers[1], E. Klotins[1], K. Kundzins[1], V.A. Trepakov[4,5] , V.Zauls[1], E.A. Kotomin[1,6]

[1] *Institute of Solid State Physics, University of Latvia, 8 Kengaraga, LV-1063 Riga, Latvia*

[2] *HASYLAB, DESY, Notkestrasse 85, D-22761 Hamburg, Germany*

[3] *Italian Institute of Technology, Via Trento 12, 10129 Turin, Italy*

[4] *Institute of Physics ASCR, 182 21 Prague 8, Czech Republic*

[5] *A.F. Ioffe Physico-Technical Institute, 194021 St. Petersburg, Russia*

[6] *Max Planck Institute for Solid State Research, D-70569 Stuttgart, Germany*

e-mail: popov@ill.fr

Luminescence emitted by a pure $SrTiO_3$ at low temperatures under exposure to UV or x-ray radiation has been known for a long time and is generally ascribed to the decay of intrinsic self-trapped excitons, which can be roughly depicted as a tightly bound state of a hole polaron and a Ti^{3+} electronic polaron [1].

In this talk, for the first time the luminescence properties of $SrTiO_3$ were studied under vacuum ultraviolet (VUV) and ultraviolet (UV) synchrotron radiation (3.6 – 25 eV) emitted from DORIS III storage ring at SUPERLUMI station [2], HASYLAB DESY, Hamburg, in the wide temperature range of 10–293 K. As it is well known, $SrTiO_3$ experimentally determined indirect band gap energy Eg=3.25 eV, whereas the direct band gap energy is 3.75 eV [3], and thus use of synchrotron radiation provides ideal conditions for the multiplication of electronic excitations, when each absorbed photon produces two or more electronic excitations. To study this effect, we have measured the appropriate excitation spectra of the so-called green emission (~500 nm). In particular, a prominent threshold for excitation multiplication at ca. 12.5 eV (as high as (3-4) Eg) was discovered. The results obtained are compared with the reflectivity and valence electron-energy loss spectroscopical data [3]. A comparison with the results of electronic structure calculations is also presented.

References

1. R. I. Eglitis, E. A. Kotomin, G. Borstel, *Eur. J Physics B* 2002, 27, 483-486

2. G.Zimmerer, *J Luminescence*, 2006, 119, 1.

3. K. Van Benthem, C. Elsässer and R.H. French. *J. Appl. Phys.*, 2001, 90, 6156.

PO-90

LUMINESCENCE PROPERTIES OF YAG:Ce^{3+} NANOCRYSTALS IN VACUUM ULTRAVIOLET SPECTRAL RANGE

L. Shirmane[1], A. Kotlov[2], A.I. Popov[1], W. Łojkowski[3], T. Chudoba[3], P. Gluhowski[4], D. Hreniak[4], W. Strek[4], V. Pankratov[1]

[1]*Institute of Solid State Physics, University of Latvia, 8 Kengaraga, LV-1063 Riga, Latvia,*

[2]*HASYLAB, DESY, Notkestrasse 85, D-22761 Hamburg, Germany,*

[3]*Institute of High Pressure Physics, Sokolowska 29, 01-142, Warsaw, Poland,*

[4]*Institute of Low Temperature and Structure Research, Okolna 2, Wroclaw, Poland*

e-mail: liana.shirmane@inbox.lv

In the present study time-resolved luminescence properties in visible-vacuum ultraviolet spectral range of cerium doped $Y_3Al_5O_{12}$ nanocrystals have been studied. The measurements were carried out under pulsed synchrotron radiation (3.6 – 22 eV) emitted from DORIS III storage ring on the SUPERLUMI station [1] of HASYLAB at DESY (Hamburg).

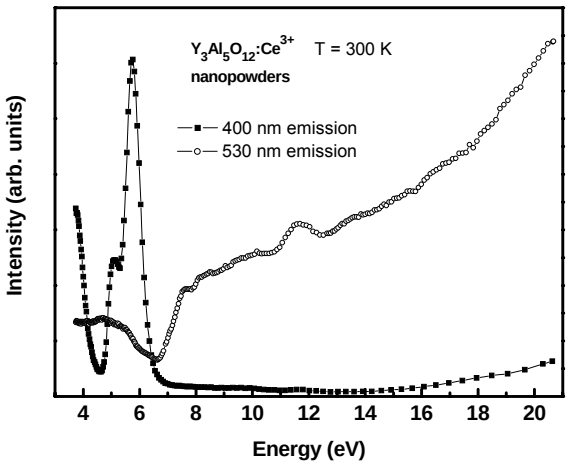

Additionally to Ce^{3+} green emission band which is well known luminescence in $Y_3Al_5O_{12}$, new emission band at 3.0 eV (~400 nm) was revealed in the luminescence spectra for all nanocrystals. This blue emission band has intensive well-resolved excitation bands in 3.6 – 7 eV spectral range and, in contrast to green Ce^{3+} emission, practically is not excited at higher energies (see figure). Moreover, such excitation spectrum has not been observed previously for any known intrinsic defect and/or impurities in $Y_3Al_5O_{12}$ [2]. Furthermore, blue emission band decays much faster then green Ce^{3+} emission in $Y_3Al_5O_{12}$. To our knowledge, this fast blue emission was not reported in literature before for both single crystals and nanocrystals and its nature will be discussed.

References

1. G. Zimmerer, *J. Luminescence*, 2006, 119, 1

2. V. Pankratov, L. Grigorjeva, T. Chudoba, W. Lojkowski, *IEEE Trans. Nucl. Sci.*, 2008, 55, 1509

PO-91

DFT SIMULATION OF GUANINE-QUARTET CHIRAL STRUCTURES

A. I. Livshits[1], L.N. Kantorovich[2]

[1]*Institute of Chemical Physics, University of Latvia,*

[2]*King's College London, London, UK*

e-mail: aliv@lanet.lv

Guanine molecules adsorbed on the Au(111) surface at room temperature are known [1] to form a heterochiral phase consisting of two homochiral G-quartet networks, called L and R. By annealing the sample at 400 K the R and L homochiral G-quartet networks are found to irreversibly transform to a heterochiral G-quartet network including both R and L G-quartets in an equal amount. Previous analysis of this intermixed G-quartet structure shows [1] that it is actually pro-chiral, since by fliipping the whole structure a geometrically different, but physically equivalent structure is obtained. Our calculations demonstrate the possibility for the G-quartet to exist in two forms, labelled I and II, with different arrangement of the H-bonds. This is why not a single G-quartet, but a pair of them must be considered as an elementary building block even in the case of homochiral structures. It increases the number of possible structures from two experimentally observed to at least six. The analysis of stability and transformations of the two experimentally observed and six numerically predicted by us G-quartet structures will follow.

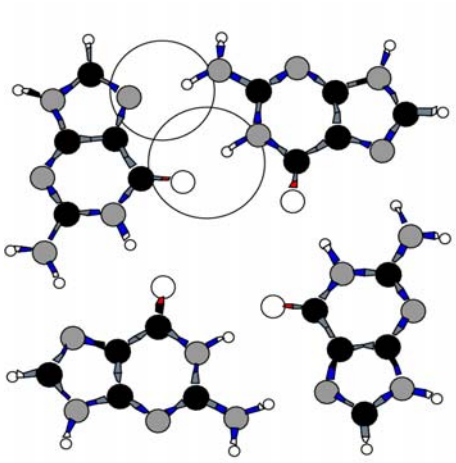

G quartet form I

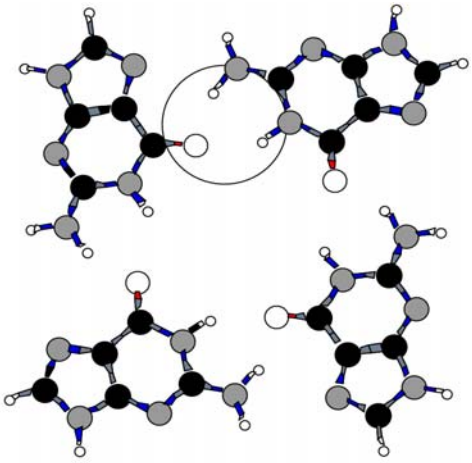

G quartet form II

References

1. W.Xu, R.E.A.Kelly, H.Gersen, E.Lægsgaard, I.Stensgaard, L.N.Kantorovich, F.Basenbacher., *Small* 2009, X, X, 1-5

PO-92

AB INITIO CALCULATIONS OF YTTRIUM AND VACANCY POINT DEFECTS FOR ODS STEELS MODELING

A. Gopejenko[1], Yu.F. Zhukovskii[1], P.V. Vladimirov[2], E.A. Kotomin[1], A. Möslang[2]

[1]*Institute of Solid State Physics, University of Latvia, LV-1063 Riga, Latvia,*

[2]*Forschungszentrum Karlsruhe, Institut für Materialforschung-I, Karlsruhe, Germany*

e-mail: agopejen@inbox.lv

Reduced activation steels strengthened by yttria precipitates are considered as promising structural materials for future fusion- and advanced fission-reactors [1]. They are usually produced by mechanical alloying for several tens of hours followed by hot isostatic pressing (HIPping) at temperature around 1000-1200°C and pressure ~100 MPa. This process is being continuously refined and optimized in our department to obtain better mechanical properties at high operation temperatures as well as excellent radiation resistance. Further optimization of the manufacture process would require deep understanding of atomic scale mechanisms of oxide particle formation. Up to now these mechanisms were not known. Recent experimental data suggest that yttrium oxide particles are, at least partly, dissolved during mechanical alloying and later precipitate again during hipping.

The kinetics of oxide particle growth is controlled by diffusion of solute atoms as well as by their chemical affinity to oxygen. The large-scale *ab initio* modeling of yttrium atom diffusion is performed using the Nudge Elastic Band (NUB) method interfaced with the *VASP* computer code [2], which is based on the plane-wave basis set combined with the non-local exchange-correlation functional constructed in the framework of Generalized Gradient Approximation (GGA). Results of these NUB first-principles calculations can be then employed for the lattice kinetic Monte Carlo (LKMC) simulations on the matrix and interstitial sublattices for Y_2O_3 cluster growth.

References

1. R. Lindau, A. Möslang, M. Schirra, P. Schlossmacher and M. Klimenkov, *J. Nucl. Mater,* 2002, 307–311, 769.

2. G. Kresse and J. Hafner, *VASP-5.2 User's Manual*, 2009. University of Vienna.

PO-93

FIRST PRINCIPLES LCAO STUDY OF PHONONS IN $NiWO_4$

A. Kuzmin[1], A.Kalinko[1], R.A. Evarestov[2]

[1]*Institute of Solid State Physics, University of Latvia, Latvia,*

[2]*Department of Quantum Chemistry, St. Petersburg University, Russia*

e-mail: a.kuzmin@cfi.lu.lv

At ambient conditions nickel tungstate $NiWO_4$ and zinc tungstate $ZnWO_4$ adopt wolframite-type structure and are isostructural. The electronic, structural and phonon properties of $ZnWO_4$ have been studied by us previously [1,2] within the periodic linear combination of atomic orbitals (LCAO) method [3], and the best agreement between experimental and theoretical structural and electronic parameters has been found for hybrid PBE0 (25%) Hamiltonian [1]. However, the IR and Raman phonon bands in $ZnWO_4$ have been reproduced rather qualitatively [2]: in particular, the theory tends to overestimate the Raman phonon frequencies, especially, at high energies where the observed difference reaches 50 cm^{-1}.

In this work we extend our studies to $NiWO_4$, which represents even more difficult case, since at low temperatures (≤67 K), it undergoes cooperative transition to antiferromagnetically-ordered state [4]. The electronic, structural and phonon properties of $NiWO_4$ have been studied using first-principles spin-polarized LCAO calculations by the CRYSTAL06 code [3]. Hybrid Hartree-Fock (HF)-DFT Hamiltonian (PBE0) was employed in the SCF calculations with different percentages of HF contribution (i.e. different correlation strength [5]). The calculations of phonon frequencies were performed by the direct (frozen phonon) method. We have found that the agreement between calculated and experimental phonon frequencies can be significantly improved by selecting the correlation strength equal to 13%.

References

1. A. Kalinko, A. Kuzmin, R.A. Evarestov, *Solid State Commun*., 2009, 149, 425.

2. R. A. Evarestov, A. Kalinko, A. Kuzmin, M. Losev, J. Purans, *Integr. Ferroelectrics*, 2009, 108, 1.

3. R. Dovesi et al., *Crystal 06, Users manual,* University of Turin, 2006.

4. H. Weitzel, *Solid State Commun*., 1970, 8, 2071.

5. J.P. Perdew, M. Ernzerhof, K. Burke, *J. Chem. Phys*., 1996, 105, 9982.

PO-94

ELECTRONIC EXCITATIONS IN $ZnWO_4$ AND $ZnWO_4$:Ni USING VUV SYNCHROTRON RADIATION

A. Kalinko[1], A. Kotlov[2], A. Kuzmin[1], V. Pankratov[1], A.I. Popov[1], L. Shirmane[1]

[1]*Institute of Solid State Physics, University of Latvia, Riga, Latvia,*

[2]*HASYLAB, DESY, Hamburg, Germany*

e-mail: a.kuzmin@cfi.lu.lv

The optical and luminescent properties of wolframite-type $ZnWO_4$ have been widely studied in the past more than once. In particular, the intrinsic luminescence band, observed at room temperature at about 2.5 eV, has been attributed to a charge transfer between oxygen and tungsten ions in the $[WO_6]^{6-}$ molecular complex [1].

In the present study, the luminescence spectra and luminescence excitation spectra of pure $ZnWO_4$ (nanocrystalline and microcrystalline) and Ni-doped $ZnWO_4$ are discussed. Measurements were performed at room temperature exploiting ultraviolet (UV) and vacuum ultraviolet (VUV) synchrotron radiation (3.6–20 eV) emitted from DORIS III storage ring at SUPERLUMI station (HASYLAB DESY, Hamburg).

The origin of luminescence and excitation spectra will be discussed based on our previous electronic structure calculations [2] and luminescence spectra/kinetics measurements [3-5].

References

1. V.N. Kolobanov, I.A. Kamenskikh, V.V. Mikhailin, I.N. Shpinkov, D.A. Spassky, B.I. Zadneprovsky, L.I. Potkin, G. Zimmerer, *Nucl. Instrum. Methods A*, 2002, 486, 496 and references wherein.

2. A. Kalinko, A. Kuzmin, R.A. Evarestov, *Solid State Commun.*, 2009, 149, 425.

3. A. Kalinko, A. Kuzmin, J. Lumin., 2009, 129, 1144.

4. V. Pankratov, L. Grigorjeva, D. Millers, S. Chernov, A.S. Voloshinovskii, *J. Lumin.*, 2001, 94-95, 427.

5. L. Grigorjeva, D. Millers, S. Chernov, V. Pankratov, A. Watterich, *Radiat. Meas.*, 2001, 33, 645.

PO-95

ANALYSIS OF VOID SUPERLATTICE FORMATION IN CaF_2

P. Merzlakovs[1], G. Zvejnieks[1], V.N. Kuzovkov[1], E.A. Kotomin[1], K.D. Li[2], L.M. Wang[2]

[1]*Institute of Solid State Physics, University of Latvia,*

[2]*Dept. Materials Science & Engineering, and Department of Nuclear Engineering & Radiological Sciences, University of Michigan, USA*

e-mail: pavels.merzlakovs@gmail.com

Irradiation of many metallic and insulating solids with energetic particles, such as heavy ions, neutrons, electrons, can result in a formation of ordered structures including periodic defect walls, bubble lattices, void lattices and periodic compositions in alloys [1-3]. The particular ordered structures arising in such open dissipative systems far from equilibrium depend on a type, energy, and flux of the energetic particles as well on the temperature. It was noticed [3] that despite the difference in the appearance, a similar underlying mechanism may be invoked to explain the selforganization behavior of these structures.

In this work, we quantitatively analyze the experimental results of halogen gas void formation in an electron-irradiated CaF_2. The filter is developed that digitalize the TEM micrographs and determine both void cluster distribution and characteristic void spacing (superlattice) depending on irradiation dose. Moreover, the void superlattice parameter scaling function with void hopping rate is proposed. The scaling function is crosschecked with kinetic Monte Carlo simulations in 2D using simplified model that includes void defect creation, migration and aggregation due to attractive defect interaction.

References

1. W. Jaeger and H. Trinkaus, *J. Nucl. Mater.*, 1993, 205, 394.

2. A. M. Stoneham, *Rep. Prog. Phys.*, 2007, 70, 1055.

3. H.C. Yu and W. Lu, *Acta Mater.*, 2005, 53, 1799.

PO-96

AB INITIO CALCULATIONS OF Nb-DOPED $SrTiO_3$

R. I. Eglitis[1], E. A. Kotomin[1,2]

[1]*Institute of Solid State Physics, University of Latvia,*

[2]*Max-Planck Institute fur Festkorperforschung, Heisenbergstr. 1, Stuttgart, Germany*

e-mail: reglitis@yahoo.com

Nb-doped $SrTiO_3$ is a promising material for several high tech applications including anodes of solid fuell cells [1] and non-volatile switching resistance memories [2]. We present the results of the large scale calculations of Nb impurities substituting for Ti ions using *ab initio* computer code CRYSTAL and several supercells containing up to 135 atoms. The local structure optimisation, the electronic charge redistribution, chemical bond covalence and the band-structure changes induced by the defect are analysed. Total charge density map for Nb-doped $SrTiO_3$ calculated by means of the hybrid B3PW method are depicted in Fig. 1. We demonstrate that Nb is a shallow donor and discuss also its segregation towards the surfaces/interfaces.

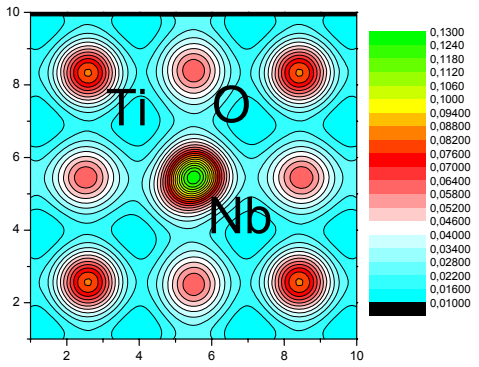

Fig.1 Total charge density map for Nb doped $SrTiO_3$ calculated by means of hybrid B3PW method.

References

1. P. Blennow *et al*., *Solid State Ionics*, 2008, 179, 2047

2. K. Szot *et al*., *Nature Materials,* 2006, 5, 312.

PO-97

AB INITIO CALCULATIONS OF MgF_2 (001) AND (011) SURFACES

R.I. Eglitis[1], A.F. Vassilyeva[2], E.A. Kotomin[1,3], A.K. Dauletbekova[2]

[1]*Institute of Solid State Physics, University of Latvia, Riga,*

[2]*L. N. Gumilyov Eurasian National University, Astana, Kazakhstan,*

[3]*Max-Planck Institute for Solid State Research, Heisenbergstr.1, Stuttgart, Germany,*

e-mail: reglitis@yahoo.com

MgF_2 is important wide-gap optical material with numerous applications. We are not familiar with any studies of its surface properties. In this paper we present calculations for the (001) and (011) MgF_2 surfaces using *ab initio* computer code CRYSTAL and the hybrid B3PW exchange and correlation functional. Both, neutral and polar surfaces show very small relaxation and negligible increase of covalent bonding thus remaining considerably ionic. Our calculated optical band gap (9.5 eV) is in a fair agreement with the experimental value of 13 eV, while HF method considerably (19.65 eV) overestimates the band gap, but DFT-based PBE method strongly (6.91 eV) underestimate it (see also [1]). The atomic relaxation at the surface and charge redistribution are discussed along with future calculations of radiation defects in MgF_2. Total MgF_2 DOS calculated by means of hybrid B3PW method are depicted in Fig. 1.

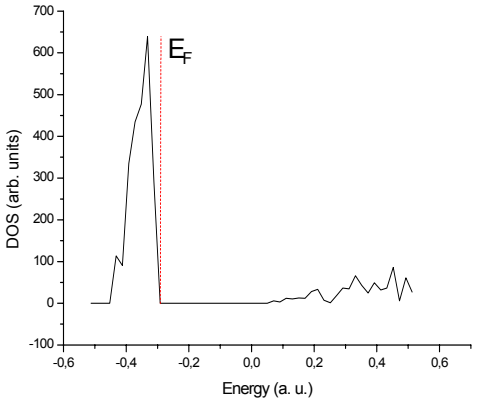

Fig.1 Total MgF_2 DOS calculated by means of hybrid B3PW method.

References

1. A. F. Vassilyeva, R. I. Eglitis, E. A. Kotomin, and A. K. Dauletbekova, *Physica B*., 2010, submitted

PO-98

AB-INITIO COMPARATIVE STUDY OF PHONONS IN DIFFERENT PHASES OF $SrTiO_3$ PEROVSKITE

E. Blokhin[1], D. Gryaznov[1], E. Kotomin[1], R. Evarestov[2], J. Maier[1]

[1]*Max-Planck Institute for Solid State Research, Stuttgart, Germany,*

[2]*Department of Quantum Chemistry, St. Petersburg State University, Peterhof, St. Petersburg, Russia*

e-mail: e.blokhin@fkf.mpg.de

$SrTiO_3$ perovskite is an excellent model material for mixed conduction investigation [1]. In the present study DFT LCAO simulations of cubic, tetragonal antiferrodistortive (AFD) and tetragonal ferroelectric (FE) $SrTiO_3$ crystals are performed via CRYSTAL06 [2] computer code. The calculations of atomic vibrations (phonons) are of great interest in perovskites as they provide the key to describe thermodynamic properties within *ab-initio* framework. The direct frozen-phonon method [3] is used for phonon calculations. The pure standard (PBE) DFT and hybrid (PBE0) HF-DFT exchange-correlation functionals are adopted. The study presented is the first step for considering defective and more complex systems.

It is well known from numerous EPR and Raman measurements that $SrTiO_3$ undergoes an AFD structural phase transition at 105K from cubic to tetragonal phase induced by the condensation of a soft phonon mode at the *R* point of the Brillouin zone (BZ). In this study the phonon dispersion over the BZ and thermodynamic properties of these two phases are discussed and the results obtained using two DFT functionals are compared. An incipient FE behavior in the low-temperature phase of $SrTiO_3$ is also taken into account considering a hypothetic FE phase. Though the FE phase transition is probably suppressed by atomic quantum fluctuations, the combination of *ab-initio* calculations and group-theory analysis permits us to examine and compare the AFD and FE instabilities.

References

1. R. Merkle and J. Maier, *Angew. Chem. Int. Ed.* 2008, 47, 3874

2. R. Dovesi, et al., CRYSTAL06 User's Manual, University of Torino, Torino, 2006

3. K. Parlinski, Z. Li, Y. Kawazoe, *Phys. Rev. Lett.* 1997, 78, 4063

PO-99

FINITE ELEMENT MODELLING OF THIN POLYMER SHELL

A. Kovalovs, S. Gluhihs, A. Chate

Institute of Materials and Structures, Riga Technical University, Latvia

e-mail: kovalovs@bf.rtu.lv

Standard methods for determining the elastic modulus of polymer materials are based on tension, compression and bending tests of specially prepared specimens. Contrary to steel, the linear elastic area of deformation of polymer materials in standard experiments is rather small. This is the reason for a noticeable measurement error in the results obtained by such methods. The method of determination of the elastic modulus described in this study is based on the solution of the problem of compression of a thin-walled circular cylindrical shell by two parallel planes with regard to the geometrical and physical nonlinearity. The account of nonlinear effects in determination of elastic modulus makes it possible to use a considerably greater range of the loading curve in the elastic region of deformation compared with that in standard methods of testing specimens for tension, compression, and bending.

The contact problem is solved by the finite-element method (ANSYS). To solve the nonlinear problem by the finite-element method, a macros-program was elaborated, which specifies the geometry, physical law, and properties of the material, boundary conditions, loading, division into finite elements, and the step scheme of the solution. The deformation of a thin polymer shell is characterized by great displacements and relatively low elastic deformations in a large range of movement of parallel planes. The solution obtained by finite element method allows making the universal loading diagram in dimensionless coordinates in the given range of thicknesses and elastic module. Equation of the universal loading diagram allows us to solve the inverse problem of determination of the elastic modulus according to experimental points on the loading diagram.

PO-100

LATTICE DYNAMICS AND PHASE TRANSITIONS OF AlF_3

J.Gabrusenoks

Institute of Solid State Physics, University of Latvia

e-mail: gabrusen@latnet.lv

The vibrational modes of cubic and rhombohedral AlF_3 phases are investigated. Calculations have been performed using hybrid exchange density functional theory as implemented within the CRYSYAL06 program to determine the equilibrium geometries and phonon frequencies in high symmetry directions of the Brillouin zone. The calculated phonon frequencies are used to adjust the parameters of a rigid ion model. The longitudinal-transverse splitting of optical modes at k=0 have been determined directly by ab initio in the directions Γ-X, Γ-M and Γ-R calculated phonon dispersions. The phonon dispersion curves show large instability region around the M-R direction.

PO-101

MOLECULAR DYNAMICS SIMULATIONS OF EXAFS IN GERMANIUM

J. Timoshenko, A. Kuzmin, J. Purans

Institute of Solid State Physics, University of Latvia, Latvia

e-mail: timoshenkojanis@inbox.lv

The accurate analysis of the Ge K-edge EXAFS in germanium is a long standing problem due to the presence of multiple-scattering (MS) contributions, which strongly influence the "classical" EXAFS analysis based on the single-scattering (SS) approach [1]. Our previous analysis [2] of thermal effects in two isotopes of ^{70}Ge and ^{76}Ge within the first three coordination shells has been performed using both SS and MS models. We found that while the ratio of the Einstein frequencies for the second and third shells agrees well for the two models, the absolute values of Einstein frequencies are slightly overestimated in the SS model [2]. Unfortunately, the MS EXAFS analysis is limited by two factors: the simplified description of thermal effects within the MS model and a large number of correlated model parameters required.

In this work we present for the first time the classical molecular dynamics (MD) simulation of the Ge K-edge EXAFS using recently developed approach [3]. The MD calculations were performed in the NVT ensemble at several temperatures for a supercell 5x5x5, containing 250 Ge atoms. The force field model included both two and three atom interaction potentials. The MD time step was 0.5 fs, and the total simulation time was 20 ps. The configuration averaged EXAFS signals were calculated from MD data and compared with the experimental EXAFS from [1, 2]. The obtained results allowed us to estimate the thermal effects within the first three coordination shells and their influence on the SS and MS contributions. The effect of the isotopic mass has been also evaluated.

References

1. J. Purans, N. D. Afify, G. Dalba, R. Grisenti, S. De Panfilis, A. Kuzmin, V. I. Ozhogin, F. Rocca, A. Sanson, S. I. Tiutiunnikov, P. Fornasini, *Phys. Rev. Lett*, 2008, 100, 055901.

2. J. Purans, J. Timoshenko, A. Kuzmin, G. Dalba, P. Fornasini, R. Grisenti, N. D. Afify, F. Rocca, S. De Panfilis, I. Ozhogin, and S. I. Tiutiunnikov, *J. Phys.: Conf. Series*, 2009, 190, 012063.

3. A.Kuzmin, R.A. Evarestov, *J.Phys.: Condens. Matter*, 2009, 21, 055401.

PO-102

EXAFS STUDY OF $ZnWO_4$ ON THE W L_3 AND Zn K EDGES

A. Kalinko, A. Kuzmin, J. Timoshenko

Institute of Solid State Physics, University of Latvia

e-mail: akalin@latnet.lv

Extended x-ray absorption fine structure (EXAFS) spectroscopy has been used to study the local atomic structure and dynamics in wolframite-type $ZnWO_4$ polycrystals, synthesized by co-precipitation technique and annealed at 900°C. EXAFS measurements were performed in transmission mode at the HASYLAB DESY C1 beamline in the temperature range of 10-300 K. Both Zn K (9659 eV) and W L_3 (10207 eV) edges were measured in a single scan (Fig. 1) at each temperature.

The static distortion and thermal disorder within the first coordination shell for both Zn and W atoms were studied as a function of temperature. The Zn-O and W-O radial distribution functions were obtained by regularization-like technique.

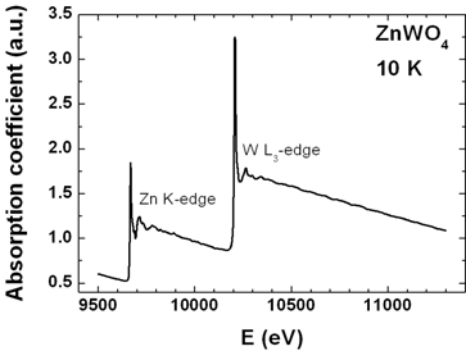

Fig.1 X-ray absorption coefficient for Zn K and W L_3 edges in $ZnWO_4$ measured at 10 K.

Our results show strong distortion of the first shell octahedra, formed by six oxygen atoms, for both Zn and W atoms: three different W-O distances are resolved, while only two Zn-O groups of distances are observed due to restricted spectral range.

The comparative analysis of our results with the recently published diffraction data [1] will be given and discussed.

References

1. D. M. Trots , A. Senyshyn, L. Vasylechko, et. al., J. *Phys.: Condens. Matter*, 2009, 21, 325402

PO-103

PROBING NiO NANOCRYSTALS STRUCTURE BY EXAFS SPECTROSCOPY

A. Anspoks, A. Kuzmin, A. Kalinko, J. Timoshenko
Institute of Solid State Physics, University of Latvia, Latvia
e-mail: aanspoks@cfi.lu.lv

The reduction in size of nanoparticles is generally followed by the atomic structure relaxation, leading to compression or expansion of nanoparticle volume. The former effect is common for metal nanoparticles, whereas the latter one is observed in most metal-oxide nanocrystals [1]. In particular, the lattice expansion has been found recently by x-ray diffraction [2] in NiO nanocrystals, having a size below about 30 nm. While different models have been proposed in the past to explain size-induced changes in the lattice volume of metal-oxide nanocrystals, the phenomenon is still not clearly understood [3]. In this work we present x-ray absorption spectroscopy study of the structure relaxation in NiO nanocrystals, having a size of about 13 nm.

The Ni K-edge EXAFS spectra of green polycrystalline (c-NiO, Aldrich, 99%) and black nanocrystalline (nano-NiO) powders were measured in transmission mode at the HASYLAB DESY C1 beamline at 300 K. Conventional single-scattering analysis of the EXAFS signals from the first two coordination shells of Ni indicates a volume expansion by about 1% in nano-NiO. To access the structure and dynamics beyond the second coordination shell, the Ni K-edge EXAFS spectra for c-NiO and nano-NiO were simulated using recently developed approach [4], based on a combination of classical molecular dynamics (MD) and *ab initio* multiple-scattering EXAFS theory. We found that a simple rigid-ion force field model [5] gives satisfactory agreement between experimental and configuration averaged Ni K-edge EXAFS signals for bulk c-NiO, but not for nano-NiO. However, the proper modification of the force field allowed us to account for the nanocrystals volume expansion and to reproduce satisfactory their EXAFS signal. The EXAFS dependence on the nanocrystals size has been also studied and will be discussed.

References

1. G. Li, J. Boerio-Goates, B.F. Woodfield, L. Li, *Appl. Phys. Lett.* 2004, 85, 2059.
2. L. Li, L. Chen, R. Qihe, G. Li, *Appl. Phys. Lett.* 2006, 89, 134102.
3. A.I. Gusev, *Nanomaterials, nanostructures, nanotechnologies*. (FIZMATLIT, Moscow, 2007).
4. A.Kuzmin, R.A. Evarestov, *J.Phys.: Condens. Matter* 2009, 21, 055401.
5. C.A.J. Fisher, *Scripta Materiala*, 2004 50, 1045.

TABLE OF CONTENTS

A

B

C

G

H

I

J

K

L

M

N

O

P

R

S

T

U

V

W

Y

Z

Notes

Notes

Notes

Notes

Notes

Notes

Notes

Notes